Universität Konstanz

Functional Characterization of the Nogo-66 Domain during Growth and Regeneration in the Fish Visual System

Dissertation

Zur Erlangung des Naturwissenschaftlichen Doktorgrades (Dr. rer. nat.)

der Universität Konstanz

Fachbereich Biologie

Vorgelegt von

Houari Boumediene Abdesselem

Tag der mündlichen Prüfung: 27.7.2009
Referentin: Prof. Dr. Claudia Stürmer
Referent: Prof. Dr. Marcel Leist

Table of Contents

Acknowledgements

I would like to express my thanks to the people who have directly or indirectly contributed to make this work happen:

-First, I would like to thank Prof. Dr. Claudia Stuermer for giving me the opportunity to make a PhD in her laboratory and under her direct supervision, and for the space and freedom she left for me for the development of my scientific experiences and skills.

-Prof. Dr. Marcel Leist and Prof. Dr. Alexander Bürkle for agreeing to take part in the evaluation of this thesis.

- I sincerely thank Dr. Edward Malaga-Trillo and Dr. Gonzalo Solis for guiding me scientifically with the molecular biology, cell biology and biochemistry works, for all advices, enthusiastic discussions and helping me whenever help was needed, and of course for being nice colleagues.

-Ulrike Binkle, Marianne Wiechers, Anette-Yvonne Loos and Silvia Hannbeck were excellent and loyal technical assistants. Thank you for your support and I wish you all the best for your future.

- I also Thank Aleksandra Shypitsyna for providing me the DNA GST-constructs to perform my functional assays.

- I extend my thanks to all the rest of the Stuermer lab for being supportive, cooperative and making enjoyable atmosphere: Yvonne Schrock, Christina Munderloh, alejandro pinzon-olejua, Emily Simpou, Alexander Reuter, Vsevolod Bodrikov, Corinna Geiss and Frau Rixe.....I wish you all the best.

- I really appreciated the financial support of the TR-SFB (DFG) and the University of Konstanz, who allowed me to pursue my Doctoral training and realize my scientific goals.

- I also want to give homage to Frau Ilonka Münch who left us few time ago. She was a great secretary with lot of human qualities.

-Last but not least: my Parents, brothers and sisters and also my good friends in Algeria, France and Germany for their great support.....Thank you all.

Summary

The mammalian central nervous system (CNS) lacks the regenerative capacity to regrow axons upon injury. RTN-4/Nogo-A, a member of reticulon-family of proteins, is a potent myelin associated inhibitor for axon growth and regeneration in the adult CNS of higher vertebrates. In stark contrast, CNS lesioned axons in the zebrafish (ZF) optic nerve regenerate readily and re-establish functional connections with the brain. This correlates well with the absence of the inhibitory NogoA-specific N-terminal domains from the zf-rtn4/nogo (reticulon-4) gene since Nogo-A blocks axon regeneration in mammals - and also in ZF retinal ganglion cell (RGC) axons *in vitro*. In addition to the N-terminal NogoA-specific domains (such as NIGΔ20) rat rtn-4/nogo carries a second inhibitory domain at the C-terminal, called Nogo-66, which is 67% identical with ZF-Nogo66. Therefore the main question we wanted to answer in this project was "Why fish is able to regenerate its lesioned axons despite the presence of the Nogo-66". Thus, we examined whether ZF-Nogo66 is inhibitory, like its Rat counterpart, and how it may affect ZF axon regeneration, using three "classical" assays. In the "outgrowth assay" ZF RGCs extended roughly 1.7 and 2.7 times more axons on ZF-Nogo66 than on Rat-Nogo66 and Rat-NIGΔ20, respectively. In the "collapse assay" 79% of the growth cones elongated unimpaired by ZF-Nogo66 whereas Rat-Nogo66 and NIGΔ20 caused collapse in 78 and 82% of ZF growth cones, respectively. Furthermore, in the "contact assay" ZF RGC growth cones showed collapse (42%) or avoidance (42%) upon contact with transfected HeLa cells expressing Rat-Nogo66 (and 63% and 20%, respectively, with Rat-NIGΔ20) as GPI-anchored EGFP-fusion proteins but grew onto cells expressing ZF-Nogo66 (65%). We further analysed the expression and distribution of ZF-Nogo66 and ZF Nogo receprors (NgRs); ZF-Nogo66 was mainly located inside the oligodendrocytes, and probably not exposed on the cell surface to be in contact with regenerating axons, but Nogo-66 on myelin debris may lye in the path of regenerating (or regrowing) axons. NgR was found on the axonal surface, and may mediate the inhibitory activity of the Rat-Nogo66 in tissue culture assays. PIPLC treatment of RGC axons abolished the inhibitory effect of the Rat-Nogo66, suggesting that a GPI-anchored receptor could mediate the Rat-Nogo66 inhibition, which is probably NgR. Our results suggest, surprisingly, that ZF-Nogo66 is functionally different from the mammalian Nogo-66, it has a growth-permissive effect on ZF axons, quite in contrast to its Rat-Nogo66 homolog which inhibits axon growth. Thus, not only the NogoA-specific domain is absent in fish, but Nogo-66, the

second inhibitory domain has non-inhibitory properties in fish so that ZF RTN-4/Nogo does not impair axon regeneration.

We also tried to render the permissive fish oligodendrocytes to inhibitory cells for axon growth by introducing the Rat-NIGΔ20. Surprisingly, cells expressing the NIGΔ20 exhibited a morphological change, they were losing their processes.

To obtain insights into the function of the zf-rtn4 gene during development, we investigated its spatio-temporal expression pattern in developing ZF embryos and larvae. Zf-rtn4 is expressed early and later during development, showing strong expression in the somites at embryonic stages, and in the brain at larval stages. RTN-4 in fish could play a role during development in neuronal and non-neuronal structures.

The present study together with earlier data imply that the fish CNS is optimized for successful neural regeneration and thus could serve as a model for the identification of parameters required for robust CNS axon regeneration in general.

Zusammenfassung

Im Zentralnervensystem (ZNS) der Säugetiere können Axone nach einer Verletzung nicht regenerieren. RTN4/Nogo-A, ein Protein der Reticulon-Familie, ist ein potenter Myelin-assoziierter Inhibitor des Wachstums und der Regeneration von Axonen im adulten ZNS der meisten Vertebraten. Im Gegensatz dazu sind verletzte Axone des optischen Nerves im Zebrafisch (ZF) in der Lage zu regenerieren und neue funktionelle Verbindungen im Gehirn zu etablieren. Letzteres korreliert mit der Tatsache, dass dem zf-rtn4/nogo (reticulon-4) Gen die N-terminale NogoA-spezifische Domäne fehlt, die in Säugetieren vorhanden ist und Axonregeneration hemmt. Dies Nogo-A spezifiche Domäne inhibitiert das *in vitro* Wachstum von ZF retinalen Ganglienzell (RGZ) Axonen. Zusätzlich zu den N-terminalen NogoA-spezifischen Domänen, wie NIGΔ20, enthalten alle Säugertier rtn4/nogo Gene eine zweite inhibitorische Domäne in ihrem C-Terminus, nämlich Nogo-66, was zu 67% identisch zu der entsprechenden ZF-Nogo-66 Domäne ist. Die Hauptfrage dieser Arbeit war, warum Fischaxone trotz der Anwesenheit von Nogo-66 regenerieren können. Diese Frage wurde mittels drei klassischer Assays untersucht. Das erste Experiment analysierte ob ZF-Nogo66 eine ähnliche inhibitorische Wirkung auf Axone aufweist wie Ratten-Nogo66. In einem "quantitativen Auswachsassay" wuchsen 1.7 und 2.7 mal mehr Axone auf ZF-Nogo66 als Substrat als auf Ratten-Nogo66 und Ratten-NIGΔ20. In einem "Kollapsassay" wuchsen 79% der Wachstumskegel unbeeinträchtigt weiter wenn ZF-Nogo66 in ihre Nähe appliziert wurde, während Ratten-Nogo66 und NIGΔ20 Kollaps von 78% und 82% der getesteten ZF Wachstumskegel hervorriefen. In einer weiteren Versuchsreihe, dem sogenannten "Kontaktassay", kollabierten ZF RGZ Wachstumskegel (42%) oder mieden den Kontakt (42%) mit Ratten-Nogo66-transfizierten HeLa Zellen. Kollaps und Vermeidung des Kontakt betrugen 63% und 20% bei Ratten-NIGΔ20-transfizierten HeLa Zellen. Dagegen wuchsen 65% der Wachstumskegel, die in Kontakt mit ZF-Nogo66-transfizierten Zellen traten frei über deren Oberfläche. Die Peptide (Nogo-66 und NIGΔ20) wurden für diese Versuche als GPI-verankerte, EGFP-Fusionsproteine auf der Zelloberfläche exprimiert. Zusätzlich analysierten wir das Expressionsmuster von ZF-Nogo66 und ZF-Nogo-Rezeptoren (NgRs) um entscheiden zu können, ob Nogo-66 und sein Rezeptor entlang des Weges regenerierender Axone vorhanden ist. ZF-Nogo66 wird vorwiegend im Inneren von Oligodendrozyten exprimiert und wird mit hoher Wahrscheinlichkeit nicht in signifikanter Konzentration auf der Zelloberfläche präsentiert, so dass regenerierende Axone mit dem Peptid nur dann in Kontakt treten wenn es durch eine Verletzung frei wird. NgR wird auf der

Axonoberfläche exprimiert, was eine Erklärung dafür liefern könnte, daß Ratten-Nogo66 auf ZF-Axone in Zellkultur inhibitorisch wirkt. Durch eine Behandlung von RGZ Axonen mit PIPLC konnte der inhibitorische Effekt von Ratten-Nogo66 aufgehoben werden, was darauf hindeutet, dass ein GPI-verankerter Rezeptor, wahrscheinlich NgR, die inhibitoriche Wirkung von Ratten-Nogo66 vermittelt.

Unsere Ergebnisse deuten darauf hin, dass sich ZF-Nogo66 von Ratten-Nogo66 funktionell unterscheidet, indem es das Axonwachstum nicht hemmt. Somit weist insgesamt ZF RTN-4/Nogo keine inhibitorische Wirkung auf Axonregeneration auf, erstens durch das Fehlen der NogoA-spezifischen Domäne und zweitens durch Besitz einer nicht-inhibitorischen Nogo-66 Domäne.

In weiteren Versuchen wurden die sonst Axonwachstum zulassenden Fisch Oligodendrozyten durch Transfektion mit Ratten-NIGΔ20 Peptid in inhibitorische Zellen umzuwandeln. Überraschenderweise zeigten NIGΔ20 exprimierende Oligodendrozyten unerwartete morphologische Veränderungen in dem sie ihre Fortsätze verloren.

Um Einblick in eine mögliche Funktion des rtn4 Gens in der Entwicklung zu gewinnen, wurde in dieser Arbeit auch das Expressionsmuster von RTN4/Nogo in den frühen Entwicklungsstadien des ZF analysiert. RTN4/Nogo wird während der gesamten frühen ZF Entwicklung exprimiert, zunächst überwiegend in den Somiten und später im Gehirn, so dass RTN-4 Protein im Fisch eine Rolle in der Entwicklung spielen könnte.

Diese Studie weist zusammen mit vorherigen Daten darauf hin, dass das ZNS der Fische für erfolgreiche axonale Regeneration optimiert ist und dass man eventuell in diesem Modell die Parameter identifizieren könnte, die die Voraussetzung für eine robuste Axonregeneration im ZNS sind.

I. Introduction

1. Neural regeneration in the adult mammalian central nervous system

The central nervous system (CNS) in adult mammals has a limited capacity to regenerate lesioned axons after injury. One of the well known and widely studied CNS injury model is spinal cord injury (SCI), which represents a clear example for regeneration failure. Following an injury to the spinal cord, the disconnected nerve fibers attempt to regrow (Ramon y Cajal, 1890) but they fail to regenerate over long distances, resulting in a permanent loss of function. An important precondition for regeneration of injured axons is the survival of the nerve cell and its capacity to respond to the lesion by forming new growth cones to initiate axonal re-growth and reconnection with the original targets (Figure 1). The closer the axonal insult to the cell body, the less likely is the survival of the neuron. Injuries that sever axons at a distance to the cell body produce severe reduction in neuronal size (atrophy) several weeks after axotomy, but the neurons normally survive the lesion and exhibit a spontaneous regenerative response called “sprouting”. Even if the cell eventually survives the injury, the nerve terminals and the entire segment distal to the lesion site (i.e. the one that has lost contact with the cell body) will degenerate by a process, called Wallerian degeneration; it is associated with myelin breakdown and the removal of axons and myelin debris (Buss et al., 2005) (Figure 1). The growth will be aborted and the new sprouts are gradually retracted as a consequence of being demyelinated and disconnected from their targets. In contrast to the CNS, in the adult peripheral nervous system (PNS) cut axons re-form growth cones that can regenerate to a significant extent back to their target (Figure 1). The reason why the CNS regenerative process fails to proceed is likely to be multifactorial. Early studies suggested a possible involvement of the adult CNS environment. In 1911, Tello (Ramon y Cajal, 1928) showed that lesioned adult CNS neurons could extend axonal processes within a permissive environment such as in peripheral nerves. This initial observation was strengthened by the elegant demonstration decades later that adult CNS neurons could indeed form long projections through peripheral nerve grafts (Benfey and Aguayo, 1982). This showed that CNS neurons are capable of regenerating axons if the environment is permissive. Thus, the difference between CNS and PNS neurons in their ability to regenerate axons can be explained by the environment of growing axons, since CNS neurons could elongate their axons within the permissive PNS (Benfey and Aguayo, 1982), but PNS neurons show only limited growth if transplanted into the hostile CNS tissue (Aguayo et al, 1981). In addition,

the PNS shows a higher re-expression of growth factors (Bolin and Shooter, 1994; Pellitteri et al., 2001; Boyd and Gordon, 2003), which are produced by Schwann cells close to the injured axons (Bhatheja and Field, 2006). Futhermore, upregulation of genes encoding growth-associated proteins such as SCG10, CAP-23, and GAP-43 by PNS neurons after axotomy correlate with the PNS axonal regeneration success, however, CNS neurons transiently upregulate these genes after axotomy, and showed prolonged upregulation of all the three molecules only when their axons regenerate into a peripheral nerve grafts (Mason et al., 2002). Thus, PNS neurons have an intrinsic capacity to respond to the lesion, and the peripheral environment positively influences the neurons to regrow their axons. Thus, several lines of evidence suggest that both cell-intrinsic and cell-extrinsic factors are reasons for the regeneration failure in the CNS.

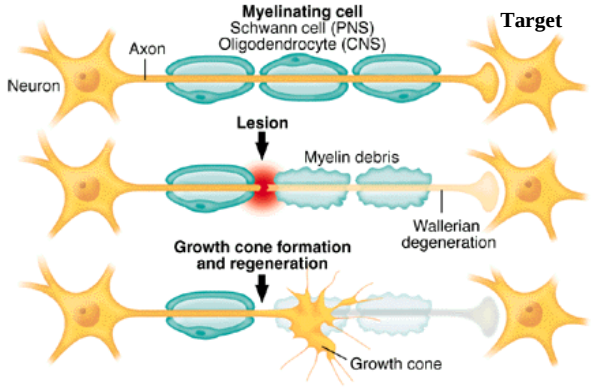

Fig 1. Growth cones direct nerve regeneration. After a lesion, the cut axon re-forms a growth cone, which attempt to regenerate a new axon segment. In the PNS, extensive regeneration is seen, whereas CNS regeneration is severely limited.

1.1. Intrinsic properties of CNS neurons

In adult CNS neurons the growth capacity is lower than during development, but re-rexpression of typical growth-associated proteins can enhance the regeneration capacity (Stuermer et al., 1992; Bomze et al., 2001; Schwab, 2004). Growth-associated proteins such as GAP-43 are typically present in growing axons during development and during PNS axonal regeneration where axonal growth in not impaired. Thus there is a difference in the growth potential in different neuronal types and in both adults and embryos, and there is an overall decrease in the vigour of axon growth with neuronal age (Fawcett, 1992). Thus, loss of intrinsic regenerative capacity in the adult CNS neurons is one of the reasons for regeneration failure.

1.2. The CNS environment

After injury to the adult CNS, axons attempting to regenerate are confronted with major obstacles: the glial scar and inhibitors in myelin and oligodendrocytes.

1.2.1. The glial scar

The glial scar is a barrier for regenerating axons in cases of lesions (Carulli et al., 2005). It contains inhibitory molecules produced by astrocytes and fibroblasts that are associated with the extracellular matrix such as chondroitin sulfate proteoglycans (CSPGs) (Mckeon et al., 1991; Niederost et al., 1999; Horn et al., 2008) being an obstacle for axonal elongation. However, the major impediments to regeneration immediately after injury are most likely to be inhibitors in myelin.

1.2.2. Myelin-associated inhibitors

CNS myelin has been proposed to inhibit regeneration (Caroni et al., 1988). It was the pioneering work of Martin Schwab and co-workers (Schwab and Caroni, 1988; Bregman et al., 1995) who showed that an antibody to an inhibitory fraction of myelin, termed IN-1, allowed regeneration and some functional recovery in rats. This work firmly established myelin as a potent inhibitor for axonal regeneration (Caroni and Schwab, 1988). This inhibitory fraction has been later identified as neurite growth inhibitor and termed Nogo (Chen et al., 2000). Interestingly, Nogo (the Nogo-A splice form) is absent from the PNS myelin where axon regeneration is possible, and when overexpressed by Schwann cells, axon regeneration is impaired after peripheral nerve injury (GrandPré et al., 2000; Pot et al., 2002). Nogo is believed to be the major inhibitory molecule for axon regeneration among all known inhibitors.

1.2.2.1. Neurite outgrowth inhibitor (Nogo)

The antigen of IN-1 was called NI220/250 (Spillmann et al., 1998). IN-1 administration results in stimulation of axonal regeneration, increase of sprouting and enhancement of functional recovery (Schnell and Schwab, 1990; Bregman et al., 1995; Broesamle et al., 2000). The sequencing of the NI220/250 (Spillmann et al., 1998) helped to identify Nogo (Chen et al., 2000; GrandPre et al., 2000; Prinjha et al., 2000). Nogo is the fourth member of the reticulons (RTN) family; RTNs are evolutionary conserved with four RTN paralogs (RTN1, RTN2, RTN3 and RTN4) and present in all land vertebrates. RTN-4/Nogo is

expressed as distinct isoforms A, B and C through differential splicing and promoter usage (Figure 2A). While the exact function of RTN1-RTN3 is unknown, mammalian RTN4/Nogo-A, the largest of the three transcripts of the rtn-4/nogo gene, was shown to inhibit axon regeneration in the mammalian central nervous system (CNS) as well as in neurons *in vitro*. There are two spatially separate inhibitory domains: an amino-terminal domain specific to Nogo-A (Amino-Nogo) (Chen et al., 2000; Prinjha et al., 2000) and an 66 amino acid sequence (Nogo-66) located within the C-terminal reticulon homology domain (RHD) which is found in all three isoforms (Figure 2A) (GrandPre et al., 2000; GrandPre et al., 2002). Furthermore, a stretch encoded by the Nogo-A specific domain called NIGΔ20 has been characterized as one of the most inhibitory domains (Figure 2A). It restricts neurite outgrowth and cell spreading and induces growth cone collapse much as the entire Nogo-A protein (Oertle et al., 2003b). Nogo-A has an endoplasmic-reticulum-retention signal, a property that is shared, however, with several myelin membrane proteins (Chen et al., 2000), the possible functional roles of Nogo-A in the endoplasmic reticulum (ER) are currently unknown. Nogo-A is present in various cell types of the adult CNS. It is found in oligodendrocyte cell bodies and membrane processes, localized in the innermost (adaxonal) myelin membranes where it is in contact with the axon (Huber et al., 2002; Wang et al., 2002) (Figure 2B). Following injury and damage to myelin and oligodendrocytes, Nogo-A is exposed so that axons can contact the inhibitor and collapse (Huber et al., 2000). Cell surface Nogo-A comprises ~1% of total cellular Nogo-A (Figure 2B), and the rest appears to be associated with the ER and may have an intracellular additional function(s) (Oertle et al., 2003b). Additionally, Nogo-A is expressed by projection neurons, in particular during development, and by postmitotic cells in the developing cortex, spinal cord, and cerebellum (Huber et al., 2002). It is also found located in growing axons of developing CNS (Tozaki et al., 2003). Regarding the two others RTN-4 Nogo products, Nogo-B and -C, Nogo-B has a widespread expression in the central and peripheral nervous systems and other peripheral tissues, while, Nogo-C was mainly found in skeletal muscle (Huber et al., 2002). However, expression of Nogo-A in other tissues and, in particular, in developing neurons and the widespread expression of the two shorter isoforms, Nogo-B and -C, suggest that the Nogo family of proteins might have function(s) additional to the neurite growth-inhibitory activity.

The C-terminal region of RTN-4/Nogo sequence shares high homology (70%) with the reticulon (RTN) protein family (Figure 2A). It contains two long hydrophobic stretches (35 and 36 amino acids) separated by the Nogo-66 segment, these hydrophobic stretches serve as transmembrane domains for integrating the protein to the cell/ER membranes (Figure 2B and

3). The Nogo-66 forms an extracellular loop detectable on the oligodendrocyte surface (GrandPre et al., 2000; McGee and Strittmatter, 2003) (Figure 2B), and has been shown *in vitro* to be exposed on the surface of the Nogo-A transfected cells (GrandPre et al., 2000). Whereas all RTNs (-1, -2, -3, and -4) have the Nogo-66, only RTN-4/Nogo-66 has been found to inhibit axonal extension and induce growth cone collapse *in vitro* (GrandPre et al., 2000). Furthermore, *in vivo* transgenic expression of the Nogo-66 domain by otherwise permissive myelinating PNS cells hinders axonal reextension after trauma (Kim et al., 2003b). In addition, evidence by blockade of the Nogo-66 using soluble Nogo-66 receptor has shown to promote axonal sprouting and enhance recovery after spinal cord injury (Li et al., 2004). Together, mammalian RTN-4/Nogo-66 represents a second most important inhibitory molecule for axonal regeneration in addition to the Nogo-A/NIGΔ20.

A

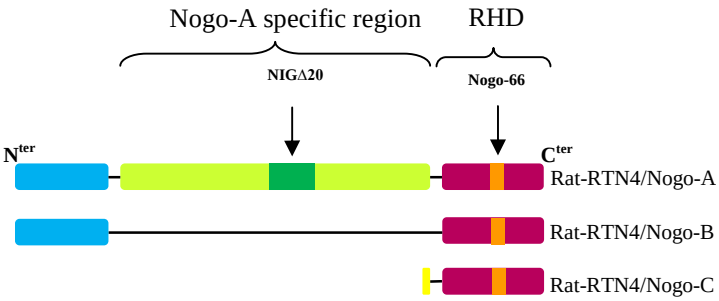

B

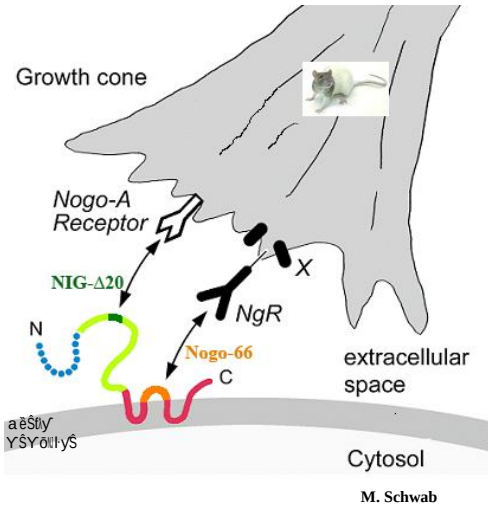

Fig 2. Rat RTN-4 protein isoforms and localization. A) Tree isoforms products are generated from the rat RTN-4 through alternative splicing (Nogo-A and Nogo-B) and promoter usage (Nogo-C), all The three isoforms contain the inhibitory domain Nogo-66 in the conserved reticulon homology domain (RHD), but only the Nogo-A isoform has the Nogo-A specific region harbouring the major inhibitory domain NIGΔ20. B) The schematic drawing shows the localization of the Nogo-A in oligodendrocyte myelin membrane, exposing its two inhibitory domains (NIGΔ20 and Nogo-66) on the extracellular space facing the growth cone of growing axon, they exert their inhibitory action via Nogo-A receptor and the Nogo-66 receptor (NgR) respectively.

The exact localization and topology of Nogo-A at the plasma surface has important biological significance (Oertle et al., 2003b) and has not been clear until recent reports. Nogo-A on the surface of oligodendrocytes inhibit neurite growth and regeneration through its N-terminus Nogo-A specific region and the Nogo-66. These domains are exposed extracellularly (Figure 2B and 3). From one hand, the Strittmatter's group proposed a topology where the Nogo-66 is exposed at the ER lumen, or at the extracellular space within a cytoplasmic N-terminus (GrandPré et al., 2000), however, The Schwab's group claims that the Nogo-A could exist in two different topologies dependent on the two transmembrane domains if they spam the membrane once or twice, leading to a similar topology proposed by Grand-Pré, but, in addition, the Nogo-A specific region is facing the extracellular space, or a topology where the Nogo-A specific region is cytoplasmic (Figure 3) (Huber et al., 2000, Oertle et al., 2003b).

1.2.2.2. Other myelin associated inhibitors

Myelin-associated glycoprotein (MAG), a protein described earlier (Everly et al., 1973) has also been identified as an inhibitory molecule for axon growth (Figure 3). Filbin and colleagues (Mukhopadhyay et al., 1994; DeBellard et al., 1996) found that MAG is an inhibitory molecule for many types of mature neurons *in vitro*. As a member of the immunoglobulin (Ig)-superfamily and sialic acid-binding glycoprotein, MAG is a Siglec family protein (Siglec 4). In the CNS, MAG is found in the periaxonal myelin membrane, and in the PNS, it is also found in the outermost membrane of the myelin sheath (Trapp, 1990).
Yet another myelin-associated inhibitor of regeneration is the glycosyl-phosphatidylinositol (GPI)-linked oligodendrocyte-myelin glycoprotein (OMgp) (Figure 3). Identified by Stefansson in 1988, OMgp has later been revealed as the inhibitor component of the fraction of bovine brain myelin initially termed arretin. OMgp is expressed not only by oligodendrocytes but also by various neurons (Wang et al., 2002). Like MAG and Nogo, OMgp inhibits axonal extension and induces growth cone collapse *in vitro* (Kottis at al., 2002; Wang at al., 2002).

1.2.3. Receptors and molecular signaling

The different myelin associated inhibitory molecules such as Nogo, MAG and OMgp are ligands for axonal receptors. Using an expression-cloning strategy, Strittmatter and colleagues identified a GPI-linked axonal surface protein, termed Nogo-66 receptor (NgR1). It consists of eight leucine-rich-repeat (LRR) domains followed by carboxy-terminal LRR (Fournier et al., 2001), and is expressed in intact and regenerating CNS neurons (Hunt et al., 2002). NgR1 can bind Nogo-66 with high affinity to mediate growth cone collapse in dorsal root ganglion (DRG) neurons (Fournier et al., 2001) (Figure 2B and 3). In addition, studies of the expression pattern of Nogo and NgR1 suggest that these proteins are both present and juxtaposed at the myelin-axon interface, which is consistent with NgR1 acting as the functional Nogo-66 receptor (Wang et al., 2002). In the study demonstrating the inhibitory role of OMgp, He's group demonstrated that the functional neuronal receptor for this molecule also is NgR1 (Wang et al., 2002) (Figure 3), and more surprisingly, also for MAG (Liu et al., 2002; Domeniconi et al., 2002) (Figure 3). In addition to NgR1, MAG also binds to NgR2 to exert inhibition. NgR2 is another member of NgR family (NgR1, NgR2 and NgR3). NgR3 seems to not bind to any of the three inhibitors, therefore it may not be involved in inhibition (Venkatesh et al., 2005). All ligands bind to the extracellular leucine-rich repeat (LRR) domain of NgR1, which provides a large molecular surface for protein-protein interactions (Barton et al., 2003; Lauren et al., 2007). Moreover, *in vivo* assays targeting NgR by administrating the Nogo-66 receptor antagonist peptide (NEP 1-40) (Figure 7) after lateral funiculus injury in the adult rat, axonal growth was promoted and functional recovery was enhanced (Cao et al., 2008). Moreover, inhibiting NgR with a soluble function-blocking NgR fragment after spinal injury allowed axonal sprouting and improved locomotion (Li et al., 2005).

Because NgR1 is a GPI-linked protein and lacks transmembrane and intracellular signaling domains, it may possess coreceptor(s) to transduce the inhibitory signal or cluster in specific microdomains which are associated with the relevant signal transduction proteins. Reports have implied the neurotrophin receptor $p75^{NTR}$ as one signal transducer for Nogo-66, MAG and OMgp-mediated inhibition (Yamashita et al., 2002; Wang et al., 2002). Later the tumor necrosis factor (TNF) receptor family member, TROY (Park et al., 2005) and LINGO-1 (Mi et al., 2004) have been found to be coreceptors for NgR1 and to transduce intracellular inhibitory signaling. Moreover, both NgR and $p75^{NTR}$ appear to be required for the activation of the small GTPase RhoA (Yamashita et al., 2002; Wang et al., 2002), known as regulator of the actin cytoskeleton. Upon interaction of Nogo-66 or MAG with NgR, $p75^{NTR}$, TROY and

LINGO-1, a receptor complex is formed and transduces intracellular signaling which lead to the activation of the GTPase RhoA and suppression of Rac1, resulting in actin disassembly and thereby growth cone collapse (Fan et al., 1993; Niederoest et al., 2002; Domeniconi et al., 2005; Mimura et al., 2006) (Figure 3). Rac1 is known to control and promote axon growth (Ng et al., 2002) and RhoA to induce growth cone collapse by activating ROCK (RhoA kinase) which stimulates LIM kinase, which then stimulates cofilin, to effectively re-organizes the actin cytoskeleton (Hsieh et al., 2006) (Figure 3). This pathway is also activated by NIGΔ20 of the Nogo-A, and mediates neurite growth inhibition by antagonistic regulation of RhoA and Rac1 independently of NgR. NgR does not, however, interact or mediate the effects of the N-terminal region of Nogo-A (amino-Nogo) (Niederost et al., 2002; Liu et al., 2002). Therefore, it has been proposed that a separate, as yet unidentified Nogo-A receptor or complex must exist (Figure 3). In addition, Nogo-A evokes a cascade of second messengers that mediate collapse of growth cones by inducing calcium release from intracellular stores (Figure 3) (Bandtlow et al., 1993; Bandtlow and Loeschinger, 1997). MAG and CNS myelin seem to affect cyclic AMP signaling (Figure 3). Cai et al (1999) found that pre-treatment (priming) of responding neurons with neurotrophins can block the inhibitory effects of MAG and CNS myelin. In addition, they showed that this priming procedure elevates cAMP levels which mediate activation of CREB leading to upregulation of genes such as Arginase I and Interleukin-6, products which have been shown to directly promote axonal regeneration (Cai et al., 2001, 2002). Thus, cAMP elevation provides mechanism for overcoming MAG and myelin-mediated neurite growth inhibition. Furthermore, MAG inhibits microtubule assembly by a Rho-kinase dependant mechanism in neurons (Figure 3) (Mimura et al., 2006). Recently, Paired immunoglobulin-like receptor B (PirB) has been shown to be an additional new receptor mediating neurite growth inhibition by Nogo-66, MAG and OMgp (Figure 3) (Atwal et al., 2008).

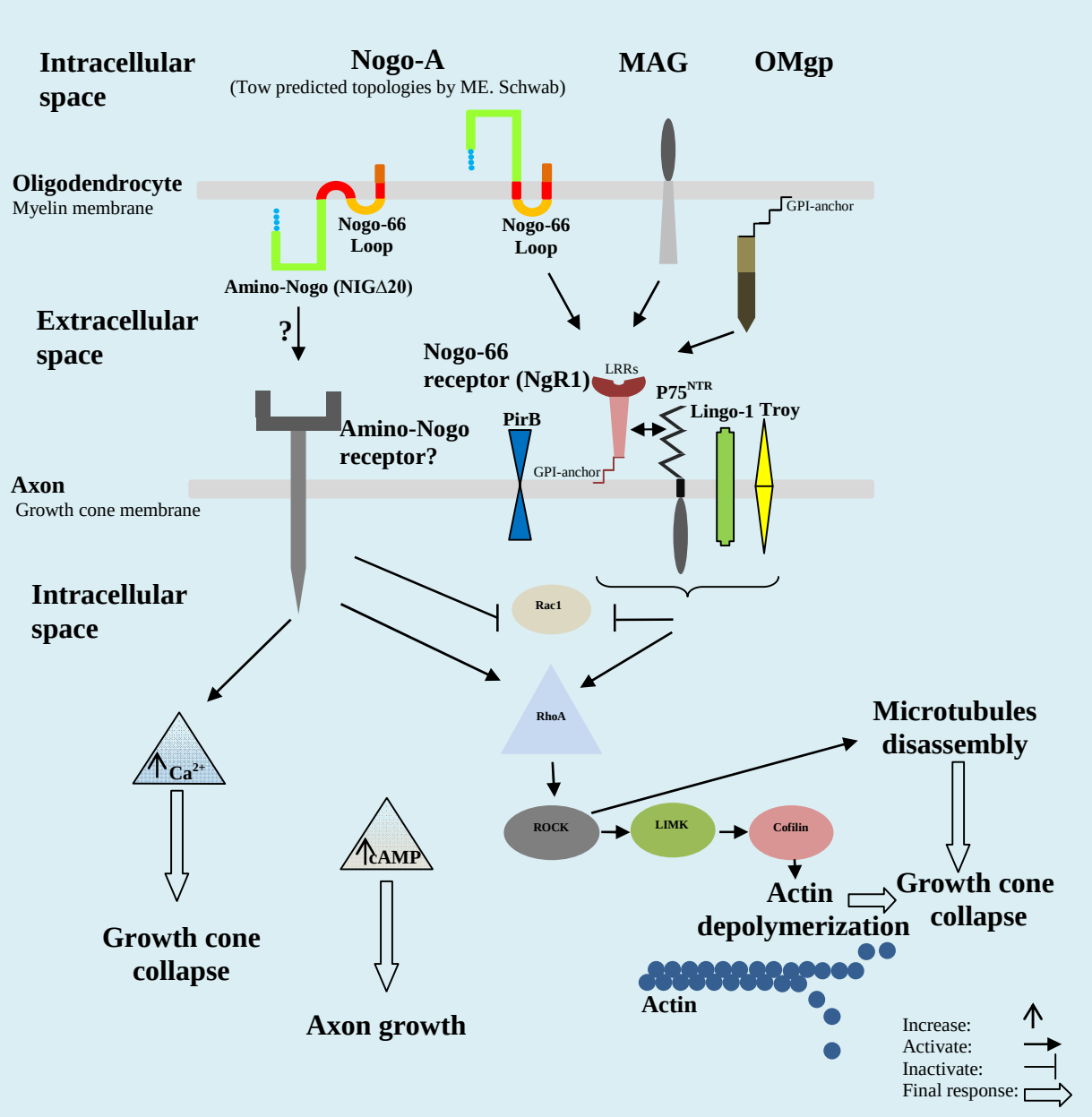

Fig 3. Myelin associated inhibitors, receptors and intracellular signaling mechanisms. Myelin inhibitors of the adult CNS include Nogo-A within two different topologies, myelin associated glycoprotein (MAG) and oligodendrocyte myelin glycoprotein (OMgp); all are expressed in the myelin membrane and facing the extracellular space. Neuronal receptors and downstream signaling pathways are involved in transducing these inhibitory signals. Nogo-66, MAG and OMgp are ligands for NgR1. Upon ligand binding, activated NgR1 interacts with $P75^{NTR}$, Lingo and Troy to transduce intracellular signaling, characterized by RhoA activation, which engages its downstream effector Rho kinase (Rock), which in turn activates LIM kinase, thereby modulating actin dynamics via phosphorylation of cofilin and inducing growth cone collapse. Other antagonistic GTPases mediating growth cone mobility signals, such as Rac1 are simultaneously downregulated. The amino-Nogo NIGΔ20 known as a major myelin inhibitor induces collapse of growing axons via interaction with Nogo-A receptor (not yet identified). This involves regulation of RhoA and Rac1 pathways.

1.3. Nogo knockout and adult neural regeneration

To investigate the role of Nogo-A on axon regeneration in the adult CNS, *in vivo* knockout mice for rtn-4/nogo were generated by three different laboratories: Nogo-A knockout mice (Simonen et al., 2003), Nogo-A/-B knockout mice (Kim et al., 2003a) and Nogo-A/-B/-C knockout mice (Zheng et al., 2003). After spinal cord lesion, Nogo-A specific knockout mice showed a moderate but clearly detectable increase in regenerative sprouting and elongation (Simonen et al., 2003). Interestingly, the same phenotype was quantitatively enhanced in Nogo-A/-B knockout mice (Kim et al., 2003a). Because Nogo-B was greatly upregulated in the Nogo-A knockout, the Nogo-66 inhibitory domain seemed to compensate partially for the absence of the Nogo-A specific site. In contradiction to these observations, the third laboratory has shown no major enhancement of sprouting or regeneration of lesioned cortico-spinal tract axons in their knockout mice for Nogo-A/-B or Nogo-A/-B/-C (Zheng et al., 2003). These controversial results can be due to the use of mice strains with different genetic background, which can differ greatly in various aspects, such as neuroinflamatory response, cell death at lesion sites, scarring response and overall behavior (Simonen et al., 2003, Schwab, 2004, Dimou et al., 2006).

1.4. Enhancing mammalian CNS regeneration after injury

With the characterization of myelin associated inhibitors and elucidation of signaling mechanisms underlying their activities, strategies can be developed in order to stimulate axon regeneration and thereby design new therapeutic approaches. Targeting inhibitors became one of the widely used strategies following the identification of the relevant molecules. Neutralizing Nogo-A by antibody administration has provided promising results as mentioned above (Broesamle et al., 2000; Liebscher et al., 2005; Seymour et al., 2005; Weinmann et al., 2006). This approach has recently been applied to non-human primates and shows that Nogo-A neutralization enhances sprouting of corticospinal axons rostral to a unilateral cervical spinal cord lesion in adult macaque monkeys (Freund et al., 2007). Other approaches are still being explored to overcome inhibition such as blockade of NgR (Li et al., 2004), targeting signaling molecules like RhoA (Fuentes et al., 2008) or delivering growth factors to the neurons (Lu and Tuszynski, 2008). Other strategies are transplantation of adult neuronal precursor cells to promote remyelination and functional recovery after spinal cord injury (Karimi-Abdolrezaee et al., 2006). Another strategy focusses on the effect of

inflammation provoked by injury on the regeneration process, such as inhibiting proteoglycans expressed by reactive astrocytes which are associated with the glial scar (Steinmetz et al., 2005) or applying chondroitinase ABC (chABC), an enzyme which selectively degrades CSPGs, leading to clear regeneration following CNS lesion (Bradbury et al., 2002; Silver and Miller, 2004).

2. Neural regeneration in the fish CNS

In contrast to mammals, fish CNS neurons readily regenerate their axons after lesion allowing functional recovery (Gaze et al., 1970; Stuermer at al., 1988a). In the fish visual system, retina ganglion cells (RGCs) grow their axons after optic nerve lesion. They make new growth cones and elongate them through myelin and axon debris in the optic nerve to reach their target cells in the optic tectum restoring connections and vision (Stuermer and Easter, 1984). Fish can also regenerate lesioned axons in the spinal cord (Becher et al., 1997). Fish are paralyzed immediately after a spinal cord transection. They tend to lye on their sides, unable to move their tail and caudal fins. After several weeks, however, their swimming ability is regained (Cohen and Wallen, 1980; McClellan, 1990). The question emerged why fish show such a capacity for axonal regeneration. This question has been a central focus of research in the Stuermer lab who aim at "trying to understand the success of axon regeneration in fish" (Stuermer et al., 1992; Diekmann et al., 2005). This requires two approaches: studying the intrinsic regenerative capacities of fish neurons and elucidating the properties of the fish CNS environment which seems to be favorable for axonal growth.

2.1. Intrinsic neuronal properties for successful regeneration

In order to regenerate successfully, a neuron whose axon has been cut has to re-induce the relevant intracellular mechanisms and synthesize the necessary proteins such as the growth-associated proteins mentioned above to support axonal growth (Stuermer et al., 1992). By using the fish visual system as a model to study axonal regeneration, various studies have been performed to verify that RGC neurons are able to reactivate the cellular machinery necessary for axonal regrowth. Molecules involved in axon growth and pathfinding are found to be upregulated in the neurons regenerating axons after nerve transection such as the cell adhesion molecules L1 (or E587), N-CAM, Thy1, TAG-1, Neurolin, Cntn1b as well as intracellular signalling molecules c-Jun, GAP43 and Reggie (Vielmetter et al., 1991; Bernhardt et al., 1996; Deininger et al., 2003; Lang et al., 2001; Paschke et al., 1992; Schulte

et al., 1997; Haenisch et al., 2005), indicating that the fish RGCs provide the necessary molecular components for growth cone elongation and navigation to their regenerating axons (Leppert et al., 1999) (Figure 4).

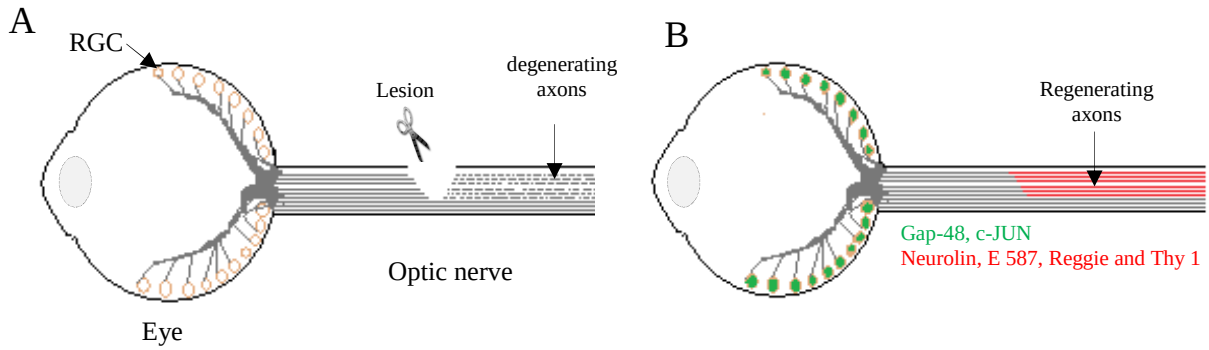

Fig 4. Upregulation of growth-associated proteins by goldfish retinal ganglion cells following optic nerve lesion. A) After lesion to the optic nerve, the post-lesion axons undergo degeneration and loose connections with their target cells in the optic tectum (not shown). The pre-lesion axons form new growth cones and start to regenerate. B) After lesion to the optic nerve, RGCs start to re-express growth associated molecules in cell bodies (green color) and in regenerating axons (red color) to support lesioned axons to regrow till they find their targets and form new connections.

2.2. Favorable environment for axonal regeneration

Since oligodendrocytes and CNS myelin interfere with axonal regeneration in mammals the most crucial question is whether equivalent glial cells and their associated inhibitors would be present in fish, if so, how they affect regeneration.

2.2.1. Fish oligodendrocytes support axonal regeneration

In fish, special properties of glial cells appear to contribute to the success of axonal regeneration after lesion. Comparison of the reaction of the fish and the mammalian CNS to the lesion has revealed striking differences. After lesion to the optic nerve in goldfish, the glial scar is formed but in contrast to mammals it represents no barrier for axon regeneration (Hirsch et al., 1995). Even if the nerve contains Nogo-66, it seems to have no negative effect on regenerating axons. Another crucial observation was that oligodendrocytes during axon degeneration and regeneration detach from degenerating axons and lose their myelin sheets. This is accompanied by the arrest of myelin proteins expression and dedifferentiation of mature to elongated cells (Ankerhold and Stuermer, 1999). Therefore, once the regenerating axons reach their targets in the optic tectum and form synapses (Stuermer and Easter, 1984),

oligodendrocytes re-differentiate to myelinating cells and ensheath the axons (Ankerhold and Stuermer, 1999). These changes are beneficial to the repair of the visual pathway. Furthermore, *in vitro* evidence has shown that fish oligodendrocyes promote axonal growth by re-expressing growth associated cell surface proteins, like the L1-adhesion molecule (or E587) that has been shown to promote RGC axon growth (Ankerhold et al., 1998). Moreover, the leading growth cones of regenerating axons are capable of growing along myelin fragments and on a wide variety of cellular surfaces of oligodendrocytes and astrocytes in the goldfish optic nerve (Strobel and Stuermer., 1994), suggesting that the fish CNS oligodendrocytes/myelin are either devoid of inhibitors such as Nogo.

2.2.2. Absence of inhibitors from fish oligodendrocytes/myelin

Earlier data indicated that fish CNS myelin is growth permissive since rat dorsal root ganglion (DRG) neurons when exposed to fish optic nerve slices as substrate, were able to extend their axons (Carbonetto et al., 1987). In cross-species co-culture assays to test the substrate properties of CNS myelin and oligodendrocytes, growth cones of rat and fish RGC axons elongated successfully upon contact with fish oligodendrocytes or fish CNS myelin (Figure 5). However, they collapsed upon contact with rat oligodendrocytes or rat CNS myelin, suggesting that fish oligodendrocytes and fish CNS myelin are devoid of inhibitors and are growth permissive (Bastmeyer et al., 1991)(Figure 5). However, when rat oligodendrocytes and rat myelin were offered to RGC axons, growth cones collapsed in contact with these inhibitory substrates suggesting that fish RGCs recognize the mammalian inhibitors. This was substantiated by treatment of oligodendrocytes/myelin with the IN-1 antibody, whereupon fish RGC axons were able to cross and grow over the cells and myelin (Bastmeyer et al., 1991) (Figure 5). Surprisingly, fish seems to possess a receptor for the mammalian neurite growth inhibitors although these proteins are apparently absent from fish CNS myelin (Figure 6B). A few years ago, the challenging task was the search for the homologs of the RTN4/Nogo-A in the fish CNS and analysis of its function. Analysis of the reticulon gene family demonstrated the absence of the neurite growth inhibitor Nogo-A in fish but showed the presence of Nogo-66 (Diekmann et al., 2005) (Figure 6).

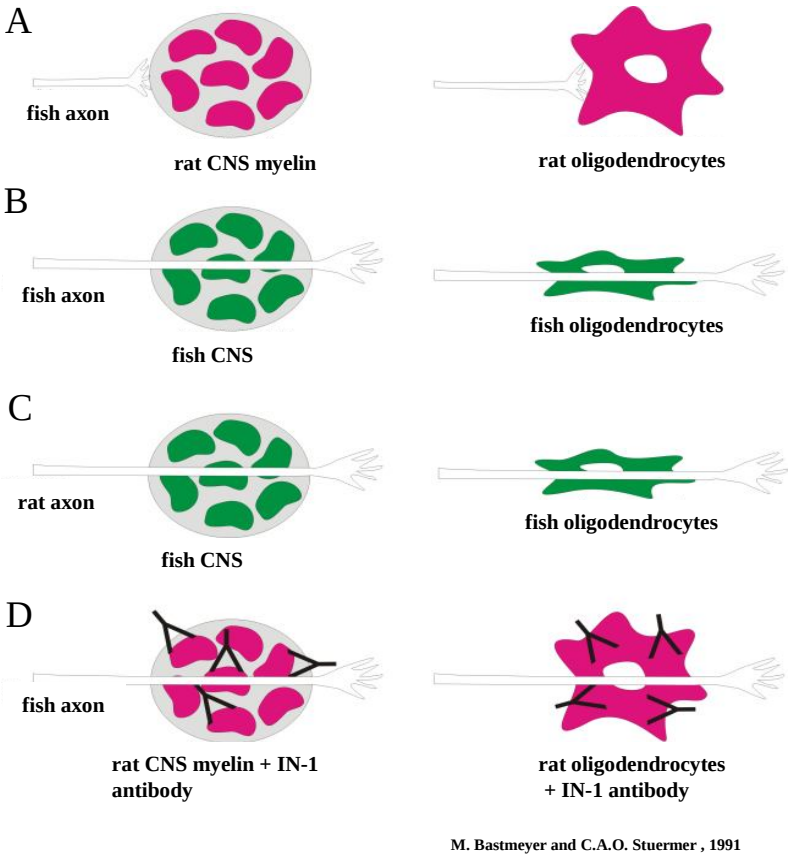

Fig 5. Cross species assays for the substrate properties of CNS myelin and oligodendrocytes. A) Fish axons collapse in contact with rat CNS myelin or oligodendrocytes (red). B and C) Fish and rat axons are able to grow over the fish CNS myelin or oligodendrocytes (green). D) When rat CNS myelin or oligodendrocytes were treated with IN-1 antibodies, the inhibition of fish axon growth was abolished, so that, fish axons were able to cross the rat CNS myelin and oligodendrocytes.

2.2.3. Fish RTN-4/Nogo and receptors

Detailed analyses of the fish reticulon gene family (Diekmann et al., 2005) has shown that the mammalian rtn4/nogo sequence is duplicated in ZF, giving rise to rtn-4 and rtn-6. zf-rtn4 encodes the three isoforms l, m and n through alternative promoter usage (Figure 6A). The C-terminal reticulon homology domain (RHD) containing the Nogo-66 stretch is highly conserved among mammals and fish. Thus, Nogo-66 is present in fish, and may not have an inhibitory function, which needs however, to be approved by the relevant experiment. However, the fish N-termini differ in length and sequence from the mammalian N-termini. They are shorter and without any homology to mammalian Nogo-A, -B, or -C. Thus, the neurite growth inhibitory region of the N-terminal portion of the Nogo-A is absent in the zf-rtn4, suggesting that this domain is an important inhibitory factor for axon regeneration. Its absence correlates with the unique ability of fish to regenerate CNS axons (Diekmann et al., 2005) (Figure 6A). Fish Rtn-4 isoforms are expressed in different adult tissues and during development (Diekmann et al., 2005). This suggests additional function(s) for the Nogo proteins in adult neuronal and non-neuronal tissues and during embryogenesis.

Four zf-ngr homologs were discovered (zf-ngr, zf-ngrH1a, zf-ngrH1b and zf-ngrH2); they are expressed early in development and prominently in the adult brain (Klinger et al., 2004). ZF-NgR is the homologous receptor for the mammalian or human NgR1 that is involved in inhibition. Having the Nogo-receptors (Klinger et al., 2004) (Figure 6B), fish RGC axons are expected to respond to Nogo-66 from fish and to its mammalian counterparts which differ from one another in 22 (roughly 33%) amino acids (aa) (Diekmann et al., 2005) (Figure 7). However, the interaction between the Nogo-66 and NgR obviously does either not exist in fish or does not lead to inhibition of axon growth, since fish axons grow over fish myelin, isolated fish oligodendrocytes *in vitro* (Bastmeyer et al., 1991; Stuermer et al., 1992) and readily regenerate *in vivo* (Stuermer et al., 1992). Therefore, fish Nogo-66 should be functionally different from its mammalian ortholog, lacking the inhibitory effect on axon regeneration or not be present in the nerve at the time at which the axons regenerate. Nevertheless, the function of the ZF homologue of Nogo-66 remains elusive, a challenging question which has to be resolved to understand further why axonal regeneration is possible in fish and not in mammals (Figure 6).

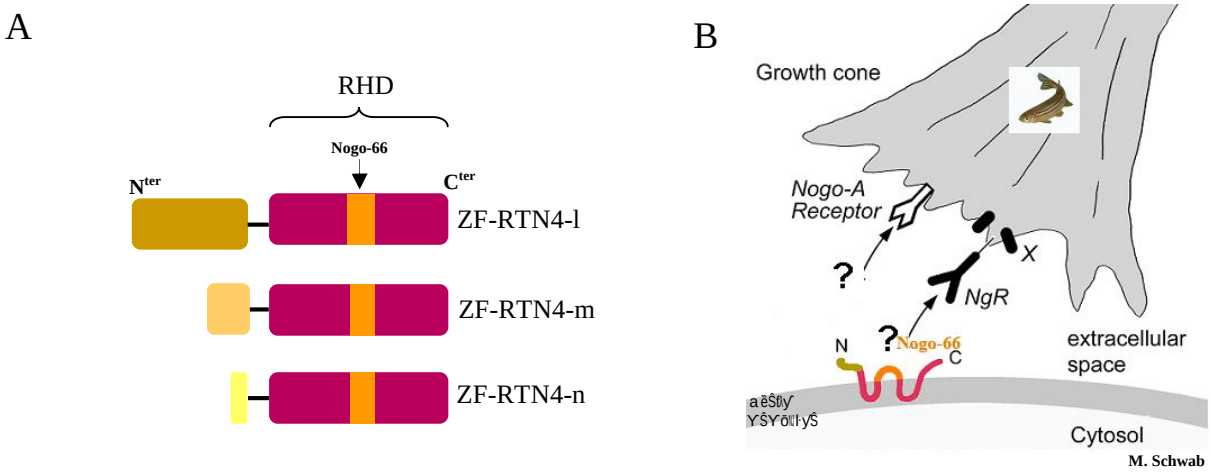

Fig 6. ZF-RTN-4 protein isoforms and localization. A) Three protein isoforms are produced by the zf-rtn4 gene (RTN4 -l, -m and -n), all three isoforms have the fish homologous version for the Rat-Nogo66 domain in the conserved reticulon homology domain (RHD) at the C-terminus. The N-terminal region is entirely different from the mammalian version and is missing the inhibitory Nogo-A specific region. B) The scheme proposes a localisation of the ZF-RTN4 in oligodendrocyte myelin membrane, in which Nogo-66 is exposed on the extracellular side to be recognized by the growth cone. The fish receptor ZF-NgR is present on the growth cone membrane where the not yet identified Nogo-A receptor should also reside.

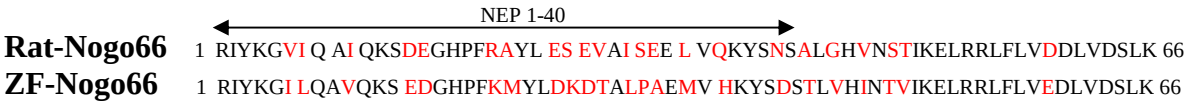

Fig 7. Amino-acid sequence alignment between the Rat-Nogo66 and ZF-Nogo66. A sequence alignment produced by BLAST. 67% of amino acids are conserved (black letters) and the differences are in red. NEP1-40 represents the Nogo-66 epitope suggested to be involved in binding the Nogo receptor NgR1.

3. Aims of the research project

Since many years, our laboratory has been involved in research focusing on axonal regeneration in fish (Stuermer et al., 1992; Diekmann et al., 2005). The absence of the Nogo-A specific region from the fish genome correlates with the success of axon regeneration in the fish optic nerve. However, as explained above, the second inhibitory system, involving Nogo-66 as the ligand in myelin and NgR as the receptor on the axons, seems to exist in fish. To shed light on the situation I have, in this thesis, investigated 1) the presence of Nogo-66 in the CNS, 2) whether it has an effect on growing fish axons by *in vitro* assays, 3) the inhibitory activity of the mammalian (Rat) Nogo-66 and NIGΔ20 on the fish RGC axons to see whether the axons recognize the mammalian molecules as growth inhibitor. 4) I also investigated whether NgR receptor is present in ZF RGC axons and tried to assess its role in inhibition mediated by Rat-Nogo66. 5) I analysed fish oligodendrocytes expressing Rat-NIGΔ20 to test if they turn to be inhibitory for axon growth. 6) Finally, in order to uncover a possible role for RTN-4/Nogo during embryogenesis by defining where it is present, its expression patterns on mRNA level were analysed in developing ZF embryos.

II. Materials and Methods

1. Materials

1.1. Technical equipment

Name	Company, Country
Agarose gel chamber	PeqLab, Germany
Amersham Hyperfilm	GE Healthcare, UK
Analytical balance	Mettler, Germany
AxioCam MRm and MRc5	Zeiss, Germany
Cell counting chamber	Neubauer, Germany
Cell scrapper	Greiner, Germany
Confocal Laser-Scaning Microscope (LSM510)	Zeiss, Germany
Coverslips	Menzel-Gläser, Germany
Filter Hybond-N^+	Amersham pharmacia biothec, UK
Fluorescent microscope axioplan 2	Carl Zeiss, Germany
Flusks	TPP, Switzerland
Heating block	NeoLab, Germany
Incubator	Heraeus instrument, Germany
Inverted fluorescent microscope	Carl Zeiss, Germany
Lumox petridishes	Greiner Bio-one, Germany
Megafuge	Sorvall Evolution , Germany
Microcon centrifugal filters	Millipore, Germany
Microinjector (Femto Jet)	Eppendorf, Germany
Micromanipulator (Inject Man NI 2)	Eppendorf, Germany
Microscope slides	Menzel-Gläser, Germany
Multifuge 4KR	Heraeus, Germany
Multi-well plates	Costar, USA
Ni-NTA spin column	Qiagen, Germany
PCR thermo-cycler	DNA engine, USA
pH meter 766	Knick, Germany
Plastic petridishes	Greiner Bio-one, Germany
Poly-prep chromatography columns	*Bio-RAD*, Germany
Power supply	Consort, Belgium and Hoefer Scientific Instruments, USA
Shaker	Heidolph Unimax, Germany

Sonifer	Branson Sonifier, Germany
Spectrophotometer	Beckmann DU530, Germany
Sterile pipettes	BD Falcon, USA
Table centrifuge 5402 and 5415C	Eppendorf, Germany
Teflon plate	Uni Konstanz, Germany
Tissue shopper	Mickle Laboratory engineering, UK
Tweezers	A.Dumand & Fils, Switzerland
UV light DNA analysis equipment	BIORAD, Germany
Vacuum filtration unit 125ml	Schleicher & Schnell, Germany
Vivaspin 0.5 centrifugal filter	Millipore, USA
Water bath	GFL, Germany

1.2. Reagents and chemicals

Name	**Company, Country**	**Name**	**Company, Country**
Acetic acid	Roth, Germany	Laminine	Sigma-Aldrich, Germany
Acrylamide 30	Roth, Germany	L-Glutamine	GIBCO, USA
Agarose	Roth, Germany	Methyl cellulose	Sigma-Aldrich, Germany
APS	Sigma-Aldrich, Germany	β 2-Mercaptoehanol	Merck, Germany
BCIP/X-phophate	Roche, Germany	MS222	Sigma-Aldrich, Germany
B-PER	Pierce, Germany	Isopropanol	Roth, Germany
Bradford assay	Sigma-Aldrich, Germany	Methanol	VWR Prolabo, France
Bromophenol blue	Merck, Germany	$MgCl_2$	Riedel-de Haën, Germany
BSA	Sigma-Aldrich, Germany	Milk powder	Rapilait, Germany
Chloroform	Roth, Germany	Mowiol	Calbiochem, Germany
Citric acid	Roth, Germany	NaCl	Roth, Germany
Coomassie violet	Merck, Germany	NaH_2PO_4, Na_2HPO_4	Merck, Germany
DNA Ladder 100bp	Fermentas and *Bio-RAD*, Germany	NaOAc	Merck, Germany
DNA ladder 1Kb	PeqLab, Germany	Ni NTA agarose	Qiagen, Germany
DTT	Fluka, Germany	NTB	Roche, Germany
EDTA	Roth, Germany	PFA	Riedel-de Haën, Germany
Effectene	Qiagen, Germany	PeqGold TriFast	PeqLab, Germany
Ethidium bromide	Sigma-Aldrich, Germany	Phenol red	Riedel-de Haën, Germany
Formamide (deionized)	Sigma-Aldrich, Germany	Poly-lysine	Sigma-Aldrich, Germany
Fugene	Roche, Germany	Ponceau S dye	Serva, Germany
Glutathione (Reduced)	Sigma-Aldrich, Germany	Protease inhibitor	Roche, Germany

Glutathione-Sepharose 4B	GE Healthcare, Sweden	SDS	Roth, Germany
Glycerol	Roth, Germany	SSC	GIBCO BRL, Germany
Glycine	Roth, Germany	TEMED	Sevra, Germany
Hepes	Sigma-Aldrich, Germany	Tris base	Sigma-Aldrich, Germany
Heparin	Sigma-Aldrich, Germany	Triton X-100	Sigma-Aldrich, Germany
HCl	Merck, Germany	tRNA	GIBCO BRL, Germany
Imidazol	Sigma-Aldrich, Germany	Tween-20	Sigma-Aldrich, Germany
IPTG	Roth, Germany	Urea	VWR Prolabo, Belgium

1.3. Kits

Name	**Company, Country**
DIG RNA Labeling Kit	Roche, Germany
ECL Kit	Thermoscientific, USA
pCRII-TOPO vector Kit	Invitrogene, Germany
QIAprep Miniprep Kit	Quigen, Germany
QIAquick Gel Extraction Kit	Qiagen, Germany
QIAquick PCR purification Kit	Qiagen, Germany
RNeasy Mini Prep Kit	Qiagen, Germany
RED Taq™ DNA polymerase Kit	Sigma-Aldrich, Germany
SuperScript II RT Kit	GIBCO BRL, Germany

1.4. Enzymes

Name	**Company, Country**
AgeI endonuclease	Fermentas, Germany
BamHI endonuclease	Fermentas, Germany
CIAP	BioLabs, Germany
Collagenase	Seromed, Germany
Dispase	Boehringer, Germany
DNaseI	GIBCO BRL, Germany
EcoRI endonucleases	Fermentas, Germany
HindIII endonuclease	Fermentas, Germany
Lysozyme	Sigma-Aldrich, Germany
NotI endonuclease	Fermentas, Germany
PIPLC	Sigma-Aldrich, Germany
Proteinase K	Roche, Germany
RNaseH	GIBCO BRL, Germany
SP6 RNA polymerases	GIBCO BRL, Germany

Trypsin	GIBCO, USA
T4 DNA ligase	Fermentas, Germany
T7 RNA polymerases	GIBCO BRL, Germany

1.5. Growth medium and antibiotics

Name	**Company, Country**
Ampicilin	Roth, Germany
Chicken serum	Invitrogene, Germany
Chloranphenicol	Roth, Germany
FCS	Invitrogene, Germany
F12 medium	Invitrogene, Germany
LB medium	BD, France
L-15 medium	Biochrom, Germany
MEM medium	Biochrom, Germany
Penicillin	GIBCO, USA
Kanamicin	Roth, Germany
Streptomycin	GIBCO, USA

1.6. Antibodies (ABs)

Primary ABs		**Secondary ABs**	
Name	**Company, Country**	**Name**	**Company, Country**
Goat Polyclonal ABs anti GST	Amerscham Biosciences, USA	Donkey anti mouse IgG, Cy3 conjugated	Jackson Immunoresearch, UK
Rabbit polyclonal ABs anti ZF-Nogo66	C.A.O.Stuermer, University of Konstanz, Germany	Donkey anti rabbit IgG, Cy3 conjugated	Jackson Immunoresearch, UK
Mouse monoclonal ABs Anti-dig-AP	Roche, USA	Goat anti mouse IgG, Cy3 conjugated	Jackson Immunoresearch, UK
Mouse monoclonal ABs11C7 anti NIGΔ20	M. Schwab, University of Zurich, Switzerland	Goat anti mouse IgG, Alexa-488 conjugated	Jackson Immunoresearch, UK
Mouse monoclonal ABs M802 anti goldfish Thy1	C.A.O.Stuermer, University of Konstanz, Germany	Goat anti rabbit IgG Alexa-488 conjugated	Jackson Immunoresearch, UK
Mouse monoclonal ABs ZN5 anti ZF-Neuroline	DSHB,USA	Goat anti mouse IgG, HRP conjugated	Jackson Immunoresearch, UK
Mouse monoclonal ABs N518 anti goldfish Neuroline	C.A.O.Stuermer, University of Konstanz, Germany	Goat anti rabbit IgG, HRP conjugated	Jackson Immunoresearch, UK
Mouse monoclonal ABs anti GFP	Roche, Germany	Rabbit anti goat IgG, HRP conjugated	Jackson Immunoresearch, UK

1.7. Plasmids and bacteria strains

1.7.1. Plasmids

Constructs in pGEX-KG prokaryotic expression vector encoding the GST-Rat-Nogo66, GST-ZF-Nogo66 and GST-Rat-NIGΔ20 fusion protein were provided by Aleksandra Shypitsyna and constructs in pET-28a prokaryotic expression vector encoding the His-Rat-NIGΔ20-His and His-Rat-Nogo66-His peptides as well as construct in pEGFP-C1 eukaryotic expression vector encoding Rat-Nogo-A were kindly provided by M.E. Schwab (University and ETH Zurich, Switzerland) (Figure 8).

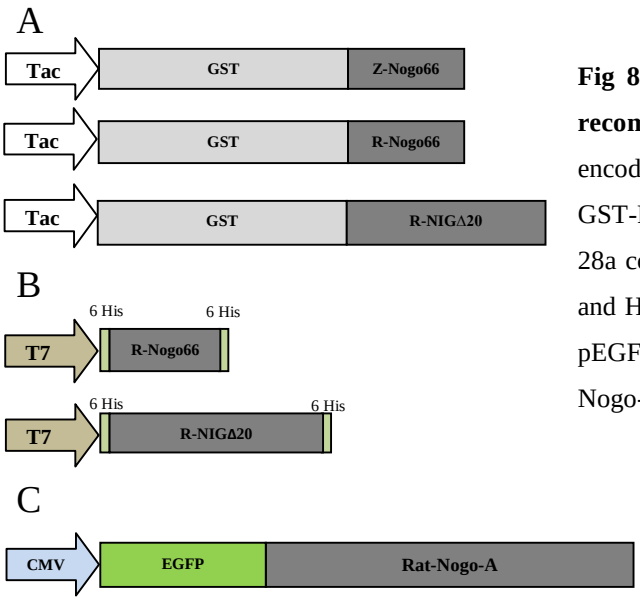

Fig 8. Diagrams for constructs plasmid encoding for recombinant proteins. A) pGEX-KG constructs plasmid encoding for GST-ZF-Nogo66, GST-Rat-Nogo66 and GST-Rat-NIGΔ20 peptides under Tac promoter. B) pET-28a constructs plasmid encoding for His-Rat-Nogo66-His and His-Rat-NIGΔ20-His peptides under T7 promoter. C) pEGFP-C1 construct plasmid encoding for EGFP-Rat-Nogo-A recombinant protein under CMV promoter.

1.7.2. Strains

E-coli competent cells	Company, Country
Top10	Invitrogene, Germany
BL21 Star	Invitrogene, Germany
BL21-codon+	Stratagene, USA

2. Methods

2.1. Animal model system

2.1.1. Adult fish

Wild type adult zebrafish (ZF) (*Danio rerio*) and goldfish (*Carassius auratus*) with the size of 2-2,5 and 5-7cm long, respectively were maintained at 28°C and room temperature (RT),

respectively in our breeding colony in the central animal facility "Tierforschungsanlage" (TFA) of the University of Konstanz.

2.1.2. Fish embryos

ZF embryos (*Danio rerio* wild type strain) were raised at 28°C in the central animal facility "Tierforschungsanlage" (TFA) of the University of Konstanz. Embryos were staged in hours post fertilization (hpf) and days post fertilization (dpf) according to Kimmel et al. (1995). Prior to fixation, embryos later than 20 somites (19 hpf) were dechorionated and anaesthetized in 0.03% aminobenzoic acid ethyl ester (MS222). For long term storage, embryos were maintained in 100% methanol and kept at -20°C.

2.2. Animal surgery

2.2.1. Fish optic nerve transection

The ZF optic nerve as well as goldfish optic nerve were transected in compliance with animal welfare legislation. In brief, adult ZF and goldfish were anesthetized with 0.03% MS222 for 3-5 min (minute) till the fish stopped moving. Under the dissecting microscope, fish was covered with wet tissue paper, the eye was pulled out and the optic nerve was cut with scissors very carefully to not destroy the blood vessel tissue.

2.2.2. Goldfish optic nerve tract preparation

10 to 15 days (d) after optic nerve transection, fish was sacrificed by overdose in 0.03% MS222 anaesthesia after more than 15 min. Fish brain was taken out of the head and put in petridish filled with L-15 medium. Under dissecting microscope, using fine tweezers and scissors the optic tract and the chiasm were separated from the eyes and the tectum opticum to be taken out of the brain (Figure 9) (Bastmeyer et al., 1991; 1993).

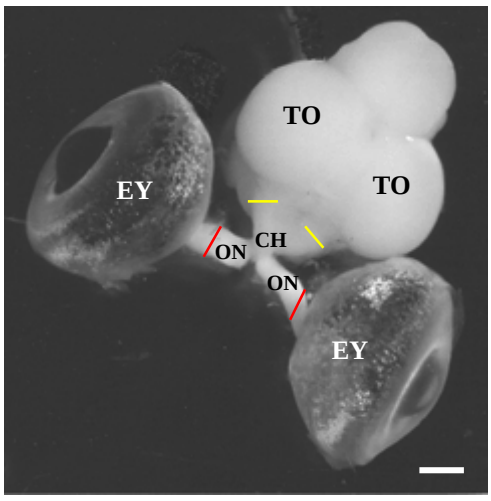

Fig 9. Isolation of the optic nerve tract from the goldfish visual system. The optic tract is a part of the visual system in the brain. It is a continuation of the optic nerve (ON) and runs from the optic chiasm (CH). Cuts are made by scissors to separate the CH from the tectum opticum (TO) (yellow lines), and the ON from the eyes (EY) (red lines). Scale bar; 1mm.

2.2.3. Fish retina preparation

Prior surgery, fish were dark-adapted for 1 hour (h), to facilitate removal of the pigment epithelium from the isolated retina. Then, fish was exposed to an overdose in MS222 anaesthesia as mentioned above. The preparation of the retina was done following a protocol published earlier by Vielmetter and Stuermer in 1989. In brief, under the dissecting microscope, the eyes were taken out in a petriedish filled with L-15 medium. Using tweezers, the eye was dissected by removing away all eye tissues including the cornea, the iris, the lens and the vitreous body. The retina was picked up in a fresh L-15 medium with a small spoon and attached to a black filter Hybond-N^+, in a sense where the photoreceptor layer is down stick to the filter and the RGC layer is facing up (Figure 14A). By flattening the retina, the blood vessel layer covering the retinal ganglion cell layer had to be removed by tweezers, in order to make the growth of axons possible from the retinal ganglion cells, in case the retina was used for the outgrowth assays. Moreover, prepared retinae were also used for expression studies.

2.3. Molecular biology methods

2.3.1. DNA cloning methods

2.3.1.1. DNA cloning in pCRII-TOPO vector

Different DNA sequences cited in table 1 were amplified from either ZF-cDNA library or from DNA plasmid constructs by polymerase chain reaction (PCR) (see methods 2.3.2.1) using primers designed either with or without specific restriction sites for enzymes recognition (Table 4). The PCR product was ligated into the lacZ gene of TOPO cloning vector following manufacturer's instructions of pCRII-TOPO cloning Kit (Figure 10). In brief, *E.coli* competent cells (TOP10 strain) were heat-shock transformed by the ligation products, then cells were spread on LB agar selective plates, containing 50µg/ml Kanamycin antibiotics, 40µl of 20mg/ml X-gal, and 40µl of 100mM IPTG, using blue/white selection to determine transformants. The vector including the insert was isolated from white colonies, DNA insertion was checked by colony PCR (see methods 2.3.2.2) from 2-3 positive colonies. After overnight (ON) culture of each colony in 5ml Kanamicin selective LB medium at 37°C and DNA plasmids were extracted by QIAprep Miniprep Kit from 1ml ON culture following manufacturer's instruction, analysed quantitatively by spectrophotometrie and qualitatively in 1% agarose gel electrophoresis and by DNA sequencing (see methods 2.3.4). TOPO-DNA

constructs (Figure 10) in TOP10 cells were stored as glycerol stock 1:1 (bacteria / 70% glycerol) at -80°C.

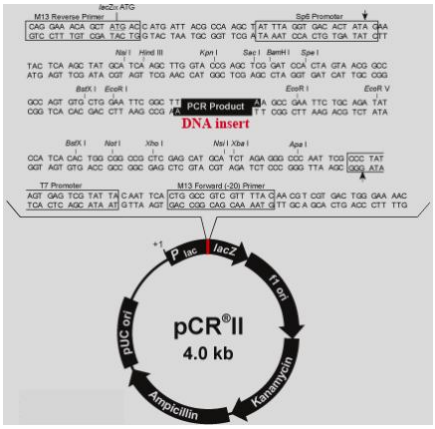

Invitrogene, Germany

Fig 10. DNA sequences cloning in pCRII-TOPO cloning vector. The scheme illustrates a map of pCRII-TOPO vector showing the LacZ gene, the site where the PCR product is inserted (red color).

Table 1. Summary of different DNA fragments cloned in pCRII-TOPO vector. PCR product sizes and the DNA sources are indicated. bp: base pair.

DNA sequence	Product size (bp)	Source
zf-rtn4-l	1.370	ZF-cDNA library
zf-rtn4-m	1057	ZF-cDNA library
zf-rtn4-n	988	ZF-cDNA library
zf-ngr	927	ZF-cDNA library
zf-ngrH1a	590	ZF-cDNA library
zf-ngrH2	390	ZF-cDNA library
zf-GAPDH	494	ZF-cDNA library
zf-ngr8LRR	558	ZF-cDNA library
zf-Nogo66	198	pGEX-zf-Nogo66 construct
rat-Nogo66	198	pGEX-rat-Nogo66 construct
rat-NIGΔ20	550	pEGFP-C1-rat-NogoA construct

2.3.1.2. DNA cloning in pEGFP-C1-ZF-PrP1-GPI vector

The ZF-Nogo66, Rat-Nogo66 and Rat-NIGΔ20 coding sequences were amplified by PCR (see methods 2.3.2.1) using specific primers containing enzymatic restriction site (Table 4) from pCRII-TOPO plasmid constructs and sub-cloned into pEGFP-C1-ZF-PrP1-GPI eukaryotic expression vector (Malaga-Trillo et al., 2009) (Table 2). Nogo DNA sequence was inserted upstream and in frame to the EGFP sequence (Enhancing green fluorescence protein) of the pEGFP-C1-ZF-PrP1-GPI vector in AgeI restriction site (Figure 11). Briefly, pCRII-

TOPO-Nogo plasmids and pEGFP-C1-ZF-PrP1-GPI vector were digested for 2 h at 37°C with a sticky-ends endonuclease AgeI. Following digestion, the vector was dephosphorilated with 1µl (10U/µl) CIAP (Calf Intestinal Alkaline Phosphatase) for 1 h at 37°C to avoid plasmid re-ligation. The digestion reaction mixture was prepared as following:

	pCRII-TOPO-Nogo insert	**Vector**
DNA	17µl (1µg)	8µl (~0.5µg)
AgeI enzyme (10U/µl)	1µl	1µl
AgeI Buffer	2µl	2µl
Distilled water dH_2O	-	To a final volume of 20µl

Once the DNA insert was purified from a 1% agarose gel using QIAquick Gel Extraction Kit and the digested vector was purified using QIAquick PCR purification Kit, they were quantitatively tested, and then the ligation reactions was performed to ligate the insert into the vector using T4 DNA ligase, for ON at RT as described in following reaction mixture:

Ligation reaction	
DNA insert	7µl (~0.5µg)
DNA vector	1µl (~0.2µg)
Ligase (1U/µl)	1µl
Ligation Buffer	1µl

5µl of ligation mixture was mixed to 25µl of *E.coli* competent cells (TOP10 strain) for Heat shock transformation at 42°C for 45 seconds (sec). Next, bacteria were grown in 250µl LB medium devoid from antibiotics for 1 h at 37°C using the shaker and then split on LB agar plates containing 50 µg/ml Kanamicin antibiotics for ON at 37°C. DNA insertion was checked by colony PCR (see methods 2.3.2.2) from 2-4 colonies using specific primers (Table 4). PCR Positive colonies were grown for ON culture in 5ml LB kanamicin selective medium for ON at 37°C. DNA plasmids were extracted, DNA was checked in agarose gel electrophoresis, the concentration was measured and the sequence checked by DNA sequencing (see methods 2.3.4). *E.coli* cells transformed with plasmids containing the gene of interest were stored at -80°C in 70% glycerol.

A

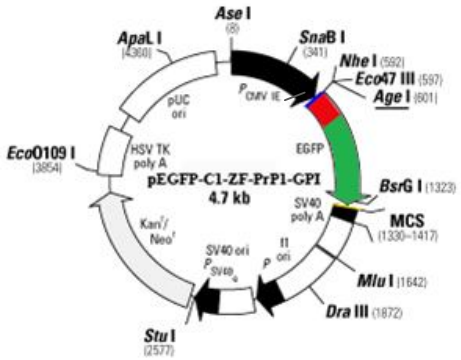

Invitrogene, Germany. Modified by H. Abdesselem

B

Fig 11. Nogo cloning in pEGFP-C1-ZF-PrP1-GPI vector. A. Restriction map of pNogo-EGFP-C1-ZF-PrP1-GPI vector. B. Diagram of the Nogo construct in pEGFP-C1-ZF-PrP1-GPI vector. DNA coding sequences of the ZF-Nogo66, Rat-Nogo66 and Rat-NIGΔ20 (red color in A and B) were inserted upstream to the EGFP sequence in AgeI restriction site (underlined restriction enzyme in A). CMV (CytoMegaloVirus) promoter, LS. Leader Sequence, EGFP. Enhanced green fluorescence protein, GPI. Glycophosphatidylinositol.

Table 2. Summary of different DNA fragments cloned in pEGFP-C1-ZF-PrP1-GPI vector. PCR product sizes and the DNA sources are indicated. bp: base pair.

DNA sequence	Product size (bp)	Source
zf-Nogo66	198	TOPO-zf-Nogo66 construct
rat-Nogo66	198	TOPO-rat-Nogo66 construct
rat-NIGΔ20	550	TOPO-rat-NIGΔ20 construct

2.3.1.3. DNA cloning in pGEX-KG vector

The zf-ngr-8LRR coding sequences was amplified by PCR (see methods 2.3.2.1)from pCRII-TOPO construct plasmids using specific primers with enzymatic restriction site sequences (Table 4) and subcloned into pGEX-KG procaryotic expression vector (Figure 12, Table 3). Nogo DNA sequence was inserted downstream and in frame to the GST (Gluthatione-S-Transferase) sequence of the pGEX-KG vector, between BamH1 and EcoR1 restriction sites. Briefly, pCRII-TOPO-Nogo construct plasmid and pGEX-KG vector were digested for 4h at 37°C with BamHI and EcoRI endonucleases. Following digestion, the vector was dephosphorilated with 1µl (10U/µl) CIAP for 1 h at 37°C. The digestion reaction mixture was prepared as following:

	pCRII-TOPO-Nogo insert	Vector
DNA	25µl (2µg)	8µl (~0.5µg)
BamHI enzyme (10U/µl)	1µl	1µl
EcoRI enzyme (10U/µl)	1µl	1µl
Common buffer for EcoRI and BamHI	3µl	2µl
Distilled water dH_2O	-	To a final volume of 20µl

After DNA purification of both insert and digested vector, ligation reaction was performed between the insert and the vector using T4 DNA ligase for ON at RT as described in following reaction mixture:

Ligation reaction	
DNA insert	5µl (~0.5µg)
DNA vector	3µl (~0.4µg)
Ligase (1U/µl)	1µl
Ligation Buffer	1µl

E.coli competent cells (BL21 codon$^+$ strain) were transformed with 5µl of ligation mixture by Heat shock at 42°C for 45 sec. Next, bacteria were grown in 250µl LB medium without antibiotics for 1 h at 37°C with shaking and then split on LB agar plates containing (100µg/ml) Ampicilin and (34µg/ml) Chloranphenicol antibiotics for ON at 37°C. DNA insertion was checked by colony PCR (see methods 2.3.2.2) from 2 colonies using specific primers (Table 4 and 5). PCR Positive colonies were grown for ON culture in 5 ml LB selective medium at 37°C. DNA plasmids were extracted and checked in 1% agarose gel, the concentration was measured and the sequence analysed by DNA sequencing (see methods 2.3.4). *E.coli* cells transformed with plasmids containing the gene of interest were stored at -80°C in 70% glycerol.

Table 3. DNA fragment cloned in pGEX-KG vector. PCR product size and the DNA source are indicated. bp: base pair.

DNA sequence	Product size (bp)	Source
zf-ngr8LRR	556	TOPO-zf-ngr8LRR construct

Fig 12. Diagrams for pGEX-KG construct plasmid encoding GST-ZF-NgR8LRR under Tac promoter.

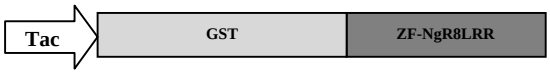

2.3.2. Polymerase chain reaction (PCR)

PCR reaction was performed using Red Taq DNA polymerase. The standard reaction was prepared as following:

2.3.2.1. PCR reaction using cDNA or DNA constructs

Template DNA	1µl
Primer (reverse and forward) (10pmol/µl)	0.6µl from each
dNTPs mixture (10mM)	1µl
10x Taq buffer	2µl
Red TaqPolymerase (5U/µl)	0.5 µl
Distilled water dH_2O	To a final volume of 20µl

2.3.2.2. Colony-PCR

A small amount of a bacteria colony including the plasmid to be tested	
Primer (reverse and forward) 10pmol/µl	0.6µl from each
dNTPs mixture (10mM)	1µl
10x Taq polymerase buffer	2µl
Red Taq DNA Polymerase (5U/µl)	0.5µl
Distilled water (dH_2O)	To a final volume of 20µl

2.3.2.3. Thermocycler PCR conditions

1. Denaturating step	1 min /94°C
2. Annealing step	1 min/ 50°C, 55°C, 60°C or 65°C depending on the primers used.
3. Elongation	1 min/72°C
Step 1 – 3 were repeated 30 times	

2.3.3. Oligonucleotides

Oligonucleotides were designed then purchased from Operon (Germany) to be used for PCR, colony PCR and sequencing. Specific restriction sequences for enzyme recognition were added to allow ligation into corresponding vector sites (Table 4 and 5).

Table 4. Overview of primers used for PCR, colony PCR and sequencing. Restriction sites are highlighted in bold. Small types (CC or CG) are bases added to prevent the loss of restriction sites during oligosynthesis. Fw: forward, Rv: reverse.

	Forward primer		Reverse primer		
DNA sequence	**Name**	**Sequence**	**Name**	**Sequence**	**Restriction enzyme**
zf-rtn4-l	Zfcontig2 sens	5'-ATGGATGATCAAATAAGCTC-3'	ZFnogo seqanti2	5'-GGCCATTTGGATTCATTTC-3'	-
zf-rtn4-m	ZfNogo RTsens4	5'-CCTGACTGGATATATGACC-3'	ZFnogo seqanti2	5'-GGCCATTTGGATTCATTTC-3'	-
zf-rtn4-n	ZfNogo	5'-ATGAGCGAGATGGATTCC-	ZFnogo seqanti2	5'-GGCCATTTGGATTCATTTC-3'	-

	RTsens5	3’			
zf-ngr	Nogo Rsens3	5’-ATGAAGACCTTAATCGTGGAG-3’	NogoR anti1	5’-GCAACCTTCCAAATCATCGCTTTTG-3’	-
zf-ngrH1a	Nogo R3sens2	5’-ACGCGGAGCCAACGCAGCTC-3’	NogoR3 antisens2	5’-TGACGCACCCTGTTGTCATG-3’	-
zf-ngrH2	Nogo R2seb	5’-AACCTGACTGGACAGACAG-3’	NogoR2as3	5’-TTTCTGCAGACAGCGATC-3’	-
zf-GAPDH	Fw GAPDH1	5’-CGTGGCCATCAATGACCCATTC-3’	RevGAPDH1	5’-GCTTCCCAGAGGGCCCATC-3’	-
zf-ngr8LRR	NgR8LR R-Fw	5’CG**GGATCC**CTCCAGAGCAACAAACTGACAGTG-3’	NgR8LR R-Rev	5’CG**GAATTC**CAGAGGGTTCATGGACTCTCCGGT-3’	BanHI-EcoRI
zf-Nogo66	FwZN66 AgeI	5’CC**ACCGGT**GAGGATATACAAAGGCATTTTA-3’	RvZN66-AgeI	5’CC**ACCGGT**GGCTTGAGCGAGTCCACCAGATC-3’	AgEI
rat-Nogo66	FwR66 AgeI	5’CC**ACCGGT**GAGGATATATAAGGGCGTGATC-3’	RvR66-AgeI	5’CC**ACCGGT**GGCTTCAGGGAATCAACTAA-3’	AgEI
rat-NIGΔ20	FwΔ20 AgeI	5’CC**ACCGGT**GACAGGTACAAAGATTGCTTAT-3’	RvΔ20AgeI	5’CC**ACCGGT**AAGTCAACTGGTTCAGATTC-3’	AgEI
pEGFP-C1-PrPGPI	FwLeader 5’NheI	5’GCTAGCATGGGGGAGTTA-3’	-	-	-

Table 5. General primers. Primers were provided from the manufacture where corresponding vectors were obtained or purchased. Fw: forward, Rv: reverse

Name	Vector	Sequence
FwM13	pCRII-TOPO	5’-GTAAAACGACGGCCAG-3’
RvM13	pCRII-TOPO	5’-GTCATAGCTGTTTCCTG-3’
Fw-pEGFP	pEGFP-C1	5’-GTGGATAACCGTATTACCGC-3’
Rv- pEGFPCMV	pEGFP-C1	5’-GGCTATGAACTAATGACCCCG-3’

2.3.4. DNA sequencing

1µg Purified DNA plasmid (~100µg/ml) was sent for sequencing to either SeqLab or GATC Biothech companies (Germany) accompanied with the primers (Table 4 and 5). Sequences were analysed by alignment with the online published sequences from pubmed (http://www. ncbi.nlm. nih.gov/pubmed) using Blast nucleotide alignment (Bl2seq) from NCBI (http: //blast.ncbi.nlm.nih.gov/Blast.cgi). Sequences were confirmed and further analysed using EditSeq sequence analysis software (DNA*, USA).

2.3.5. Total RNA (tRNA) extraction

2.3.5.1. tRNA extraction from tissue

Fish retina and optic nerve tissues were homogenized at 1:9 ratio of PeqGold TriFast reagent, incubated 5 min at room temperature (RT), then treated with Chloroform at 1:4 ratio (Chloroform / TriFast), shacked by hand briefly and incubated for 3 min until the two phases

are clear. The samples were spun down at 4°C at max speed for 15 min, the aqueous phase (upper) was transferred in a fresh eppendorf tube. 500µl Isopropanol/1ml TriFast was added for 10 min incubation at RT, then, after 15 min centrifugation at maximum speed, the pellet (extracted RNA) was washed with ethanol 75% at 1:1 ratio (Ethanol /TriFast), air dried and dissolved in RNAase free sterile water. RNA quantity was checked in 1% agarose gel electrophoresis and the RNA concentration measured by spectrophotometer. Extracted tRNAs were stored at -80°C.

2.3.5.2. tRNA extraction from animal cells

Cultured fish oligodendrocytes were scraped manually from the coverslips using a cell scrapper, collected in medium and transferred in a fresh eppendorf tube. Number of cells was measured using counting chamber. Around 1-3x10^6 cells were harvested with a short centrifugation at 1000 rpm in RT and tRNA was extracted from cell pellet using the RNeasy Mini Prep Kit following manufacturer's instructions. The RNA quality was checked in agarose gel electrophoresis and the RNA concentration was measured. Extracted tRNAs were stored at -80°C.

2.3.6. First strand cDNA synthesis and reverse transcriptase polymerase chain reaction analysis (RT-PCR)

zf-rtn4 gene expression was analysed in both ZF intact and lesioned optic nerve between 2 and 10 d after nerve transection as well as in goldfish cultured oligodendrocytes. Additionally, the zf-ngr, zf-ngrH1a and zf-ngrH2 genes expression were analysed in both intact and regenerating ZF retina. tRNAs were reverse transcribed into first-strand cDNA by using the SuperScript II RT (Reverse Transcriptase) system under standard conditions. Briefly, a 10µl RNA/primer mixture containing 5µg of total RNA, 0.5µg/µl oligo (dT) primer, 10mM dNTP mix was incubated at 65°C for 5 min to linearise the RNAs. Then, 50U Supertranscript II, 10x RT buffer, 25mM $MgCl_2$, 0.1M DTT and 1µl RNAaseOUT™ (RNAase Inhibitor) were added to the reaction, gently mixed and incubated at 42°C for 50 min. After the transcription reaction is finished, the temperature was raised up to 70°C during 15 min to inactivate the RT enzyme. Next, the reaction was chilled on ice and treated with 1µl RNaseH for 20 min at 37°C to degrade all non reverse transcribed RNAs. Finally, ZF retina, optic nerve tissues and glial cells cDNA libraries were established and stored at -80°C. Zero transcripts (without RT Supertranscript II in the reaction) were performed in parallel to control for genomic DNA contamination in subsequent PCR (see methods 2.3.2.1). zf-rtn4-l,

zf-ngr, zf-ngrH1a, zf-ngrH2 and GAPDH gene transcripts were detected with gene-specific primers targeting coding sequences across introns (Table 4) (Klinger et al., 2004; Diekmann, et al., 2005, Abdesselem et al., in revision) to exclude genomic contamination, therefore, PCR product sizes have to correspond exclusively to cDNA. The quality and the amount of different cDNA samples were controlled by comparison with the expression level of the housekeeping gene GAPDH (Glyceraldehyde-3-phosphate dehydrogenase).

2.4. Biochemical methods

2.4.1. Tissue protein extraction

Total proteins were isolated from adult ZF brain tissue. In brief, tissue was homogenised in lysis buffer at 15µl/mg tissue using glass-douncer. The lysis buffer contained 50mM Tris/HCl pH 7.4, 300mM NaCl, 5mM Triton X-100, 0.1mM SDS and protease inhibitor cocktail (1tablet/10ml). After 10 min incubation of the homogenate on ice, followed by 10 min centrifugation at 14.000 rpm and 4°C, the supernatant consisting protein lysate was collected, aliquoted, and then kept at -20°C.

2.4.2. Expression and purification of recombinant proteins

2.4.2.1. Expression of recombinant proteins

A small quantity (~20µl) of -80°C frozen glycerol stock bacteria containing the plasmids encoding His-Rat-NIGΔ20-His, His-Rat-Nogo66-His, GST-Rat-Nogo66, GST-ZF-Nogo66, GST-Rat-NIGΔ20 and pGEX-KG empty vector was inoculated in 50ml LB medium mixed with appropriate antibiotics for ON at 37°C under shaking. Bacteria ON culture was used to inoculate 450ml pre-warmed LB medium with antibiotics until OD_{600} of 0.5–0.7 was reached. At this point, the cells are induced by 1mM IPTG to express the fusion proteins for 1 h at 37°C for GST and GST-Rat-NIGΔ20, 4 h at 37°C for GST-Rat-Nogo66, GST-ZF-Nogo66, 2 h at 37°C for His-Rat-Nogo66-His and 2 h at 30°C for His-Rat-NIGΔ20-His.

2.4.2.2. Extraction and purification of GST recombinant proteins

GST-Rat-NIGΔ20 fusion protein and GST alone were extracted under native conditions, while, GST-Rat-Nogo66 and GST-ZF-Nogo66 fusion proteins were extracted under denaturing conditions. 250ml bacterial cells (BL21 $codon^+$ strain) expressing the fusion protein were harvested for 10 min at 14.000 rpm speed and 4°C. The pellet was resuspended in 20ml PBS lysis buffer supplemented with 1mM EDTA, 2mM DTT and 1mg/ml lysozyme pH 7.4. The cell lysate was incubated on ice for 20 min and sonicated five times 10 sec at

30% outputs and then centrifuged for 30 min at 14.000 rpm and 4°C. In case of the GST and GST-Rat-NIGΔ20 extraction, the supernatant containing the soluble proteins was kept on ice and used for protein purification in column. For the insoluble GST-Rat-Nogo66 and GST-ZF-Nogo66 proteins, the pellet was resuspended in 3ml PBS denaturing buffer supplemented with 8M urea, 1mM EDTA, and 2mM DTT, then sonicated four times 15 sec and centrifuged for 30 min at 14.000 rpm and 4°C. The supernatant was diluted 10 times in PBS refolding buffer supplemented with 1mM EDTA, 2mM DTT and 1%Triton X100 for proteins refolding. Then, after 30 min centrifugation at maximum speed in 4°C, the supernatant was collected for protein purification in column using Glutathione-Sepharose 4B beads. In brief, proteins in the supernatant were bound to 400µl glutathione-sepharose beads at 4°C for ON under gentle agitation or rotation. Using poly-prep chromatography columns, GST fusion proteins bound to the beads were five times washed with 10ml PBS to remove away all unbound proteins. As a last step, 300µl of PBS elution buffer supplemented with 50mM Tris pH 8.0 and 10mM reduced Glutathione was added to the beads and incubated for 10 min, then the proteins were eluted and stored at 4°C. Protein concentrations were determined by Bradford assay using 1mg/ml BSA for the standard curve, following manufacturer's instruction.

2.4.2.3. Extraction and purification of His_6-tagged proteins

His-Rat-NIGΔ20-His and His-Rat-Nogo66-His fusion proteins were extracted under native conditions using column and batch purification, respectively. 200ml bacterial cell culture (BL21 strain) was harvested; the pellet was resuspended with 15ml B-PER Bactrial protein extraction reagent, and sonicated four times 15 sec at 30% outputs. After 30 min centrifugation at 14.000 rpm and 4°C the supernatant was vacuum-filtered. The His-Rat-NIGΔ20-His was then purified in Ni-NTA spin column. In brief, filtrated supernatant was flow through the His trap columns to bind the His-tagged proteins. After washing tree times with PBS buffer supplemented with 50mM NaH_2PO_4, 300mM NaCl and 20mM Imidazol pH 8.0, His_6-tagged proteins were eluted with PBS buffer supplemented with 50mM NaH_2PO_4, 300mM NaCl and 250mM Imidazol pH 8.0, collected, aliquoted and stored at -20°C. The His-Rat-Nogo66-His was purified in batch using Ni-NTA agarose. The supernatant was filtered and applied to 500µl Ni-NTA agarose, to bind the His-tagged proteins to the agarose for 2 h under the rotator shaker. The resin was washed five times with 2ml wash buffer. Proteins were eluted twice with 250µl of PBS elution buffer, and then aliquoted and stored at -20°C. Protein concentration was determined by Bradford assay.

2.4.3. Proteins concentration

Purified GST and His tagged proteins at low quantity were concentrated using microcon centrifugal filters following manufacturer's instruction.

2.4.4. SDS-PAGE

An SDS-PAGE was performed to analyze the purity of eluted proteins. In brief, 3µl from 6x denaturing simple buffer (0.3% Bromophenol blue, 10% β 2-Mercaptoehanol, 10% SDS, 40% Glycerol and 1M Tris-HCl pH 6.8) was added to 10 µl eluted proteins, the mixture was boiled at 95°C for 5 min. Then samples were loaded in SDS gel and separated for 1 h at 120 volts. The SDS-PAGE was conducted with a 12% or 10% resolving gel according to the protein molecular weight (MW) and a 5% stacking gel (Table 6) by using Lammli electrode buffer pH 8.3 (0.25M Tris base, 2M Glycine and 1% SDS). A 5µl of protein standard markers (Fermentas and Bio-RAD, Germany) was used to determine the relative MW for the samples.

Table 6. SDS resolving and stacking gel compositions:

	Resolving gel		Stacking gel
	10%	12%	15%
Bidest H_2O	4 ml	3.3ml	4.1ml
Acrylamide 30	3.3ml	4ml	1ml
Resolving gel mix (1.5M Tris pH 8.8, 10% SDS)	2.6 ml	2.6 ml	-
Stacking gel mix (1M Tris pH 6.8, 10% SDS)	-	-	0.81ml
10% APS	0.1ml	0.1ml	0.06ml
TEMED	0.01ml	0.01ml	0.01ml

2.4.5. Coomassie staining

For protein staining with coomassie violet R150, SDS-gel was imbibed in the coomassie solution (0.1% Coomassie, 40% Methanol and 10% Acetic acid) to be fixed and stained for 10-30 min at RT on a shaker, followed by distaining solution (25% Methanol and 5% Acetic acid) for ON in order to visualize proteins bands.

2.4.6. Western Blot and immunodetection

Once the proteins are separated by SDS-PAGE, they were electrotansfered from the gel into a support membrane nitrocellulose using the corresponding blot buffer (20mM Tris base, 150mM Glycine and 25% Methanol in distilled H_2O). To control the efficiency of the blotting, the membrane was incubated with ponceau S dye for 5 min and then washed with

TBST buffer pH 7.6 (20mM Tris base, 136mM NaCl, 0.1% Tween-20). Prior to ABs incubation, the membrane was incubated in blocking solution of 3% Non-fat dry milk powder in TBST for 30 min at RT, in order to block the unspecific binding of ABs. Then, the membrane was incubated with primary ABs diluted in TBST solution for 2 h at RT or ON at 4°C. After three wash steps using TBST buffer, the membrane was incubated for 1 h and 30 min with the secondary ABs conjugated with the horseradish peroxidase (HRP) to allow a chemiluminescence detection of the antibody after incubation of the membrane with a solution containing liminol using ECL Kit for 1 min. This solution reacts with the horseradish peroxidase and emits chemiluminiscence that can be detected using an autoradiography Amersham Hyperfilm.

2.4.7. Generation of polyclonal antibodies against ZF-NgR receptor

A small peptide comprising amino acids 121-137, LDLSDNPSLRRLDGGA, from the N-terminal LRR (Leucine Reach Repeat) region of ZF-NgRH1b was selected as antigen to generate polyclonal ABs against ZF-NgRs. The peptide share 56% identity with the homolog Rat-NgR1-7E11 peptide (Figure 13), a highly antigenic peptide and known to be involved in neurite outgrowth inhibition by binding to myelin inhibitors (Li et al., 2004). ZF peptide was synthesised and conjugated with a carrier protein Diphtheria Toxoid, then, delivered soluble within 95% purity (Mimotopes, Australia). For rabbit immunisation, 0.1mg antigen solution was injected to the rabbit to produce ABs against ZF-NgRs receptors in the TFA of the University of Konstanz. Four successive immunisations have been done with an interval of two weeks. One week after the second immunisation, the first serum was collected and tested biochemically for ABs production and specificity. The 2nd and 3rd serums were tested one week after the 3rd and 4th immunisation, respectively. 1 ml prae-immune serum was collected prior immunisation in order to control the specificity of the ABs.

```
Rat-NgR1      LDLS DNAQLRVVDPTT
ZF-NgRH1b     LDLS DNPSLRRLDGGA
ZF-NgRH1a     LDLGDNPNLHRLEGGA
ZF-NgRH2      LDLGDNRYLRSLSA ET
ZF-NgR        LDI GDNSNLRI I P S TA
```

Fig 13. Peptide sequences alignment between Rat-NgR1-7E11 epitope and its four ZF homologous sequences. The 7E11 Rat-NgR1 sequence is 56% identical (yellow highlight) with ZF-NgRH1b. The ZF-NgRH1b is 75% identical with ZF-NgRH1a and 50% with ZF-NgRH2 and ZF-NgR.

2.5. Expression and localization studies

2.5.1. Immunocytochemistry

2.5.1.1. Live immunostaining

Fish RGC axons, fish oligodendrocytes and HeLa (Henrietta Lacks) cells in culture were live stained for surface expressed proteins. Briefly, cells were grown on cover slips coated poly-lysine (plus Laminin for oligodendrocytes). The culture medium was removed and cells were washed two time 5 min at RT with L-15 (for fish axons and oligodendrocytes) or PBS (for HeLa cells) supplemented with 1% BSA and then blocked for 15 min in the same buffer. Cells were then incubated with primary ABs in L-15 or PBS as mentioned above, for 1 h at RT. Next, the cells were washed three times and fixed in 4% PFA for 15 min at RT. After fixation, cells were washed in PBS and then incubated with Cy3- or Alexa-488-conjugated secondary ABs, diluted in PBS, for 1 h and 30 min at RT, followed by a strong wash with PBS of five times 5 min. Cells were mounted on slides within a drop of mowiol on the cells and a fresh glass coverslip on the top to be analysed under fluorescence microscopy.

2.5.1.2. Fix immunostaining

Fish axons and oligodendrocytes in culture were fix stained for intracellular or surface proteins. In brief, cells were washed three times 5 min with PBS and fixed with 4% PFA for 15 min at RT, and then again washed in PBS. For staining of intracellular proteins, cells were permeabilized with 0.1% Triton X-100 in PBS for 1 min and then rinsed with PBS. Thereafter, cells were blocked in PBS supplemented with 1% BSA for 15 min at RT and then incubated with primary ABs for 2 h at room temperature or ON at 4°C. Next, the cells were washed three times in PBS before incubation with secondary ABs conjugated with Cy3- or green Alexa-488 for 1 h and 30 min at RT. Following a strong wash with PBS of 5-6 times for 5 min, cells were mounted as described above in 2.5.1.1.

2.5.2. Whole-mount *in situ* hybridization (ISH)

The rtn-4 gene splice forms (Rtn4-l, -m and -n) sequences were amplified by PCR from ZF cDNA library and cloned into pCRII-TOPO vector. Labelled sense and antisense RNAs probes, specific for each Rtn-4 isoform were *in vitro* synthesized using DIG RNA Labeling Kit. First, 1µg of plasmid DNA were linearised by HindIII/NotI restriction enzymes to generate riboprobes sense/antisense of Rtn4-l, -m and -n, respectively for 2 h at 37°C. The enzyme cuts the plasmid DNA once at the flank of the insert opposite to the flank where the transcriptional promoter is located, so that the RNA polymerase falls off after transcribing the

insert. The quantity of the linearised DNA was checked in agarose gel. Samples were precipitated with 3M NaOAc mixed to 2 volume 100% ethanol at -20°C for 30 min, then centrifuged at maximum speed for 15 min and washed with 70% ethanol. Precipitated DNAs were air dried, and then resuspended in DEPC-H_2O at RT. Linearised DNAs were *in vitro* transcribed with RNA polymerase enzymes T7/SP6 to generate sense/antisense riboprobes of Rtn4-l, -m and -n. The transcription reaction contained RNA polymerase, transcription buffer, RNAase inhibitor and NTP labelling mix with Digoxigenin (DIG) to label RNA riboprobes. The transcription reaction was carried out for 2 h at 37°C. Then, RNA probes were treated with DNaseI enzyme to degrade the untranscribed DNA. RNAs solutions were filtrated using Vivaspin 0.5 centrifugal filter to remove salts and non-incorporated ribonucleotides, then treated with RNAase inhibitor, aliquoted and kept at -80°C. *In situ* hybridization experiments were performed by the following protocol:

2.5.2.1. ZF embryo whole-mount *in situ* hybridization

Fixed ZF embryos were permeabilized by treating them with 10µg/ml proteinase K in PBST (0.1% Tween-20) at RT for time ranging from 1 to 10 min depending on the age: 1 min for 2-4 somites embryos, 3 min for 9-13 somites embryos, 5 min for 18-24 hpf embryos and 10 min for 48 hpf and older embryos. After wash and fixation in 4% PFA for ON at 4°C, embryos were transferred in hybridization buffer (Hyb-buffer) pH 6.0 composed of 50% deionized Formamide, 5x SSC (saline-sodium citrate), 50µg/µl Heparin, 500µg/µl tRNA, 0.1% Tween-20 and 9mM Citric acid for 1h at 65°C in a block incubator as a prehybridization step. 100ng of riboprobes were pre-warmed in Hyb-buffer for 10 min at 65°C and then added to the embryos for hybridization step during ON at 65°C. The day after, embryos were washed twice in Hyb-buffer at 65°C and then in PBST at RT. RNAs probes hybridized to the endogenous mRNAs were detected by ABs anti-digoxigenin conjugated with alkaline phosphatase. After incubation of embryos with 1:2000 dilution antibodies Anti-dig-AP for 2 h at RT under gentle agitation, embryos were equilibrated in BCL buffer (0.1M Tris-HCl pH 9.5, 50mM $MgCl_2$, 100mM NaCl and 0.1% Tween-20) and then the color solution containing (4.5µl NTB and 3.5µl BCIP/X-phophate per ml of BCL buffer) was applied to the embryos in dark at RT, until a blue reaction product is visible, then the color reaction can be stopped by washing the embryos with an excess of distilled H_2O. Blue stained embryos are cleared with 100% ethanol then with sequential ethanol dilutions in PBST (70%, 50% and 30%) in order to accentuate the blue color and remove background staining. Finally embryos were washed in PBST, fixed with 4% PFA and mounted in glasses with glycerol.

Specificity of the antisense probes was verified by running controls experiments with sense probes.

2.5.2.2. ZF retina whole-mount *in situ* hybridization

ZF retinae were socked on the black filter as a support to keep the retina flattened (Figure 14), then fixed with 4% PFA for ON at 4°C in multiwell dishes. After washing in PBST, retinae were transferred in methanol for tissue delipidation for 5 min at RT then cooled down in -20°C for 30 min or up to several mounts storage. Retinae were brought back to RT and incubated for 5 min in sequential methanol dilutions in PBST (70%, 50% and 30%) at RT, then rinsed in PBST. They were again fixed in 4% PFA, rinsed in PBST and then permeabilized with 10µg/ml proteinase K in DEPC-PBST at RT for 10 min. After washing and fixation in PFA, retinae were transferred in Hyb-buffer for 4 h at 55°C in a water bath as a prehybridization step. 100ng of riboprobes were pre-warmed in Hyb-buffer for 10 min at 55°C and then added to the embryos for hybridization for ON at 55°C. The day after, embryos were washed twice in Hyb-buffer at 55°C and then transferred in PBST at RT. RNAs probes hybridized to the endogenous mRNAs were detected by ABs anti-digoxigenin conjugated with alkaline phosphatase. After incubation with 1:500 dilution antibodies Anti-dig-AP for 2 h at RT under gentle agitation, retinae were equilibrated in BCL buffer and then the color solution was applied. The rest of the steps including the mounting are the same as mentioned above in 2.5.2.2.

2.6. Cell biology methods

2.6.1. Cell and tissue culture

2.6.1.1. Fish retinal mini-explants tissue culture

Goldfish and ZF retinae were respectively prepared 10-15 d and 4-9 d after optic nerve transection (conditions for the RGCs to regenerate their axons (Landreth and Agranoff, 1979)) in L-15 medium following the protocol described in methods 2.2.3 (Vielmetter and Stuermer, 1989). Retinae were then transferred from the black filter to the teflon plate and shopped in 200 x 200µm squares mini-explants with tissue shopper (Figure 14A and B). Mini-explants collected in complete F12 medium (F12 supplemented with 1% fetal calf serum (FCS), 0.4% methyl cellulose, 0.04% chicken serum (ChS), 2mM L-glutamine, 25mM Hepes pH 7.4 and antibiotics (10µg/ml streptomycin and 10U/ml penicillin)) were plated on poly-lysine coated coverslips. Attached mini-explants to the coverslip start to grow out RGC

axons after 12-18 h of culture (Figure 14B). The culture was incubated at 23°C for goldfish and 28°C for ZF, under humid conditions.

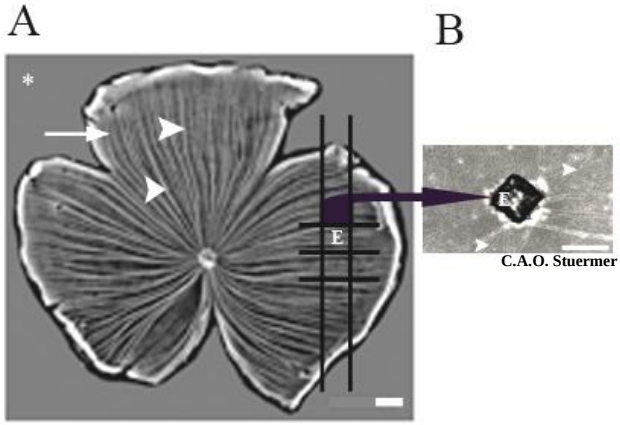

Fig 14. Fish retinal mini-explants preparation. A) Fish retina flattened on black filter (white star), the white arrow shows the RGC layer and white arrowheads show RGC axon bundles. B) Mini-explant (E) in culture with growing axons (white arrowhead in B). Scale bar; 200µm.

2.5.1.2. Goldfish oligodendrocytes culture

Oligodendrocytes were obtained from the goldfish regenerating optic nerve tract according to protocols published earlier (Bastmeyer et al., 1991; 1993). In brief, small pieces of the optic nerve tract (2 weeks after optic nerve transection, conditions for glial cells to become highly proliferative) were obtained by dissociating the tissue mechanically with tweezers in L-15 medium. Then, enzymatically to generate single cells by treating tissue pieces with 3mg/ml Collagenase and 10mg/ml Dispase for 20 min at 37°C within a gentle vortex after each 5 min. Dissociated pieces of tissue were explanted onto poly-lysine/laminin-coated coverslips prepared as follow: 14mm of diameter round coverslips coated with 4mg/ml poly-lysine diluted in PBS 1:20 for 1 h, washed in milliQ water, air-dried and then coated with 1mg/ml laminin diluted in PBS 1:50 for 1 h. Glial tissue culture were kept in complete F12 medium at 23°C. The medium was changed twice a week and the culture was kept humid. After 2-3 weeks the cells reached a confluence of 50–90%.

2.5.1.3. HeLa cell line culture

HeLa cells were cultured in 75cm^2 flasks in complete MEM medium (MEM supplemented with 10% FCS and 1% penicillin/streptomycin) at 37°C and 5% CO_2. Cells were split regularly three times a week as following: after removing the medium and washing the cells with PBS, 0.05% trypsin was added to the cells for 5 min incubation, in order to detach the cells from the surface. Then, 8ml fresh medium was added to resuspend the cells, and then cells were collected in 15ml falcon tube. After 5 min centrifugation at 800 rpm, the pellet was

resuspended in 6 ml fresh medium and then 1ml of cells was mixed to 15ml fresh medium in a new flask.

2.6.2. DNA transfection of cells

2.6.2.1. Primary oligodendrocytes transfection

Goldfish oligodendrocytes cultures, around two weeks older within a confluence of 50-70% corresponding to (2-4 x 10^5 cells) were selected for the transfection. DNA transfection was performed using Effectene Transfection Reagent kit. In brief, for transfection of one oligodendrocytes culture, 4µg of purified DNA plasmids encoding the Rat-NIGΔ20-EGFP-GPI peptide or EGFP-GPI peptide was added to 160µl of DNA condensation buffer (EC), after a short vortex, the mixture was incubated for 5 min at RT. Then, 30 µl of Enhancer reagent was added to the DNA-mixture, and incubated for 10 min at RT in order to condensate the DNA. 30 µl Effectene reagent was then added to the mixture for 10 min at RT, to form micelles structures. Effectene-DNA complexes were mixed to complete F12 medium to a final volume of 1ml and then directly added to the cells. Cells were incubated for 48-72 h with DNA-transfection reagents at 23°C, for both cell transfection and overexpression of the recombinant protein. Afterwards, the medium containing the transfection reagents was replaced with a fresh complete F12 medium and cells expressing Rat-NIGΔ20-tagged EGFP proteins were analysed under fluorescent microscopy.

2.6.2.2. HeLa cell line transfection

DNA plasmids encoding the Rat-NIGΔ20-EGFP-GPI, Rat-Nogo66-EGFP-GPI and ZF-Nogo66-EGFP-GPI fusion peptides were transfected into HeLa cells using Fugene Transfection Reagent as described previously (Schrock et al., 2009). In brief, 1.5µg DNA plasmid was mixed to 100µl MEM medium without serum and 4µl Fugene reagent. The mixture was incubated for 15 min at RT and then added to the cells. Cells were incubated for 5 h in transfection mixture contained in 1ml complete MEM medium. Then, the medium was replaced with a fresh medium and cells were incubated ON for the overexpression of the recombinant proteins. GFP-expressing cells were analysed under fluorescent microscopy.

2.7. Functional neurobiology assays

2.7.1. Quantitative axon outgrowth assay

Square coverslips 18x18 mm were first coated with 4 mg/ml poly-lysine diluted to 1:20 in PBS for 1 h, rinsed in milliQ water and air-dried. Then, fresh purified proteins GST-ZF-

Nogo66, GST-Rat-Nogo66, GST-Rat-NIGΔ20 and GST alone kept in 4°C up to 1 week were applied at a concentration of 50µM to poly-lysine-coated coverslips for ON at 4°C under humid conditions, and rinsed prior to use (three times with cold L-15 medium). For the His-tagged proteins Rat-Nogo66 and Rat-NIGΔ20, 3µg/µl protein concentration was used for the coating. Isolated goldfish retinae as well as ZF retinae were prepared 10-15 d and 4-9 d, respectively, after optic nerve lesion and divided into 200 x 200µm pieces with a tissue chopper. Ten mini-explants were plated on each coverslip and incubated at 28°C in complete F12 medium. After 24 h, either the number of axons growing from the retina mini-explants or the number of mini-explants with growing axons were determined in an inverted microscope Axiovert 200M under phase contrast. Student's *t*-test and OriginLab pro 7.5 were used for statistical analysis.

2.7.2. Quantitative axon outgrowth assay using enzymatic PIPLC treatment

A same axon outgrowth assay was performed as described above in 2.7.1, but with treating the growing axons with 0.5U/ml PIPLC enzyme (Phosphatidylinositol Phospholipase C). In brief, the enzyme was mixed to the medium used for fish RGC axon outgrowth in order to cleave off all GPI-anchor proteins exposed on the surface of RGC axons and then quantify after 24 h of culture the number of growing axons on the different Nogo substrates. Experiments were performed side by side with control experiment without enzymatic treatment. The activity of the enzyme was controlled by immunostaining of the PIPLC-treated axons after 24h with antibodies against the GPI–anchored protein Thy1.

2.7.3. Axon collapse assay with soluble ZF-Nogo66, Rat-Nogo66 or Rat-NIGΔ20

ZF RGC axons from retina mini-explants were cultured on poly-lysine-coated coverslips in lumox petridishes for 24 h at 28°C. Femtotips of 0.5µm tip diameter connected to a microinjector were loaded with either 100µM of GST-ZF-Nogo66, GST-Rat-Nogo66, GST-Rat-NIGΔ20 or GST alone in elution buffer along with 1:20 phenol red. The tips were positioned at a distance of 50µm or 50-100µm, from the individual growth cone by a micromanipulator (Inject Man NI 2) under phase contrast. Each peptide was delivered continuously to the growth cone under injection pressure (Pi) of 115 hPa (hecto-pascal). Time-lapse images were captured at 1 min intervals with the AxioCam MRm camera using Axio Vision Rel. 4.7 image acquisition software. A test for axon growth was performed for 30 min without reagent release to assure that the selected growth cone advances well. Time-lapse images were collected for an average of 150 min and the behavior of the growth cone was classified as either 'growing' (growth cone elongation) or 'collapsing' (growth cone

collapse). The Student's *t*-test was used for statistical analysis.

2.7.4. Contact assay: Co-cultures of ZF RGC axons with Nogo peptide-expressing HeLa cells

HeLa cells transfected with different constructs encoding the EGFP-coupled Nogo-GPI fusion proteins or EGFP-GPI as control, were cultured for 5 h in complete MEM medium at 37°C and 5% CO_2. Cells were washed in PBS, treated with 0.05% trypsin and harvested by centrifugation 5 min at 800 rpm. The pellet was resuspended in fresh complete MEM medium, and a drop of cells was added to 15mm coverslips coated with poly-lysine in 1ml complete MEM medium in multiwell dishes. After 12 h at 37°C, cells were transferred to complete F12 medium, a condition which is appropriate for ZF cells and which allows survival and heterologous expression of HeLa cells in cross-species assays. Mini-explants were added and cocultured with HeLa cells at 28°C. After 24 h, the ZF growth cones were monitored when they contacted the transfected cells. Time-lapse images were captured at one min intervals for an average of 75 min as described above, and the behavior of the growth cone was classified as either 'growing' (growth cone elongates and grows across the cell) or 'collapsing' (growth cone collapses after contact with the cell) or 'avoiding' (growth cone avoids to cross the cell and grows around it) (Bastmeyer et al., 1991). The Student's *t*-test was used for statistical analysis.

2.8. Microscopic analysis

ISH transcription patterns for ZF-Rtn4 mRNAs on ZF embryos and ZF-NgR mRNAs on ZF retina as well as immunostained cells and axons were visualised under fluorescent microscope Axioplan 2 using 10x to 40x lenses. For ISH, embryos and retina were photographed with incorporated camera Zeiss Color Axiocam MRc5, while, for immunofluorescent cells Zeiss HRm Axiocam was used. Additionally, oligodendrocytes immunofluorescence was recorded using 100x oil lens either in a confocal Laser scaning microscope (LSM510) and in total internal reflection microscopy (TIRFM). Growing fish axons were visualised under phase contrast using 40x lens in an inverted microscope and time-lapse images were captured at one minute intervals with AxioCam MRm camera. Images were analysed using image acquisition Axiovision Rel 4.7 or LSM 510 softwares (Carl Zeiss, Germany) and then further processed with Adobe photoshop CS2 (Adobe Systems Incorporated, USA).

III. Results

1. Functional characterization of ZF- and Rat-Nogo66 peptides in fish RGC axon growth

1.1. Quantitative outgrowth assay: ZF-Nogo66 promotes and Rat-Nogo66 inhibits ZF axon outgrowth

To examine the substrate properties of ZF-Nogo66 in comparison to Rat-Nogo66, the Rat-Nogo66 peptide was expressed and purified as His-tagged fusion protein His-Rat-Nogo66-His (Figure 15). In these first growth assays, goldfish retinal axons were used and Rat-Nogo66 was tested for its effect on goldfish axon growth by a quantitative outgrowth assay (Vielmetter and Stuermer, 1989). Number of retinal mini-explants with growing axons on His-Rat-Nogo66-His was compared to the growth on the His-tagged Rat-NIGΔ20 peptide (Figure 15), known as the most inhibitory region of Nogo-A (Oertle et al., 2003b), used as an "inhibition control" and compared to the growth on poly-lysine alone as "growth control" (Figure 16). After 24 h in culture, explants with axons on His-Rat-Nogo66-His coated coverslips were very few (14% explants with axons) as compared to explants on poly-lysine (27% explants with axons) (Figure 16). Comparison between Nogo-66 and NIGΔ20 substrates in their ability to inhibit growth of axons showed that NIGΔ20 (6% explants with axons) seems to inhibit the growth of axons more than Nogo-66 (14% explants with axons), but statistically they are not different (Figure 16). However, statistical analysis showed significant differences between poly-lysine and the two Nogo substrates. Thus, we found that growth of fish axons is inhibited by the mammalian NIGΔ20 and Rat-Nogo-66. This data give rise to intriguing question: whether fish Nogo-66 whould also have inhibitory effects on fish growing axons.

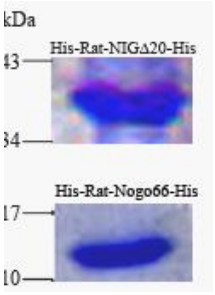

Fig 15. Coomassie staining of purified His-tagged Nogo peptides. His-Rat-NIGΔ20-His and His-Rat-Nogo66-His peptides were expressed in *E-coli*, purified under native conditions using columns (His-Rat-NIGΔ20-His) or using batch assays (His-Rat-Nogo66-His). His-Rat-NIGΔ20-His is 37 kDa and His-Rat-Nogo66-His is 13 kDa.

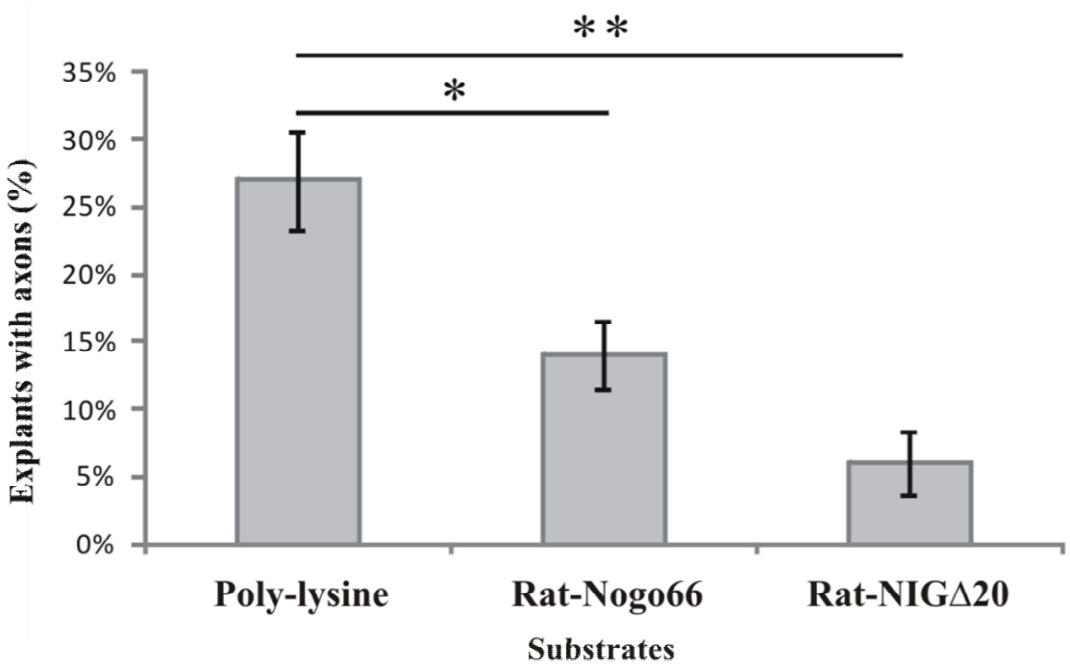

Fig 16. Goldfish axon outgrowth assay. Histogram showing the percentage of goldfish retinal mini-explants with axons after 24 h in culture. Axon growth on His-Rat-Nogo66-His or His-Rat-NIGΔ20-His peptides is lower than that on poly-lysine. Bars in each column represent standard error, asterisks indicate significant difference (* $P< 0.05$), (** $P< 0.01$) by student's *t*-test.

In parallel experiments, however, we realized that ZF retinal axons are more sensitive than their goldfish counterparts, and that GST-fusion proteins are easier to purify. Therefore, the core experiments were with ZF axons and GST-tagged Nogo peptides. To determine whether ZF-Nogo66 has inhibitory properties like its mammalian orthologue, GST-fusion proteins of Rat- and ZF-Nogo66 were produced in *E-coli* and purified (Figure 17) for use in *in vitro* growth assays testing their effects on growing fish axons in the "quantitative outgrowth assay". From six independent experiments including roughly 100 retinal explants for each substrate (Table 7), the number of axons growing on recombinant GST-ZF-Nogo66 or GST-Rat-Nogo66 as substrate was determined. These values were compared to the number of axons on the inhibitory substrate GST-Rat-NIGΔ20, which served as "inhibition control". Axon growth on GST served as "growth control" (Figure 19). The average number of axons on Rat-Nogo66 with 19 axons/explant was significantly reduced compared to the GST control showing an average of 27 axons/explant. The number of axons on Rat-NIGΔ20 with 12 axons/explant was significantly lower than on Rat-Nogo66 (Figure 19). ZF-Nogo66, however, had no inhibitory effect on growing axons: the number of axons (33 axons/explant)

was (statistically) not different from the control substrate GST but was roughly 2.7 and 1.7 times higher than on Rat-NIGΔ20 and Rat-Nogo66, respectively (Figure 18 and 19). Thus, ZF-Nogo66 appears to be permissive for axon growth in contrast to Rat-Nogo66 which negatively affects the growth of fish axons.

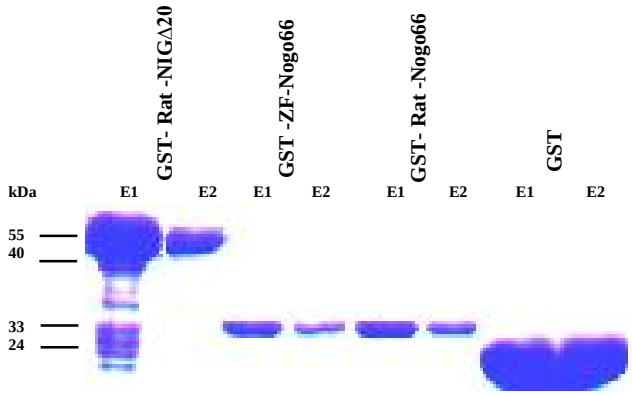

Fig 17. Coomassie staining of purified GST fused -Nogo proteins. GST-Rat-NIGΔ20, GST-Rat-Nogo66, GST-ZF-Nogo66, and GST alone proteins were expressed in *E-coli*, purified in batch under native conditions (GST-Rat-NIGΔ20 and GST) and under denaturing conditions with 8M urea (GST-Rat-Nogo66, and GST-ZF-Nogo66). GST is 26 kDa, GST-Rat-NIGΔ20 is 47 kDa, GST-ZF-Nogo66 and GST-Rat-Nogo66 are 34 kDa. E: Elution, 1 and 2 are different elutions.

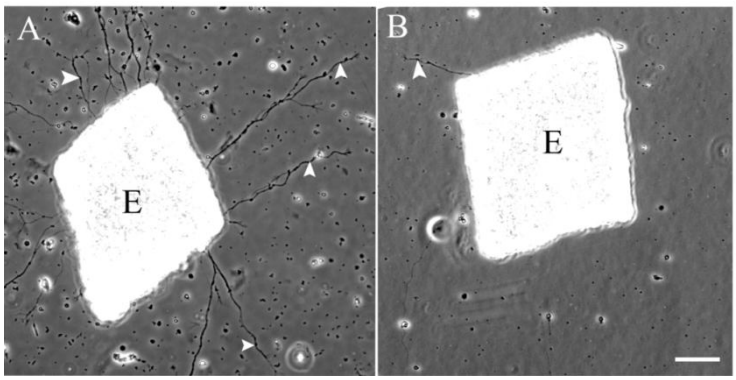

Fig 18. ZF retina mini-explants with growing axons on different substrates after 24 h in culture. A) Category "growth": Many axons (arrowhead) grow out of the mini-explant on ZF-Nogo66 substrate. B) Category "inhibition": few axons are growing out of the mini-explant on Rat-Nog66 substrate (arrowhead). E: Explant. Scale bar; 50 µm.

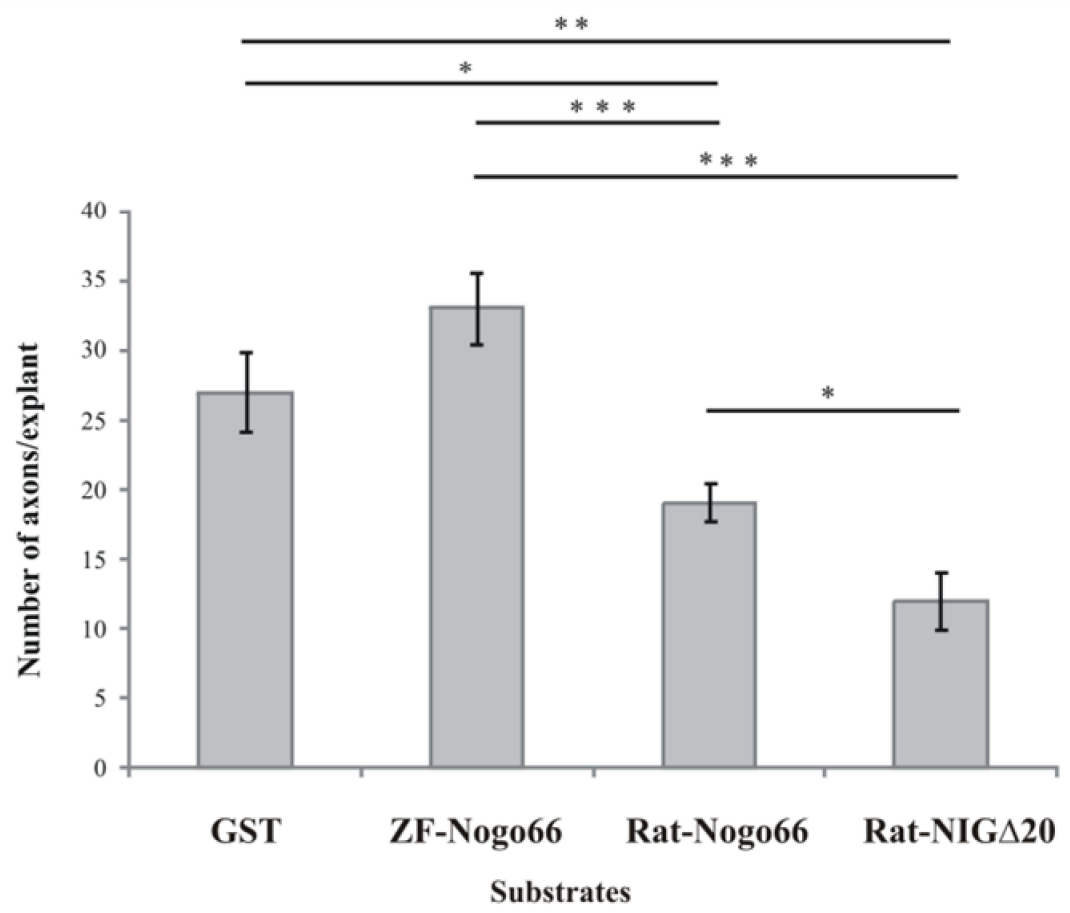

Fig 19. ZF axon outgrowth assay. Histogram showing the average number of ZF RGC axons per retina mini-explant after 24h in culture. The quantification includes six separate experiments with a total number of roughly 100 retina mini-explants per substrate. Substrates are as indicated below each column. GST was used as a positive control for axon outgrowth. Number of axons per explant on ZF-Nogo66 is significantly higher compared to Rat-Nogo66, and growth on Rat-Nogo66 is significantly higher compared to Rat-NIGΔ20. Bars in each column represent standard error and asterisks indicate significant difference (* $P < 0.05$), (** $P < 0.01$) and (*** $P < 0.001$) by Student's *t*-test.

Substrate	N° explants	N° axons
GST	87	2349
GST-ZF-Nogo66	98	3302
GST-Rat-Nogo66	100	1840
GST-Rat-NIGΔ20	100	1275

Table 7. Quantitative outgrowth assay. Number of ZF mini-explants used in the outgrowth assay and number of counted ZF RGC axons grown on various GST-Nogo peptides and GST as control.

1.2. Collapse assay: Rat-Nogo66 in contrast to ZF-Nogo66 causes collapse of ZF growth cones

To investigate whether Rat-Nogo66 but not ZF-Nogo66 causes collapse, we used time-lapse microscopy and monitored the reaction of RGC growth cones upon application of GST-ZF-Nogo66, GST-Rat-Nogo66, GST-Rat-NIGΔ20 and GST at a distance of either 50µm (Figure 21A) or 50-100µm (Figure 21B) to the growth cone, over an average time of 150 min. Selected images of time-lapse movies (Figure 20) illustrate RGC growth cone responses which are quantified in Table 8. GST control protein application did not affect extension or motility (Figure 20A, B and C) in 73% of the tested growth cones whereas 27% collapsed. We consider this as the "background collapse rate", which was observed earlier in such assays with fish RGCs and rat dorsal root ganglion neurons and proteins isolated from goldfish CNS myelin (Wanner et al., 1995) which is growth permissive for fish and mammalian neurons (Bastmeyer et al., 1991). Bovine CNS myelin-derived proteins caused 75-80% collapse of fish RGC growth cones in these former assays (Wanner et al., 1995). Here, with GST-ZF-Nogo66, 79% of growth cones continued to grow (Figure 20D, E and F; table 8) and 21% collapsed suggesting that ZF-Nogo66 has no collapsing activity beyond the background rate. The growth cone in Figure 14F was striking in so far as it grew towards the source of ZF-Nogo66 and established intimate contact with the tip of the micropipette – a behavior not seen with the other peptides. In contrast, GST-Rat-Nogo66 and GST-NIGΔ20 induced collapse in 78% and 82% of growth cones, respectively (Table 8) with its typical features (Figure 20G, H, I and J, K, L): arrest of elongation with loss of lamellipodia and filopodia followed by retraction of the growth cone and retraction bulb formation culminating in the loss of motile activity. Thus, the percentage of collapsed growth cones during the application of GST-ZF-Nogo66 was three to four times lower (statistically significant $P < 0.05$, $P < 0.01$) (Figure 21A) than with GST-Rat-Nogo66 (78%) or GST-Rat-NIGΔ20 (82%) (Table 8) which caused collapse of the vast majority of growth cones. Even when applied at 50-100µm (Figure 21B) percentage of collapse on GST-ZF-Nogo66 was statistically different ($P < 0.01$) from the GST-Rat-Nogo66. These findings confirm the inhibition exerted by Rat-NIGΔ20 on ZF RGC growth cones and show as a new result that Rat-Nogo66 has an inhibitory influence on fish axon growth. Importantly, ZF-Nogo66 added to elongating ZF growth cones, does not impair growth cone advance (beyond the

background collapse rate) and hence is growth permissive – in contrast to its mammalian counterpart.

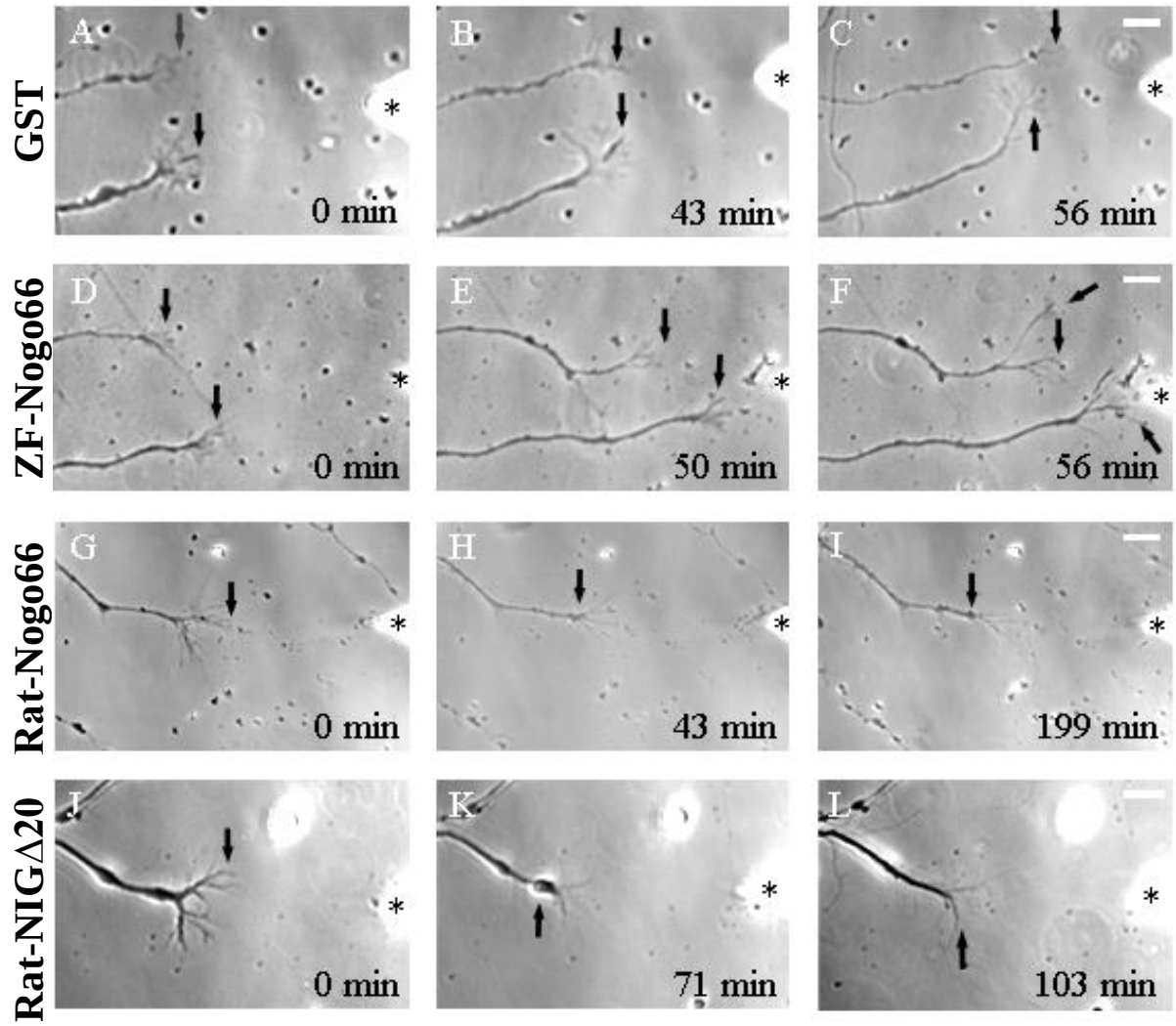

Fig 20. Collapse assay. Time-lapse microscopy of ZF RGC growth cones responding to GST alone (A, B, C), to GST-ZF-Nogo66 (D-F), GST-Rat-Nogo66 (G-I), and GST-Rat-NIGΔ20 (J-L). Time of application in minutes is indicated. The position of the femtotip is marked by an asterisk. A-F: The growth cones (arrow) elongate after application of soluble GST (A-C) and GST-ZF-Nogo66 (D-F), respectively. G-L) Cessation of growth cone motility after application of GST-Rat-Nogo66 (G-I) or GST-Rat-NIGΔ20 (J-L). Arrowhead indicates retraction bulbs of collapsed growth cones. Note the contact between the lower of the two growth cones (F, arrow) and the tip of the needle (*). Scale bar; 10 µm.

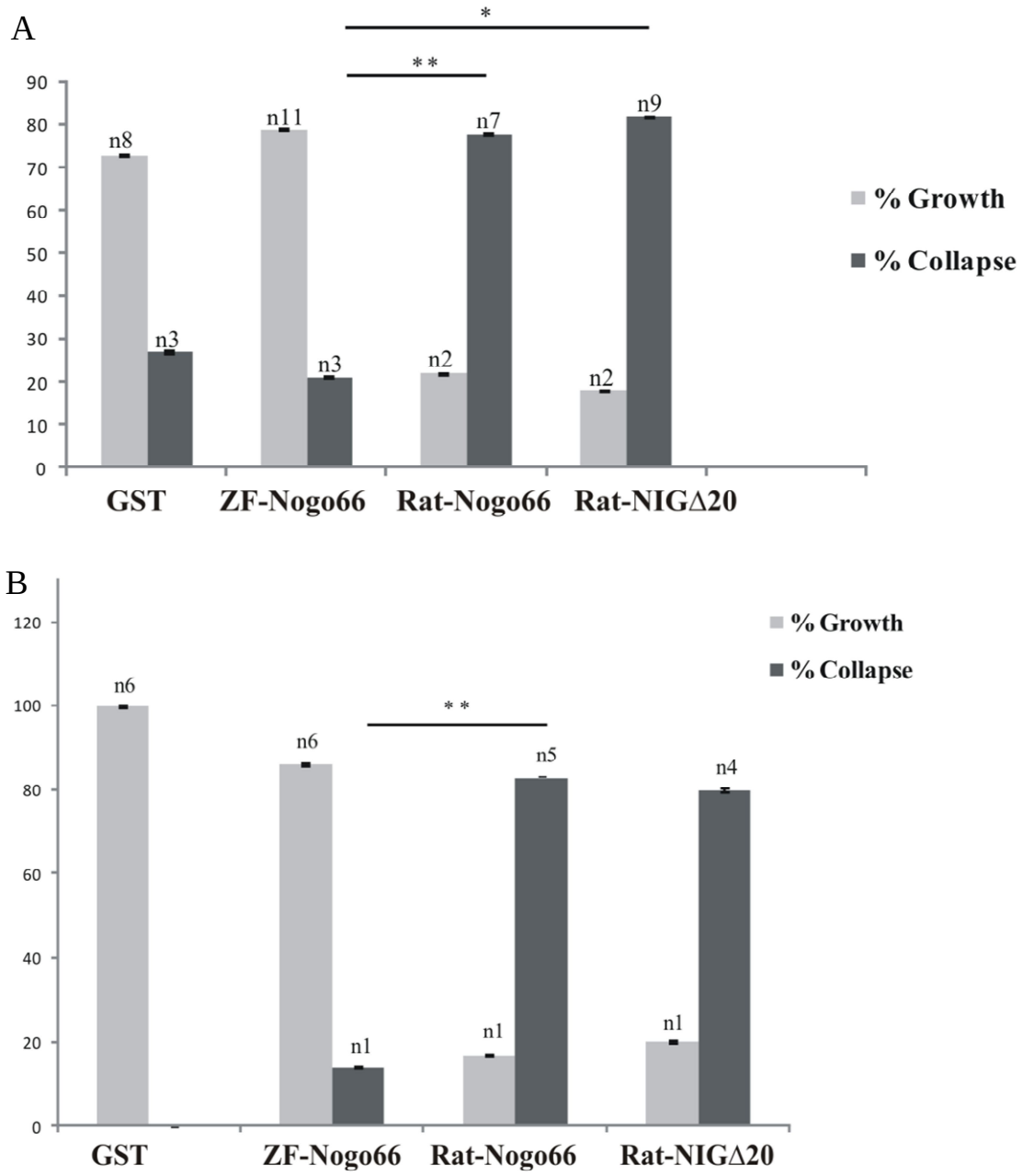

Fig 21. Collapse assay. Quantification of growth cone responses: growth (grey bars), collapse (black bars) following application of GST-ZF-Nogo66, GST-Rat-Nogo66, GST-Rat-NIGΔ20 and GST. Peptides were applied at 50µm distance from the growth cone (A) and at 50 to 150 µm distance from the growth cone (B). A statistical difference exists between all experiments but only the most important ones in are indicated by asterisks (* $P < 0.05$ and ** $P < 0.01$ according to Student's *t*-test). Note that in (A) ZF-Nogo66 allows a significantly higher percentage of growth as opposed to Rat-Nogo66 and Rat-NIGΔ20 which cause collapse in 79 and 82%, respectively, of the growth cones. GST was used as positive control for axon growth. Bar in columns, standard error; n is the number of growth cones.

Peptide	N	N collapse	% growth	% collapse
GST	11	3	73	27
GST-ZF-Nogo66	14	3	79	21
GST-Rat-Nogo66	9	7	22	78
GST-Rat-NIGΔ20	11	9	18	82

Table 8. Collapse assay. Number and percentage of ZF RGC growth cones which collapse and grow when exposed to the various GST-Nogo peptides and GST as control at 50µm distance.

1.3. Contact assay: Axons contacting HeLa cells expressing Rat- and ZF-Nogo66, respectively

To analyse whether ZF and Rat-Nogo66 as well as Rat NIGΔ20 affect RGC growth cones when exposed on the surface of cells, we fused the relevant peptides to a GPI-anchor from ZF Prion protein (PrP) and EGFP for the transfection of HeLa cells. This cell line was used because it is easily transfected as opposed to primary fish oligodendrocytes which we would have preferred for these experiments but which gave a smaller than 1% transfection rate. That HeLa cells expressed the GPI-anchored EGFP-fusion peptides on the cell surface was confirmed by live staining with ABs against the various Nogo peptides (Figure 22). EGFP-GPI transfected HeLa cells served as control. By co-culturing the Nogo transfected HeLa cells with fish ZF RGCs axons, three main categories of axon responses were observed following contact with the HeLa cell: collapse (growth cone collapses upon contact with the cell), avoidance (growth cone avoids to grow over the cell after contact and prefers to grow away from or around the cell) and growth (growth cone grows over or under the cell following contact) (Figure 23). After testing more than 20 contacts for each peptide expressing HeLa cells and quantifying the growth cone responses, we found that HeLa cells expressing NIGΔ20-EGFP-GPI caused collapse in 63% and avoidance in 20% of the growth cones, and 17% crossed the cells (Figure 24; table 9). However, HeLa cells expressing ZF-Nogo66-EGFP-GPI showed the opposite: 16% collapse, 19% avoidance and 65% growth across the cells, but the Rat-Nogo66-EGFP-GPI gave 42% collapse and 42% avoidance, and only 16% crossed the cells (Figure 24; table 9). Thus, ZF-Nogo66 allows four times more cell crossings than Rat-Nogo66 and NIGΔ20. In contact with non-transfected cells, growth cone collapse and avoidance occurred in 18% and 15%, respectively, and 67% crossed untransfected cells, ratios similar to ZF-Nogo66. In contact with EGFP-GPI transfected cells,

collapse amounted to 20%, avoidance to 40% and growth across to 40% (Figure 24; Table 9). Why EGFP-GPI expressing cells caused an increase in avoidance cannot be readily explained but puts even more weight on the lower avoidance rate caused by the ZF-Nogo66 fusion protein and underscores its permissiveness. Thus, ZF growth cones collapse in contact with Rat-Nogo66 and Rat-NIGΔ20 expressed on the cell surface which markedly differs from ZF-Nogo66 which had no collapsing activity beyond the background rate also seen with untransfected cells and EGFP-GPI. A new evidence showing a functional difference between the fish and mammalian Nogo66 for their ability to affect growth of axons.

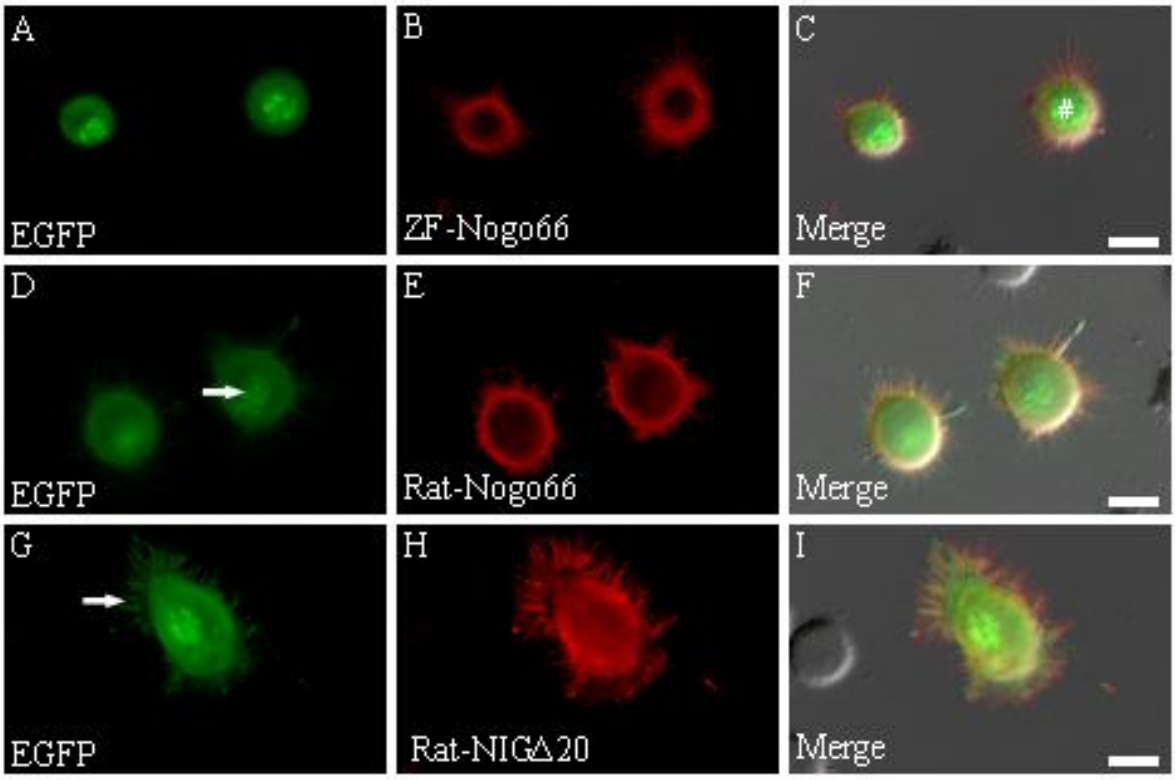

Fig 22. Contact assay and expression of Nogo-EGFP-GPI fusion proteins on the cell surface. Live HeLa cells expressing Nogo fusion proteins with GPI-anchor and EGFP (green) of ZF-Nogo66 (A-C), Rat-Nogo66 (D-F) and Rat-NIGΔ20 (G-I) were exposed to Nogo ABs-staining (red) at 1:1000 dilutions which resulted in cell surface staining in each case. Scale bar; 10µm.

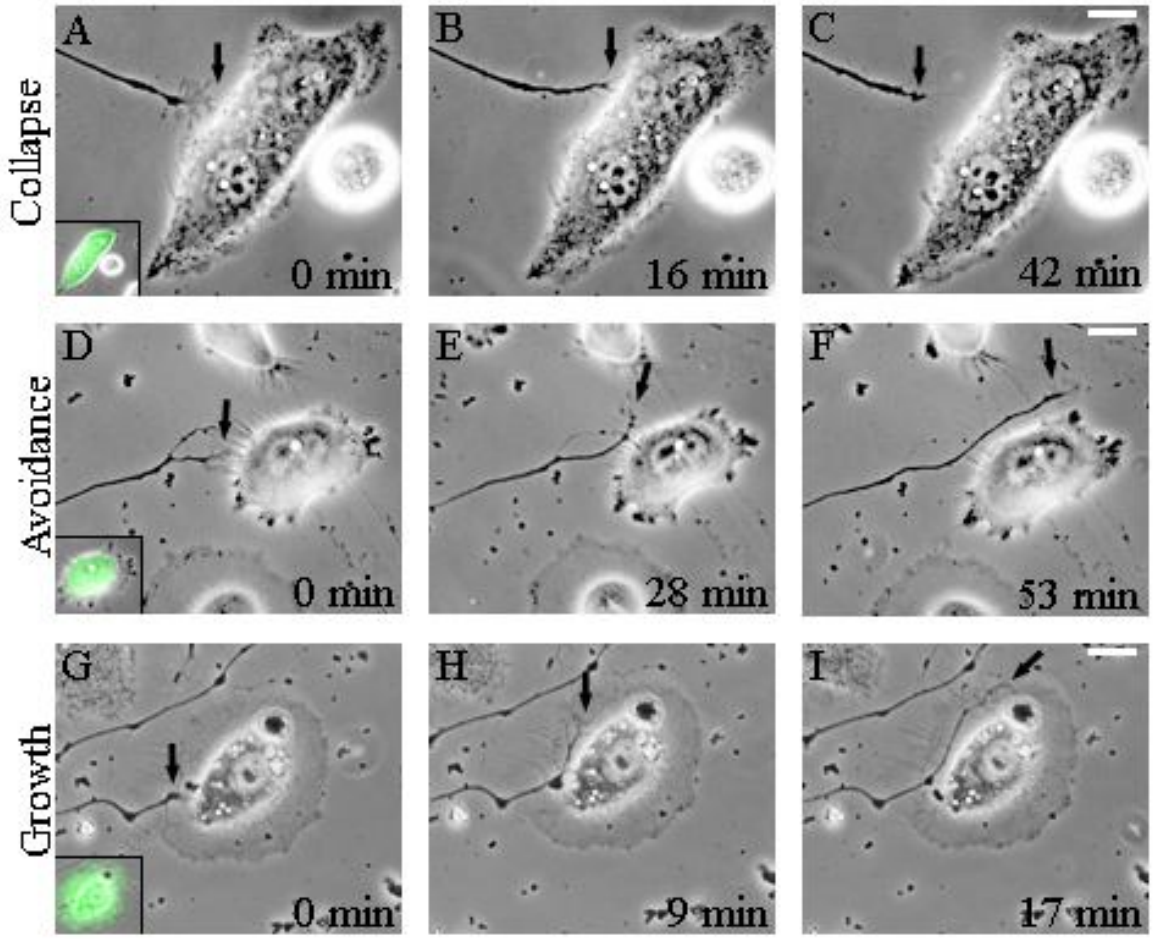

Fig 23. Contact assay. ZF RGC axons were co-cultured with control HeLa cells and HeLa cells expressing either ZF-Nogo66-GPI-EGFP, Rat-Nogo66-GPI-EGFP, Rat-NIGΔ20-GPI-EGFP, and EGFP-GPI (green fluorescence in insert). Growth cone (arrow) contact with cells resulted in growth cone collapse, avoidance and growth on the cell as exemplified in A-C; D-F; G-I. Scale bar; 20µm.

Tested peptide	N° of axons	N° of grown axons	N° of avoiding axons	N° of collapsed axons	% growth	% avoidance	% collapse
Non transfected	27	18	4	5	67	15	18
EGFP	20	8	8	4	40	40	20
ZF-Nogo66- EGFP	26	17	5	4	65	19	16
Rat-Nogo66-EGFP	24	4	10	10	16	42	42
Rat-NIGΔ20-EGFP	30	5	6	19	17	20	63

Table 9. Contact assay. Number and percentage of ZF RGC growth cones which collapse, avoid to cross and grow onto/across transfected HeLa cells expressing Nogo peptides as EGFP-GPI fusion proteins on the cell surface.

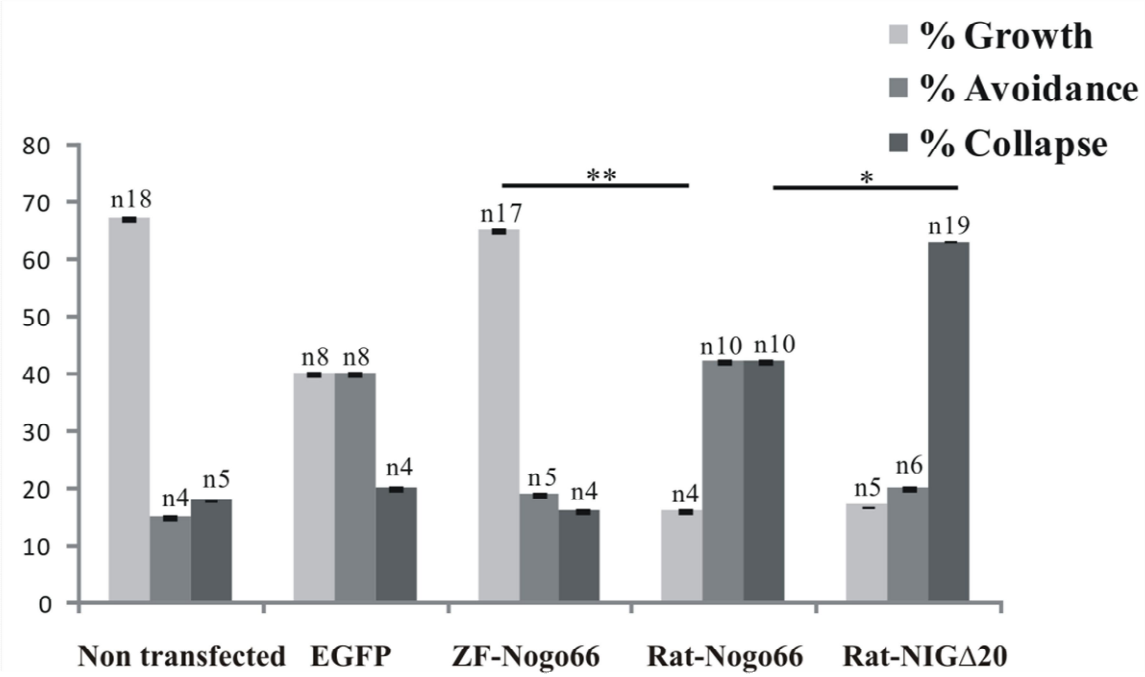

Fig 24. Contact assay. Quantification of the growth cone responses in dependence of the expressed Nogo peptide. All differences between substrates are significant but only the two most important ones are labeled accordingly (* $P < 0.05$) and (** $P < 0.01$ according to Student's *t*-test). n, number of growth cones; bar in column, standard error.

2. Fish oligodendrocytes expressing the mammalian NogoA-NIGΔ20

In contrast to mammals, fish oligodendrocytes are devoid of inhibitors such as Nogo-A (Diekmann et al., 2005) and are permissive for axonal growth and regeneration (Bastmeyer et al., 1993). To investigate *in vitro* the inhibitory characteristics of the mammalian Nogo-A in the fish system, we used primary cultured goldfish oligodendrocytes as a cellular model for Nogo-A inhibition of fish RGC axons in a co-culture assay. We transfected the cells with the most inhibitory stretch of the Nogo-A, NIGΔ20 -fused to EGFP and the GPI anchor from prion protein to target the protein to the cell surface (Figure 25). Unfortunately, the rate of transfection was too low (~1%) that no contact between the Rat-NIGΔ20-EGFP expressing oligodendrocytes and growing axons has occurred in co-culture assays. Interestingly, after reviewing 19 and 11 recorded time-lapse movies for NIGΔ20-EGFP expressing oligodendrocytes and EGFP control expressing oligodendrocytes, respectively (Figure 26), an

unexpected behaviour has been observed only in cells expressing the inhibitory NIGΔ20. We found that cells expressing the Rat-NIGΔ20-GFP-GPI lose their membrane processes (Figure 35A-C); therefore, they no longer have the elongated morphology of goldfish oligodendrocytes in culture characterized earlier by C.A.O. Stuermer, 1989. 63% of Rat-NIGΔ20 expressing cells were losing their processes, the rest did not show any morphological change, and the two groups are statistically different (P <0.01) (Figure 27). Moreover, we did not observe this morphological change in the control cells expressing GFP-GPI (Figure 27 and 26D and E), where cells kept their elongated shape. Thus, we found that the Rat-NIGΔ20 inhibitory molecule affects fish oligodendrocyte morphology, when expressed on their cell surface.

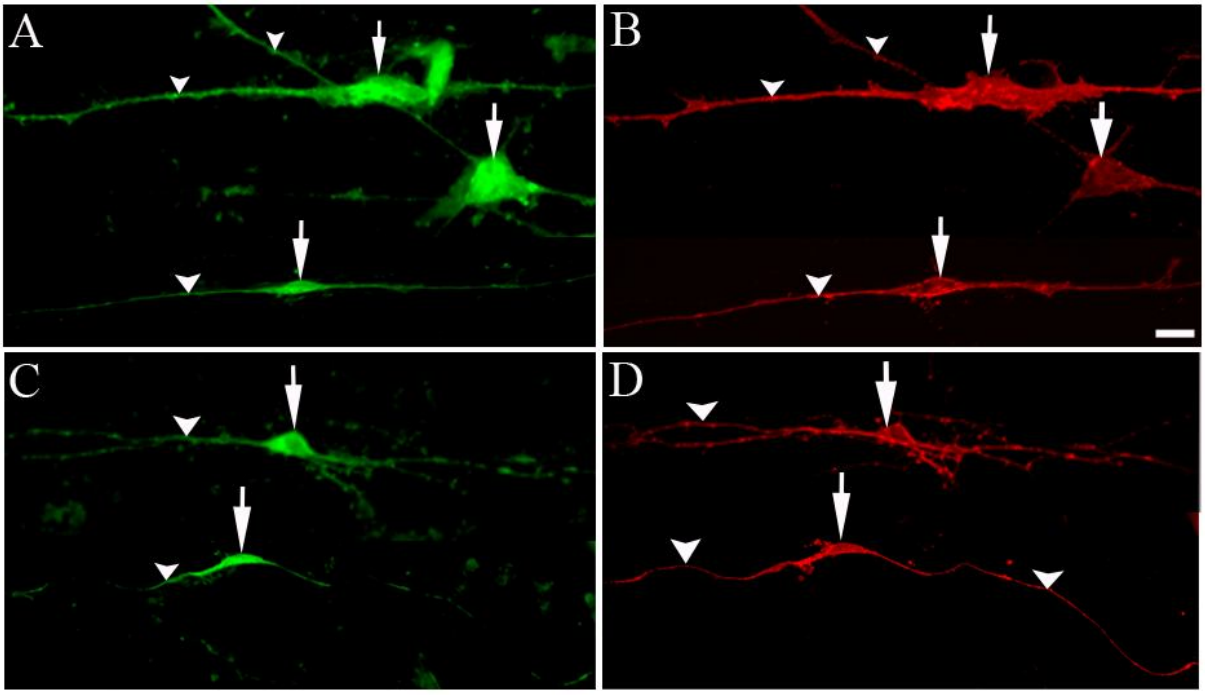

Fig 25. Rat-NIGΔ20 is exposed on the cell surface of cultured goldfish oligodendrocytes. A-D) Live goldfish oligodendrocytes expressing Rat-NIGΔ20 fusion protein with GPI-anchor and EGFP (GFP green fluorescence in A and C) were exposed to ABs 11C7 against NIGΔ20 (B) and ABs against GFP (D), which resulted in cell surface staining in membrane processes (arrowheads in B and D) and cell bodies (arrows in B and D). Primary antibodies were used in a dilution of 1:500 for 11C7 ABs and 1:1000 for GFP ABs, and Cy3 conjugated secondary antibodies were used in a dilution of 1:1000. Scale bar; 10μm.

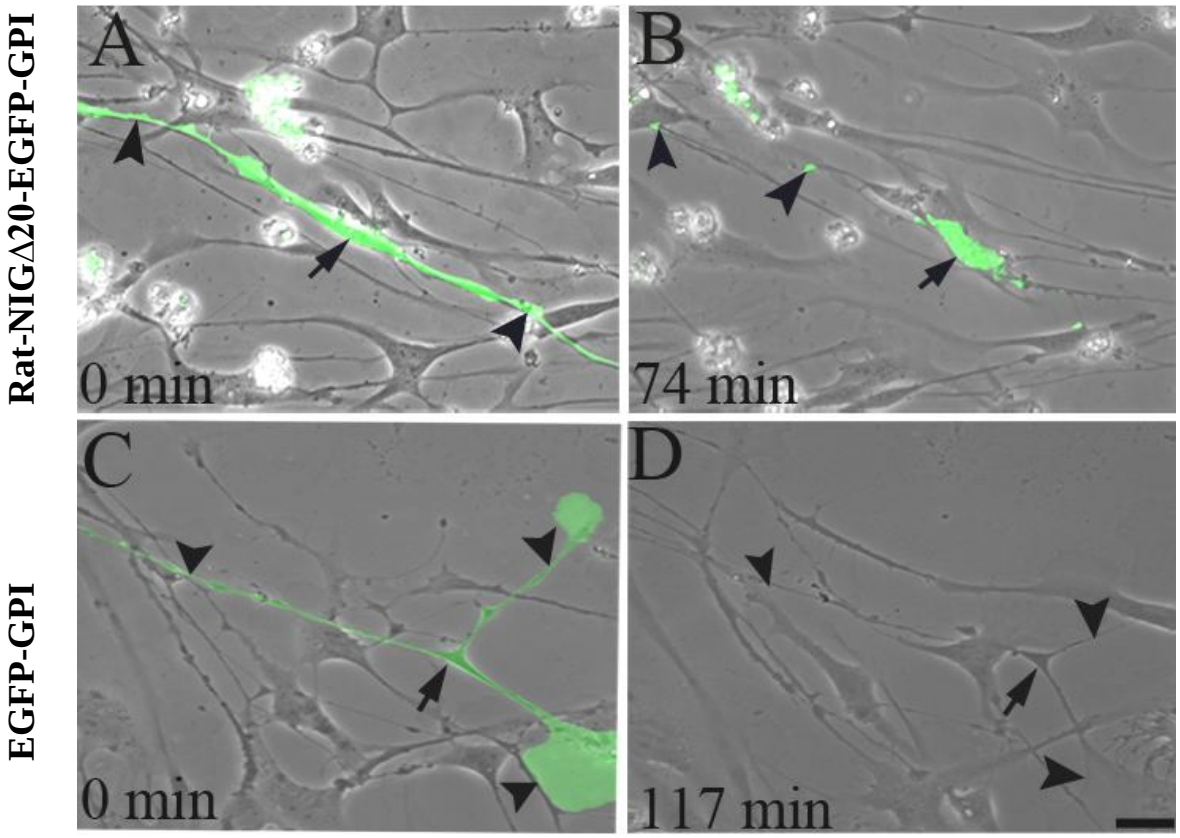

Fig 26. Rat-NIGΔ20 affects goldfish oligodendrocyte cell morphology. Time-lapse microscopy of goldfish oligodendrocytes expressing either Rat-NIGΔ20-EGFP-GPI (A and B) or EGFP-GPI (C and D). GFP positive cells are green (green GFP fluorescence in A and C). Time in minutes is indicated. A and B) GFP positive cells expressing the NIGΔ20 lose their processes (arrowhead in A, B) and only the cell body persists (arrow in B). C and D) Cells expressing the control GFP do not lose their processes (arrowhead in C and D). Scale bar; 10µm.

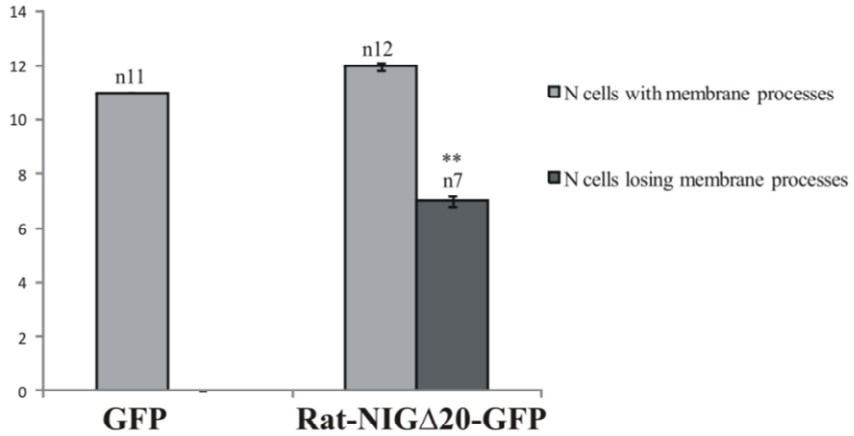

Fig 27. Quantification of loss of membrane processes by oligodendrocytes expressing Rat-NIGΔ20-EGFP-GPI or EGFP-GPI alone. Loss of processes (black bar) and no loss of processes (gray bars). Bar in columns, standard error; n is the number of cells. A statistical difference is indicated by asterisks (** $P < 0.01$) according to Student's *t*-test).

3. Gene expression analysis for Rtn-4/Nogo-66 in the adult fish visual system

3.1. Rtn-4 mRNAs are expressed in fish regenerating optic nerve and cultured oligodendrocytes

The zf-rtn4 gene has three different transcripts l, m and n (Klinger et al., 2004). All of them have the Nogo-66 region in the conserved RHD and are expressed in different adult fish tissues, including the CNS (Diekmann et al., 2005). To further clarify why ZF-RTN4/Nogo-66 has no inhibitory properties on regenerating fish axons, we first examined its expression in the intact and regenerating optic nerve as well as in cultured oligodendrocytes. The mRNA expression level of the Rtn4-l transcript (the largest of the splice variants Rtn4-l, -m and -n; Diekmann et al., 2004) was analyzed by RT-PCR. Total RNAs were extracted from the optic nerve tissue and from cultured oligodendrocytes for cDNA synthesis by reverse transcriptase, and Rtn4-l was amplified by PCR reaction. We found Rtn4-l expressed in both normal and regenerating optic nerve (Figure 28A), and the intensity of the band was similar between the normal and regenerating optic nerve, which excludes up or down regulation of the gene during regeneration. Moreover, Rtn4-l transcript is also present in isolated oligodendrocytes (Figure 28B). Thus, Rtn4-l isoform is expressed in cells in the environment where the axons are growing during the regeneration process.

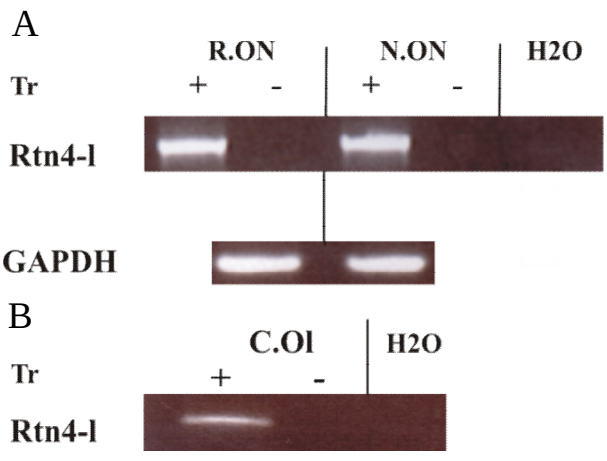

Fig 28. RT-PCR analysis of ZF-Rtn4 mRNA expression in the ZF optic nerve and in goldfish oligodendrocytes. A) RT-PCR analysis on normal (N.ON) and regenerating ZF optic nerves (R.ON) shows expression of ZF-Rtn4-l mRNA. B) Rtn4-l mRNA are detected by RT-PCR in goldfish cultured oligodendrocytes (C.Ol). A reverse transcriptase negative control (Tr (-); without Superscript II enzyme was performed with each primer pair. RT-PCR with GAPDH-specific primers (GAPDH) served as a loading control in each reaction. Abbreviation: H2O, no template, control.

3.2. Nogo-66 peptide is localized inside the goldfish oligodendrocytes

In mammals, the Nogo-66 domain seems to be exposed on the cell surface of oligodendrocytes (GrandPre et al., 2000), or it faces the extracellular space (Huber et al., 2000). The Nogo-66 localization on the surface of oligodendrocytes is important for its inhibitory action on axon growth and regeneration in mammals. Fish oligodendrocytes, known to be permissive for axonal growth (Bastmeyer et al., 1993), seem to be devoid from all kinds of inhibitors. Still, if fish Nogo-66 is recognized by axons it should be surface-exposed. To investigate the cellular distribution of the RTN4-Nogo66 protein, cultured goldfish oligodendrocytes were stained with polyclonal antibodies against ZF-Nogo66. Here, we show in permeabilized cells a diffuse staining of the Nogo-66 inside the cells including cell body and membrane processes (Figure 29A, C and D). Non-permeabilized cells show a weaker and non-uniform staining (Figure 29B), which can be either an artifact possibly from a partial pemeabilization of the cell due to the fixation process or the protein is on the surface but in low level and not distributed in the entire cell. Furthermore, live cells were not stained for Nogo-66 (data not shown). Thus, Nogo-66 is localized inside the cell and may not be present on the cell surface of fish oligodendrocytes.

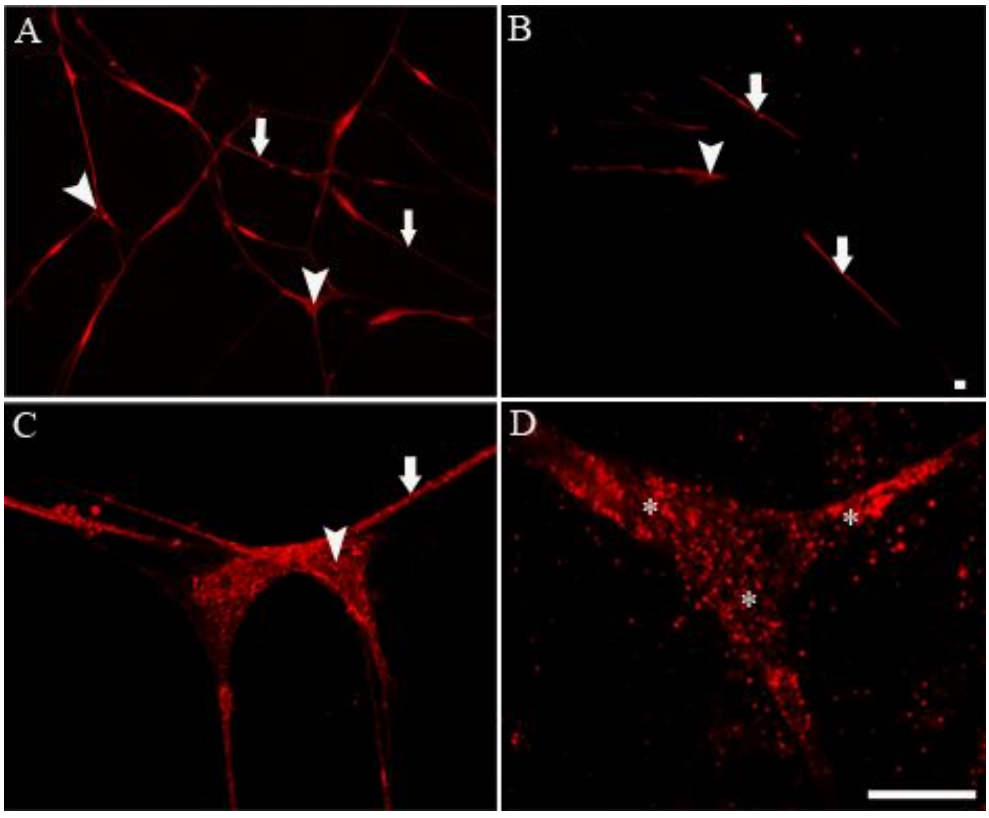

Fig 29. Nogo-66 protein expression in cultured oligodendrocytes. A-D) Fixed oligodendrocyte were incubated with (1:1000) antibodies against the ZF-Nogo66, washed and then incubated with (1:1000) Cy3-conjugated secondary antibodies. A, C and D) Permeabelized cells with triton X100 show strong and uniform staining inside the cell including cell bodies (arrowhead in A and C) and membrane processes (arrow in A and C) and in organelles (arrowhead in C and asterisks in D), Nogo-66 seems to be located inside the cell. B) Umpermeabilized cells show a non uniform staining (only in some regions) on membrane processes and cell bodies (arrow and arrowhead in B, respectively). In A and B images were taken with the 40x lens under a conventional fluorescence microscope, and in C with the 100x lens within confocal-laser scanning microscope (LSM*)* and D with total internal reflection fluorescence *(*TIRF) at an inverted microscope. Scale bars; 10μm.

4. Gene expression analysis of the Nogo receptor (NgR) in the adult fish visual system

4.1. NgR mRNAs are expressed in the fish retina

In mammals, the Nogo-66 receptor NgR has been proposed to play an important role in the mediation of axonal growth inhibition (Fournier et al., 2001). The fish NgR homolog has been identified and found to be predominantly expressed in the brain but also in eye and heart (Klinger et al., 2004) and its function remains unclear. Because CNS axons regenerate successfully in fish, the function of fish NgR is likely to differ from the mammalian function as transducer for growth inhibition. However, NgR might be involved in the mediation of the inhibitory effect of the mammalian Nogo-66 on fish axons *in vitro*. In this context, we set out to study its expression, cell localization and role during regeneration in the fish visual system. Gene expression of the four ngr genes (zf-ngr, zf-ngrH1a, zf-ngrH1b and zf-ngrH2) was analysed by RT-PCR in the ZF retina. We found ZF-NgR, ZF-NgRH1a and ZF-NgRH2 mRNAs in both normal retina and in the retina after optic nerve lesion but not the ZF-NgRH1b (Figure 30) which is absent in both retinae. Moreover, the amount of transcripts seems not to significantly differ between the normal retina and retina after optic nerve lesion, meaning that axon regeneration does not apparently affect the regulation of NgRs expression. To check whether these NgR mRNAs are expressed by RGCs, we performed *in situ* hybridization (ISH) on whole mount retinae. Here, we show that ZF-NgR mRNAs are present in RGCs (blue dots in Figure 31A) (Figure. 31B control). Thus, ZF-NgR is expressed by RGCs. The question remains is whether NgR proteins is produced by and localized in regenerating axons.

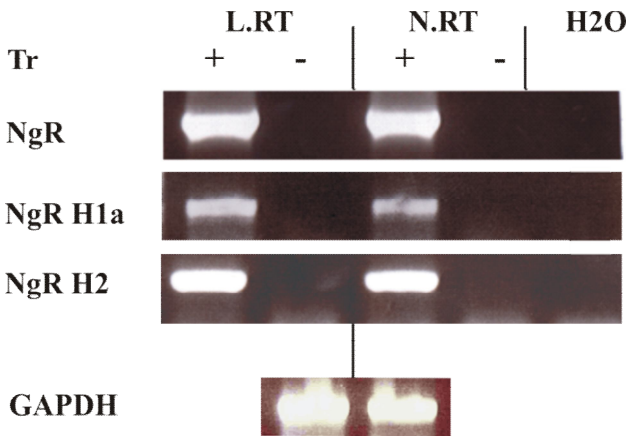

Fig 30. RT-PCR analysis of ZF-NgR, ZF-NgRH1a and ZF-NgRH2 mRNAs expression in ZF retina. Expression of different ZF-NgRs mRNAs was examined in normal ZF retina (N.RT) and ZF retina after optic nerve lesion (L.RT). A reverse transcriptase negative control Tr (-) without Superscript II enzyme was performed with each primer pair. RT-PCR with GAPDH-specific primers (GAPDH) served as a loading control in each reaction. Abbreviation: H2O, no template, control.

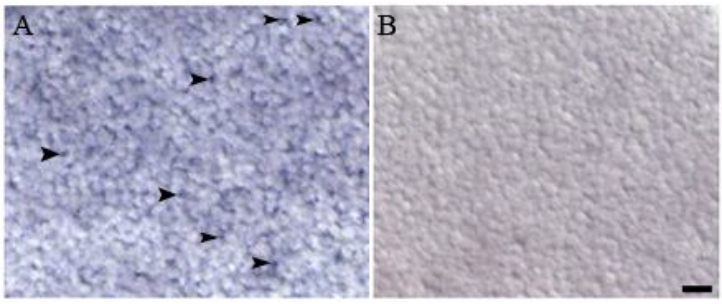

Fig 31. ISH analysis of ZF-NgR mRNA expression in RGCs. Expression of ZF-NgR mRNA was examined in a retina whole mount. A) NgR anti-sense riboprobe. B) NgR control sense riboprobe. In A, arrowheads show the stained RGCs neurons (blue dots). Control is blank (B). Scale bar; 50 µm.

4.2. ZF-NgR is present in ZF brain and expressed in growing axons

In order to analyze the expression and localization of ZF-NgR on fish growing axons, we generated polyclonal antibodies against a 16 amino-acids epitope from the N-terminal leucine reach repeat region (LRR) of the ZF-NgRH1b (see methods 2.4.7). Rabbit anti serum (AS923) was tested biochemically for its specificity on proteins from the ZF brain as well as on purified GST-ZF-NgR8LRR recombinant protein (Figure 32C). By western blots, AS923 ABs revealed a band at ~54 kDa in brain (Figure 32 A) corresponding to one of the four ZF-NgRs (54 kDa for ZF-NgR, 52 for kDa for ZF-NgRH1a, 52 for kDa for ZF-NgRH1b and 54 kDa for ZF-NgRH2). This band was absent in the control prae-immune serum (Figure 32A). Furthermore, these antibodies recognized the 46 kDa recombinant protein GST-ZF-

NgR8LRR as compared with antibodies against GST (Figure 32B and C). Therefore, AS923 seems to recognize all ZF-NgRs since the epitope against which antibodies were raised is identical in the four NgRs (see methods 2.4.7). Moreover, we show here that ZF-NgRs are expressed in ZF brain.

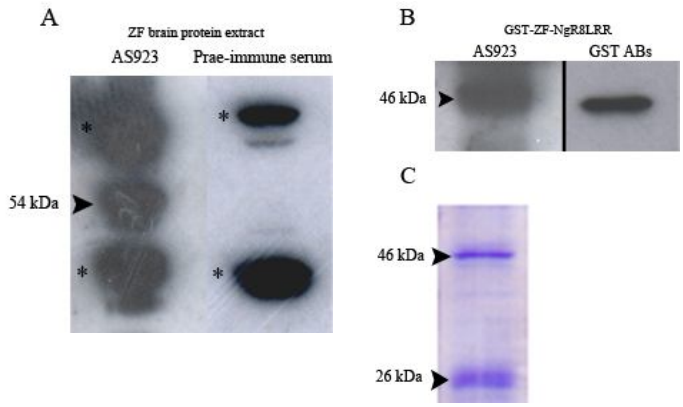

Fig 32. Test for specificity of AS923 polyclonal antibodies and NgR protein expression in the ZF brain. A-B) Western blot analysis with ZF brain extract (A) and recombinant proteins GST-ZF-NgR8LRR (B). A) AS923ABs against ZF-NgRs detect 54 kDa in brain, which is absent in the prae-immune serum, both AS923 and prae-immune recognize other proteins (asterisks in A). B) AS923 recognizes GST-ZF-NgR8LRR. ABs against GST were used as control.

C. Coomassie staining for purified GST-ZF-NgR8LRR recombinant protein, 46 kDa is the recombinant protein and 26 kDa is GST alone. AS923 ABs and GST ABs were used at 1:1000 dilution and HRP conjugated secondary antibodies 1:10.000.

Furthermore, this antibody served to look for the localization of the NgRs in ZF growing axons (Figure 33). Axons showed no staining when they were exposed to the ABs unfixed, but after fixation the ABs labeled the axons (Figure 33, arrowhead in B). The staining was stronger compared to the control prae-immune serum (Figure 33H and I) with a weak staining in some axonal regions (Figure 33, arrowhead H and I), which can be background staining. Other axons were not stained (Figure 33, arrows in I). Moreover, when axons were treated with PI-PLC enzymes to cleave-off all GPI-anchored proteins such as NgRs, the staining with AS923 was absent (Figure 33E and arrows in F), or very weak in some axonal regions (Figure 33, arrowhead in F). This is evidence that the AS923 recognized a GPI anchored protein on the axonal surface, which is probably NgR. Thus, NgR seems to be exposed on the surface of ZF axons and probably in the growth cones.

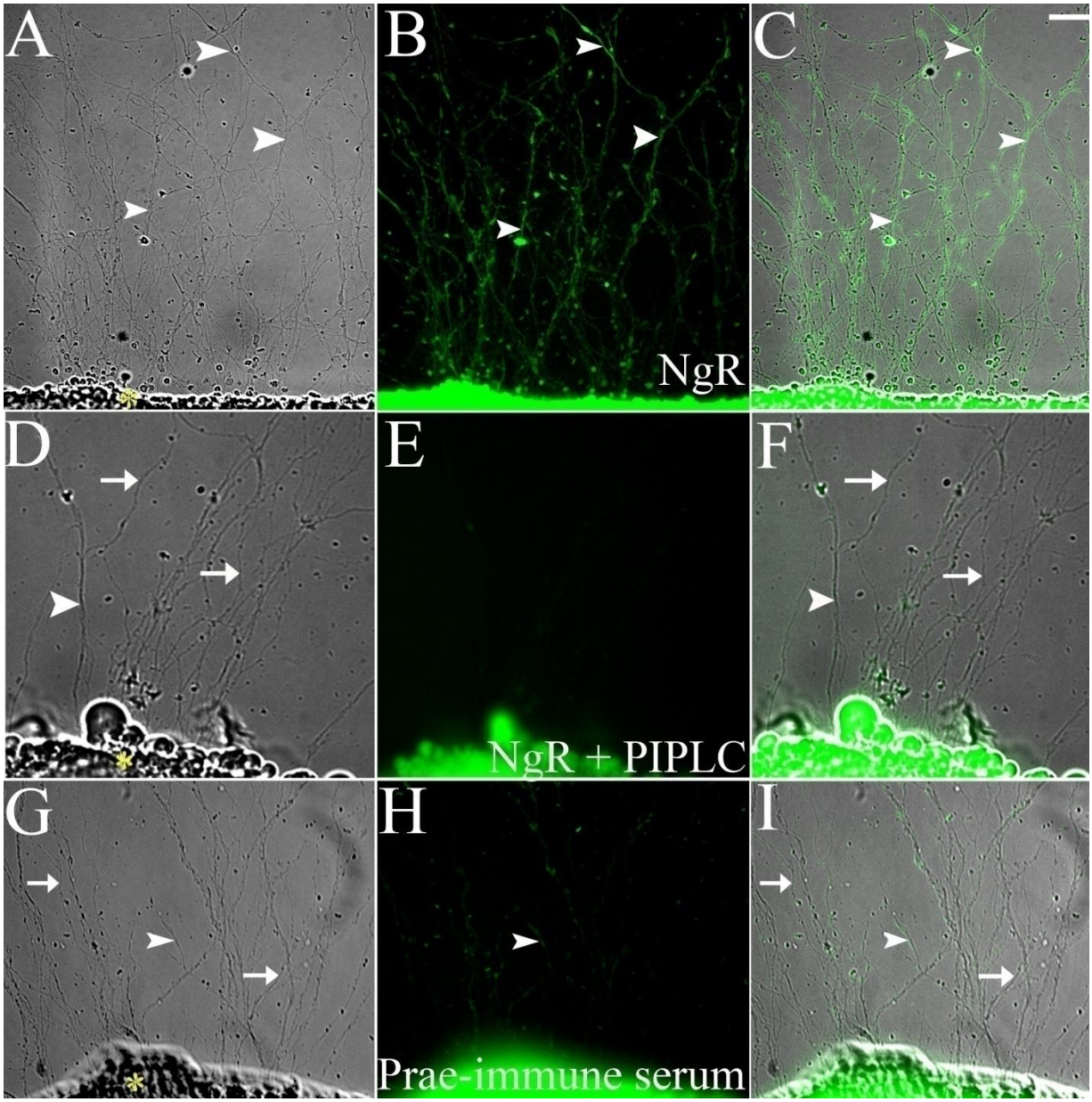

Fig 33. Staining of ZF RGC axons with AS923 ABs against ZF-NgRs. A-I) Fixed ZF axons, growing out of the mini-explants (asterisks in A, D and G) were stained for NgRs. A-C) ZF axons are stained with AS923 ABs (arrowhead in A, B and C). D-F) When axons were treated with 0.5U PI-PLC enzyme, axons were weakly stained (arrowhead in D and F) or not stained at all (arrows in D and F). G-I) Weak staining (arrowhead in G, H and I) or no staining (arrows in G, H and I) of axons within the prae-immune serum. C, F and I are merged images. AS923 and the prae-immune serum were used in a dilution of 1:100 and Alexa-488 conjugated secondary antibodies were used at 1:1000. Scale bar; 20 µm.

5. Rat-Nogo66 inhibits ZF axon growth probably via NgR receptor

To determine whether the inhibition of Rat-Nogo66 on ZF RGC axons involves the fish NgR receptor, we performed a quantitative outgrowth assay using GST-tagged ZF- and Rat-Nogo66 substrates (Figure 17) and we treated ZF RGC axons with PIPLC enzyme to cleave-off the GPI-anchored proteins, including NgR receptor from the surface. First, the PIPLC enzymatic activity was controlled by immunostaining on ZF RGC axons for a GPI and non-GPI-anchored proteins after PIPLC treatment (Figure 34). The percentage of axon growth on different substrates was determined when PIPLC treatment was applied. Parallel experiments without PIPLC treatment were performed as controls (Figure 35). We found more growth of RGC axons (120%) when Rat-Nogo66 is used as substrate in presence of PIPLC, compared with PIPLC-non-treated axons, which reach only 37% of growth (Figure 35). Growth of PIPLC-treated axons on Rat-Nogo66 is not statistically different from the GST control, which means that RGC axons are not sensitive to the Rat-Nogo66 when are treated with PIPLC. Interestingly, growth of RGC axons on ZF-Nogo66 substrate decreased from 154% without PIPLC to 87% with PIPLC (statistically different, $P< 0.01$). However, this decrease in growth did not reach the inhibition state, since growth of PIPLC-treated RGC axons on ZF-Nogo66 (87%) is statistically different from the growth of PIPLC-non-treated RGC axons on Rat-Nogo66 (34%) ($P< 0.05$). Moreover, growth on ZF-Nogo66 (154%) without PIPLC treatment is statistically different from the growth on control GST (100%) ($P< 0.05$) (Figure 35), suggesting that ZF-Nogo66 has probably not only growth-permissive properties but also growth-promoting. Here we bring two new information, first Rat-Nogo66 seems to inhibit growth of ZF axons via a GPI-anchored receptor, which is probably NgR, and secondly, ZF-Nogo66 may promote growth of axons via GPI-anchored receptor.

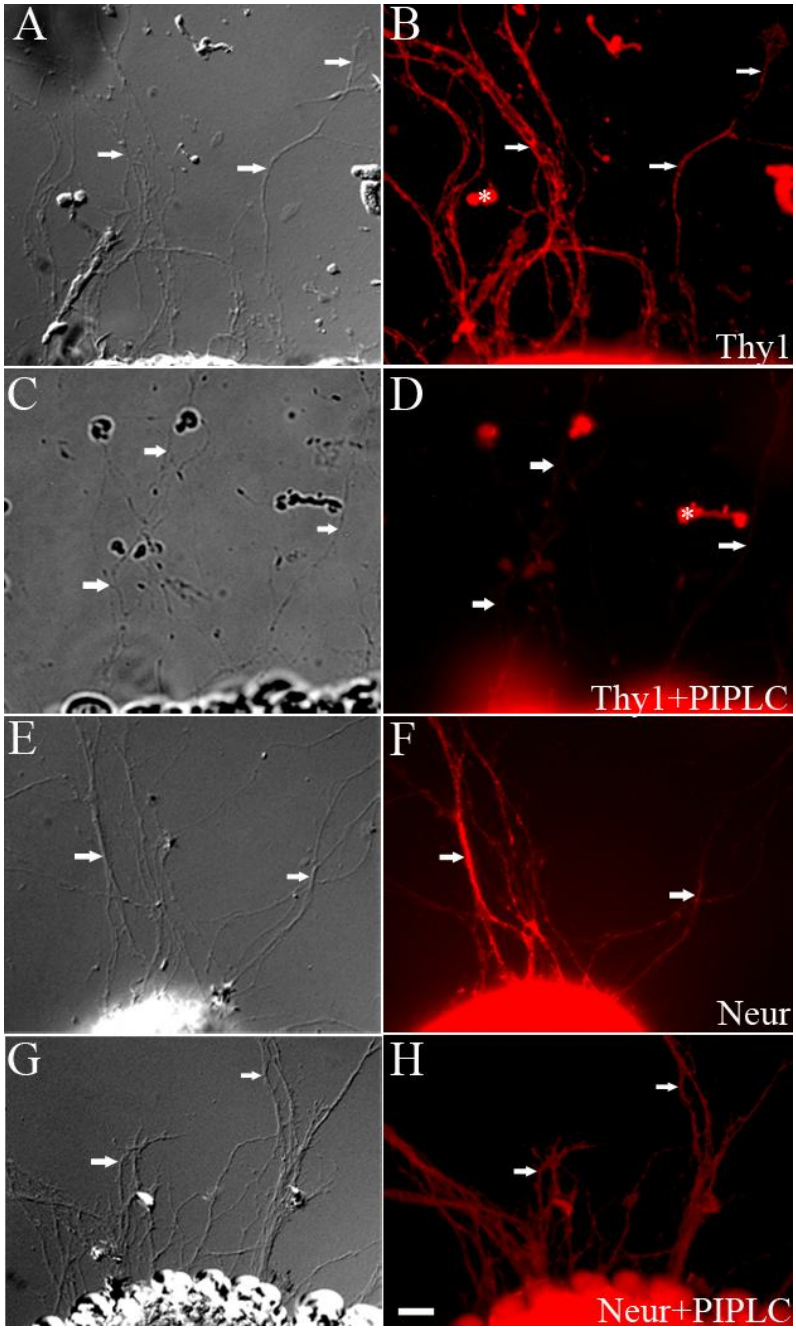

Fig 34. Control of PIPLC enzymatic activity on fish axons. A-H) Fish axons growing out of mini-explants. A-D) Fixed goldfish axons. E-H) Fixed ZF axons. A and B) Axons were stained with M802 ABs against the GPI-anchored protein Thy1 (white arrows in B). C and D) Axons were treated with PIPLC prior to fixation and staining with M802 ABs. Note that the staining is absent or very week after PIPLC treatment (white arrows in D).E and F) Axons were stained with ZN5 ABs, against the non- GPI-anchored protein Neurolin in the presence or absence of PIPLC (white arrows in F and H). Asterisks in B and D is unspecific staining. Primary ABs as well as red Cy-3 conjugated secondary ABs were used in a dilution of 1:1000. Scale bar; 20 µm.

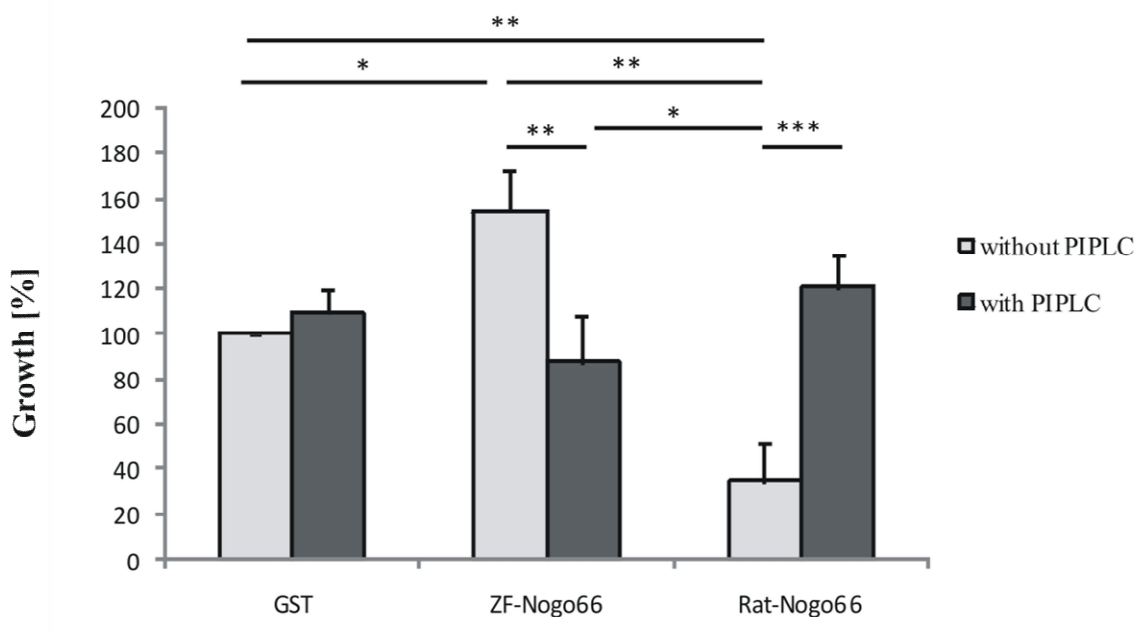

Fig. 35. Axon outgrowth assay using PIPLC enzymatic treatment. Percentage of ZF RGC axon growth after 24h in culture. With PIPLC treatment more axons are growing on Rat-Nogo66 substrate, and less axons are growing on ZF-Nogo66 substrate, compared to the non-treated axons. GST substrate was used as growth control. Bars in each column represent standard error and asterisks indicate significant difference (* $P< 0.05$, ** $P< 0.01$ and *** $P< 0.001$) by student's *t*-test.

6. Expression analysis for the rtn-4 gene during ZF embryonic development

The rtn-4 gene is highly conserved among species (Oertle et al., 2003a), and its function might therefore be conserved. Besides the inhibitory role of the mammalian RTN4-Nogo-A in axonal regeneration, RTN4 proteins may have functions in the endoplasmic reticulon (ER), where they are most heavily expressed (Oertle et al., 2003b). They also seem to function during CNS development since RTN4-Nogo-A is present in neurons (Huber et al., 2002). In fish, previous studies on the expression of ZF-Rtn4 mRNA by RT-PCR have shown the presence of the three transcripts Rtn4-l, -m and -n during ZF development (Diekmann et al., 2005). To assess where zf-rtn4 is expressed and active during development, we performed whole mount *in situ* hybridization (ISH) on ZF embryos. Transcription of ZF-Rtn4-l was examined in 6 hpf to 48 hpf old embryos (Figure 36A-E), and in 3 dpf to 10 dpf old larvae (Figure 36F-I). ZF-Rtn4 mRNA transcripts are present in all tested stages (Figure 36).

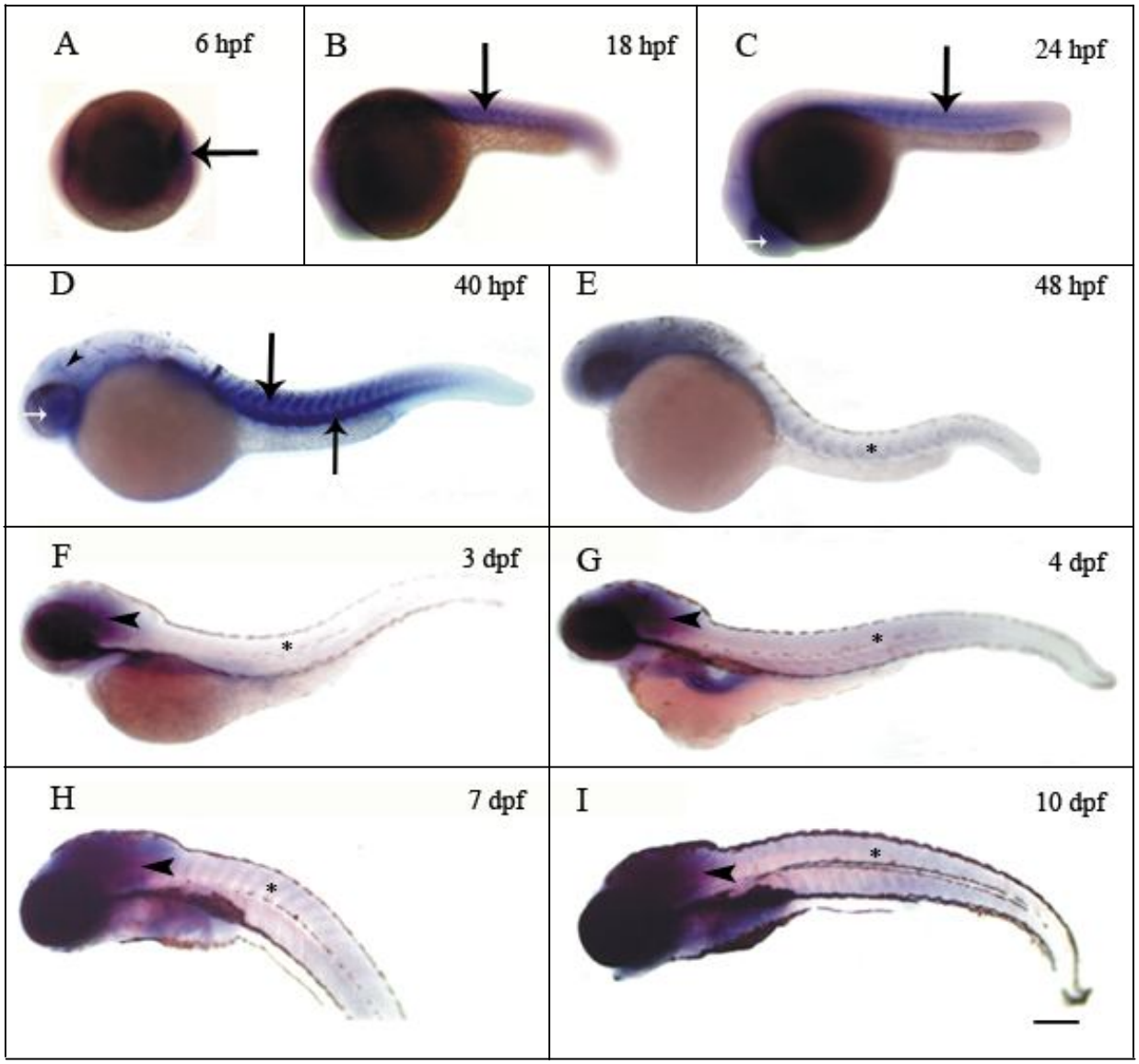

Fig 36. Expression patterns of Rtn4-l mRNAs in 6 hpf –10 dpf ZF embryos. A-I) Lateral view. A) at 6 hpf ZF-Rtn4 mRNAs are detected by *in situ* hybridization in cells at the embryonic shield (black arrow). B-D) from 18 hpf (C) until 40 hpf (D) increased expression of ZF-Rtn4 mRNAs is detected in the somites (black arrow) as well as in the eye lens (white arrow). At 40 hpf, ZF-Rtn4 mRNAs are expressed in some brain structure (black arrowhead). E-I) Expression pattern of ZF-Rtn4 disappear from the somites (asterisk) and increase progressively in the entire brain (black arrowhead). hpf is hour(s) post fertilization, dpf is day(s) post fertilization. Scale bar; 200µm.

At 6 hpf ZF-Rtn4-l mRNAs are detected in cells from the embryonic shield (black arrow in A), and are from 18 hpf to 40 hpf increasingly expressed in the somites (black arrow in B, C and D), in the eye lens (white arrow in C and D), and in some brain structure (black arrowhead in D). Interestingly, Rtn4-l expression pattern in the somites disappears completely within the first 48 hpf (asterisk in E). However, from early to late larvae (3 dpf to 10 dpf) the entire brain becomes a new expression domain, where the Rtn4-l mRNAs are increasingly expressed (black arrowhead in F-I). In parallel, the two other Rtn4-m and -n splice forms were analyzed from 6 hpf to 40 hpf. Interestingly, they had exactly the same expression pattern as the Rtn4-l (data not shown). Here, we found that the three transcripts Rtn4-l, -m and -n have related spatio-temporal expression patterns, at least up to 40 hpf, showing weak expression at early stages and a developmental increase in the signal, particularly restricted to the somites, and Rtn4-l is increasingly expressed in the brain of larval stages. Thus, ZF Rtn-4-Nogo mRNAs are strongly expressed in ZF embryonic somites and larval brain, and might play a role in the development of neural and non-neural structures.

IV. Discussion

Results in this thesis have uncovered a new cause underlying successful axon regeneration in the fish CNS: Nogo-66 of fish RTN-4 has no inhibitory effect on fish RGC axon growth and is, instead, growth-permissive. Rat-Nogo66, however, which is known to inhibit axon growth in mammals, also inhibits fish axon growth in the present cross-species *in vitro* assays. Thus, ZF- and Rat-Nogo66 have opposite effects on growing axons in spite of being 67% identical. In similar assays, Rat-NIGΔ20 of the NogoA-specific domain, a well-known and strong inhibitor of axon growth, hinders ZF RGC axon elongation in culture. Yet, the NogoA-specific domain is absent from the zf rtn-4/nogo gene (Diekmann et al., 2005). Our results, therefore, imply that the ZF version of RTN-4/Nogo exerts no negative influence on axon regeneration in fish, neither in tissue culture, nor *in vivo*. This view is supported by recent results with mammalian hippocampal neurons showing that ZF-Nogo66 supports neurite extension whereas Rat-Nogo66 blocks neurite growth. In addition, ZF RGC axons may respond to the Rat-Nogo66 inhibitory action via the GPI-anchored receptor NgR, since RGC axons became less sensitive to Rat-Nogo66 when treated with the enzyme PIPLC.

1. ZF-Nogo66 versus Rat-Nogo66 and NIGΔ20

Our conclusion concerning the growth-permissive properties of ZF-Nogo66 is derived from three independent assays with growing fish axons. The “quantitative outgrowth assay” with Nogo-peptides as substrates for RGCs demonstrated that ZF-Nogo66 has growth-permissive substrate properties for fish axons whereas Rat-Nogo66 and Rat-NIGΔ20 blocked axon growth. The “collapse assay” showing collapse in 82% and 78% of the growth cones exposed to NIGΔ20 and Rat-Nogo66, respectively, revealed elongation instead of collapse in 79% of the growth cones when ZF-Nogo66 was applied. Likewise, in the “contact assay” with HeLa cells expressing ZF-Nogo66-EGFP-GPI on their surface, long lasting exploratory growth and crossing occurred in 65% of the growth cones in contact with the cells, whereas Rat-Nogo66-EGFP-GPI expressing cells were avoided (42%) and caused collapse (42%) in altogether 84% of the growth cones thereby preventing growth across the cells. NIGΔ20-EGFP-GPI expressing cells elicited collapse in 63% of ZF growth cones and avoidance in 20%, and therefore blocked growth in 83% of the growth cones.

The assays testing the influence of the Nogo peptides on fish RGC axons exhibited a collapse/avoidance rate of less than 25% with ZF-Nogo66, with the non-inhibitory GST and with EGFP-GPI transfected and untransfected cells. This percentage was the same as in

earlier work with growth-permissive substrates/reagents and fish RGC axons as well as with rat dorsal root ganglion cell axons (Wanner et al., 1995) so that we consider this rate as "background collapse" as opposed to the three times higher collapse/avoidance rates prompted by inhibitory substrates/reagents. This finding is consistent with earlier results showing the growth-permissive properties of fish CNS myelin for fish and mammalian axons (Bastmeyer et al., 1991; Wanner et al., 2005).

Thus, the new and central result of our work is the finding that ZF-Nogo66 is growth-permissive and does not impair ZF RGC axon growth *in vitro* and obviously also not *in vivo*. Together with earlier findings showing the lack of the entire N-terminal portion of the rtn-4 gene encoding the Nogo-A specific domain (Diekmann et al., 2005), the present results suggest that absence of the Nogo-A specific inhibitory domain and the transition from inhibitory to growth-permissive properties of Nogo-66 correlates with and seems to be causally linked to the success of axon regeneration in fish.

In addition we noted when analysing the ZF-Nogo66 effect on growth of RGC axons in the three assays that ZF-Nogo66 tended to promote growth of more axons compared with controls. In the collapse assay, growth cones showed an interesting response to the soluble ZF Nogo-66. They grew towards the source of the peptide as shown in Figure 20 F, probably because these growth cones interpret the ZF-Nogo66 as an attractive molecule, and thus moved towards it. Moreover, in the outgrowth assay where the percentage of growth was measured, 154% of axon growth was measured for the ZF-Nogo66, compared with 100% for the GST control and 34% for the Rat-Nogo66, which are statistically different. Thus, ZF-Nogo66 seems to not only permit the growth of axons but to promote growth. If this is so, ZF-Nogo66 influences growth cones into the opposite direction than the mammalian version. Not surprising, since the fish visual system seems to be equipped with an environment favourable for successful axon regeneration. The growth-promoting influenced properties have to be proven in further *in vitro* assays. For instance; the length of the growing axons on ZF-Nogo66 can be determined. Perhaps, ZF-Nogo66 participates in the neuronal upregulation of growth associated molecules, and an *in vivo* knockdown of RTN-4/Nogo-66 may clarify whether it is essential for axon regeneration.

2. Rat-Nogo66 versus Rat-NIGΔ20

By comparing the strength of growth inhibition between the two mammalian inhibitory molecules, Rat-NIGΔ20 and Rat-Nogo66, we found an interesting difference. In contact

assays, when the growth cone collapse and avoidance responses are added, Rat-NIGΔ20 and Rat-Nogo66 affect ZF growth cones to almost the same extent (83-84%, respectively). However, NIGΔ20 causes more collapse (63%) than Rat-Nogo66 (42%). Together with the outcome of the outgrowth assay demonstrating significantly fewer ZF axons on NIGΔ20 than on Rat Nogo-66, these observations may suggest that Nogo-A is a stronger growth inhibitor than Rat Nogo-66, - at least for ZF RGC axons. This difference may be due to the fact that the Nogo-A induced- collapse or -inhibition is not only caused by the Rho/Rock pathway which is also known to be regulated by Rat-Nogo66, but also by a signal transduction pathway leading to rise in intracellular calcium, through calcium release from intracellular stores (Bandtlow et al., 1993) (Figure 3). Whether Rat-Nogo66 provokes a similar affect has not been published. Moreover, Nogo-A is the only myelin-associated inhibitor which has been proven to affect axon regeneration *in vivo.* Application of the antibodies IN-1 against Nogo-A to the lesioned spinal cord resulted in regeneration of small number of axons (Schnell and Schwab, 1990). So far, no *in vivo* evidence for the inhibitory activity of Nogo-66 has been reported.

3. Presence of Rtn-4/Nogo-66 in the environment of regenerating ZF axons

Cell culture assays, as important they are to evaluate substrate properties, permit reasonable conclusions if the substrates under consideration are present along the pathway of regenerating axons; and so are the growth-permissive properties of ZF-Nogo66 relevant only if axons encounter this peptide on the glial cell surface or myelin/cell debris in the fish retinotectal pathway after optic nerve lesion. First, RT-PCR demonstrated mRNA expression of ZF rtn-4/nogo-66 in regenerating optic nerve tissue and cultured glial cells of the optic nerve. By immunostainings with ABs against ZF-Nogo66 we could reveal the cellular localisation of Nogo-66 in glial cells derived from the regenerating optic nerve. We found Nogo-66 only inside the cells and not exposed on cell surface in live cells. This however, does not exclude that small amounts may be surface-exposed as demonstrated with sophisticated methods in case of Nogo-A (Dodd et al., 2005). Moreover, RTN4-Nogo66 proteins may be found in cellular debris at the lesion site following nerve crush, where regenerating axons contact Nogo-66. Additionally, in our lab parallel *in vivo* experiments analysing the Nogo-66 localization with ABs against ZF-Nogo66 demonstrated the presence of Nogo-66 in glial cells, RGC axons and CNS myelin (A. Shypitsyna). Yet, since ZF-

Nogo66 in the optic nerve is associated with myelin and myelin debris, which is contacted by regenerating axons (Strobel and Stuermer, 1994), growth cones are expected to come in contact with Nogo-66 repeatedly along their path to the brain *in vivo*. These *in vivo* expression analyses for Nogo-66 provide new evidence for the permissiveness of Nogo-66, which is consistent with the *in vitro* findings described above.

4. Nogo receptors and ZF growing axons

With *in vitro* assays we have shown that ZF RGC axons respond to the inhibitory activity of Rat-Nogo66. Growing ZF axons need a receptor for this inhibitor in order to get inhibited when confronted with Rat-Nogo66, as substrate or soluble molecule. As it is known that NgR1 is the receptor for the Nogo-66 (Fournier et al., 2001), mediating inhibition and collapse, fish axons also have a receptor (Klinger et al., 2004), a homolog of Rat-NgR1. So why do fish have a receptor for inhibition, when they are able to regenerate? Is ZF-NgR not binding to the ZF-Nogo66 but binding to the Rat-Nogo-66 to mediate inhibition *in vitro* assays? To solve this question we tested whether NgR is expressed by RGCs and exposed on the surface of growing axons. On the mRNAs level using RT-PCR and ISH we found the ngr gene expressed in retina and more specifically in RGC neurons. Moreover, by immunostaining, NgR protein was found localized on the surface of growing axons. This finding confirms that NgR is a candidate receptor mediating inhibition by the Rat-Nogo66. To bring evidence for a possible NgR implication in Rat-Nogo66-mediated inhibition, we treated RGC axons with PIPLC to cleave off all GPI-anchored proteins on the surface, the inhibitory effect of the Rat-Nogo66 on growing axons was highly reduced. This means that probably NgR or other unknown GPI-anchored receptors are involved. More interesting, ZF-Nogo66-permissive effect for axon growth was reduced when RGC axons were treated with PIPLC, which means probably that ZF-Nogo66 promotes growth of axons by acting via a GPI anchored receptor.

But still in order to prove NgR involvement more functional assays have to be performed. One experiment along these lines is the blockade of NgR using antibodies, in order to reverse inhibition exerted by the Rat-Nogo66. It will be more interesting to perform *in vitro* binding assays between the ZF-NgR receptor and the Rat versus ZF Nogo-66 ligands. The issue of these assays is to know whether Rat-Nogo66 binds to ZF-NgR and ZF-Nogo66 to ZF or Rat-NgR. If only the Nogo-66 from rat who binds to ZF-NgR, this will support its inhibitory role in fish axons and may clarify why one Nogo-66 is inhibitor (Rat) and the other one not (ZF). But if both bind to the receptor, this may mean probably that Rat-Nogo66 binds and activates

NgR while the ZF-Nogo66 binds without activating the receptor. Then we may speculate that other co-receptors complexes assemble and signal following ZF-Nogo66 binding. Also, using biochemical tools, it has to be tested if the collapse signaling pathway is active when ZF axons grow on Rat-Nogo66 but not when growing on ZF-Nogo66. This will be necessary to understand the difference of their effect on axon growth.

Interestingly, we found that three NgRs are expressed in the retina (ZF-NgR, ZF-NgRH1a and ZF-NgRH2). They are probably all expressed on axons but may function differently. We can speculate that ZF-Nogo66 may bind to NgR which has no inhibitory effect. Binding can also occur via NgRH2 the homolog of mammalian NgR3, which has no inhibitory activity in mammals (Venkatesh et al., 2005). If these issues are solved we can better understand why ZF axons respond differently to the Rat- and ZF-Nogo66.

Rat-NIGΔ20 has already been shown to inhibit ZF axon growth (Dieckmann et al., 2005). The fact that ZF axons as well as Rat axons collapse in contact with NIGΔ20 suggest that they both have a receptor Nogo-A NIGΔ20. This rises an intriguing question: why do fish a have a receptor for Nogo-A, while not having the Nogo-A domain as ligand. Once the receptor is identified in mammals, we will try to find its homolog in fish, and prove its involvement in mediating inhibition by binding to NIGΔ20. The presence of the Nogo-A receptor in fish could be explained if the Nogo-A ligand may have existed very earlier in evolution in fish ancestors perhaps with diffrent function, and co-evolved together with the Nogo-A receptor. But teleost fish lost the ligand as is suggested by Diekmann et al (2005).

5. Absence of axon growth inhibitors and plasticity

The absence of Nogo inhibitors from the fish CNS correlates not only with axon regeneration but also with the remarkable plasticity of nerve connections in the fish retinotectal pathway (Gaze, 1970; Stuermer and Easter, 1984). The fish retinotectal projection is continuously re-organised in a process known as shifting connection (Stuermer and Easter, 1984; Easter and Stuermer, 1984), and such plasticity might require absence of inhibitory Nogo domains. It is also conceivable that absence of inhibitory substrates permits the exploratory behaviour of regenerating fish axons and the formation of the exuberant axon branches (Schmidt et al., 1988; Stuermer, 1988a,b) characteristic for fish RGC axons *in vivo*.

It has been demonstrated that axon regeneration is negatively affected by a number of other myelin/oligodendrocyte-, macrophage- and astrocyte/fibroblast-associated molecules (Schwab, 2004; Yiu and He, 2006), but no glial scar-associated growth inhibiton was found

earlier in goldfish (Hirsch et al., 1995). Glial cell-derived soluble factors actually support axon regeneration (Schwalb et al., 1996). From the vigorous re-growth that fish RGC axons exhibit upon optic nerve lesion we would assume that MAG, OMgp and further myelin proteins negatively affecting axon growth in mammals (Yiu and He, 2006), probably have no or only weak inhibitory influence on fish axon growth - if not absent altogether.

In fish, however, it is not only the growth-permissive nature of glial cells in the optic nerve which allows axon regeneration, but other parameters contribute to the success of axonal regeneration. The extraordinary neuron-intrinsic properties bring axotomized fish RGCs into an optimal growth state (Stuermer et al., 1992; Munderloh et al., 2009) and the fibroblasts at the transection site provide physical support for growing axons during regeneration (Hirsch et al., 1995).

6. Nogo inhibitors in fish axon regeneration?

Nogo-A in mammals interferes with sprouting of CNS axons (Meyenburg et al., 1998; Buffo et al., 2000) and counteracts plasticity. It is tempting to speculate that fish RGC axon regeneration might be blocked and the retinotectal plasticity might be less effective if the mammalian version of the Nogo gene would be expressed in the fish CNS. It will be interesting to test whether Rat-Nogo66 as well as the Rat-Nogo-A specific region can be introduced into ZF-myelinating cells transgenically, and to see if this will affect regeneration and plasticity. One way towards testing this speculation was the transfection of fish oligodendrocytes in culture with the rat Nogo-A derived NIGΔ20 sequence linked to a GPI-anchor from fish PrP. In the co-culture assays we looked for contact between NIGΔ20 transfected oligodendrocytes and growth cones, but no contact has been found, because of the low transfection rate of oligodendrocytes. Primary adult oligodendrocytes are known to be difficult to transfect. If NIGΔ20 is sufficient to turn growth supportive into inhibitory cells, this will be remarkable in so far, as fish oligodendrocytes in culture (and *in vivo*) are highly growth supportive, not only for fish but also for mammalian neurons (Batsmeyer et al., 1993).

When monitoring the successfully transfected fish oligodendrocytes, cells expressing the NIGΔ20 were seen to loose their processes. Oligodendrocytes in culture are known to be proliferative and to have the tendency to form a cell carpet (Bastmeyer et al., 1989). Obviously, they use their processes, which are rich in cell adhesion molecules such as E587 (L1 family) for cell motility and cell-cell contact formation (Ankerhold et al., 1998). Why these cells undergo morphological change when expressing Rat-NIGΔ20 is unclear but may

result from overexpression of intracellular NIGΔ20 or surface exposed NIGΔ20. NIGΔ20 may be toxic for cells, being a foreign molecule or when surface exposed, NIGΔ20 may negatively affect contact formation between cells. To discriminate between the possibilities, we will have to express NIGΔ20 without GPI anchor which should exclusively remain in the cell, to see if cells are still retracting processes.

7. Was the Nogo-associated inhibition lost from the fish CNS or acquired in the tetrapod CNS during evolution?

In light of the difference between the fish and tetrapod nogo genes, two main questions arise 1) have fish lost Nogo-66 inhibition and the entire NogoA-specific domain or, 2) have tetrapods acquired an inhibitory version of Nogo-66 and – even more important – did they gain Nogo-A during evolution:

1) Loss of inhibition in fish: As stated above, fish possess a RTN-4-specific RHD and the relevant rtn-4 gene (Diekmann et al., 2005). Yet, the N-terminus of fish rtn-4/nogo has no similarity neither in sequence or in length with the mammalian N-terminal Nogo-A specific region. In contrast to rtn-4, another member of the rtn family, rtn-1, has the same exon-intron structure in fish as in mammals (Diekmann et al., 2005). Thus, it would seem that teleosts lost all exons corresponding to the Nogo-A domain during evolution. Moreover, comparison between the genomic organisation of the mammalian rtn-4 and fish rtn-4 have revealed that genes upstream to rtn-4 gene (MTIF2 and RPS27A) were conserved in fish, but the gene nearest to the N-terminal rtn-4 called FLJ31438 was absent (Figure 37) (Diekmann et al., 2005), suggesting that during evolution a genomic region containing FLJ31438 gene and the inhibitory Nogo-A N-terminal region have been lost in fish rather than being acquired in land vertebrates (amphibians, birds and mammals). This hypothesis needs to be substantiated by a thorough analysis of the genomes of sharks and vertebrate ancestors of fish, to see whether it existed before teleosts. Should Nogo-A turn out to be the most crucial myelin-associated inhibitor for axon growth, it also appears possible that mammals did not lose the ability to regenerate but rather that teleosts acquired this ability through loss of exons in the rtn-4 gene.

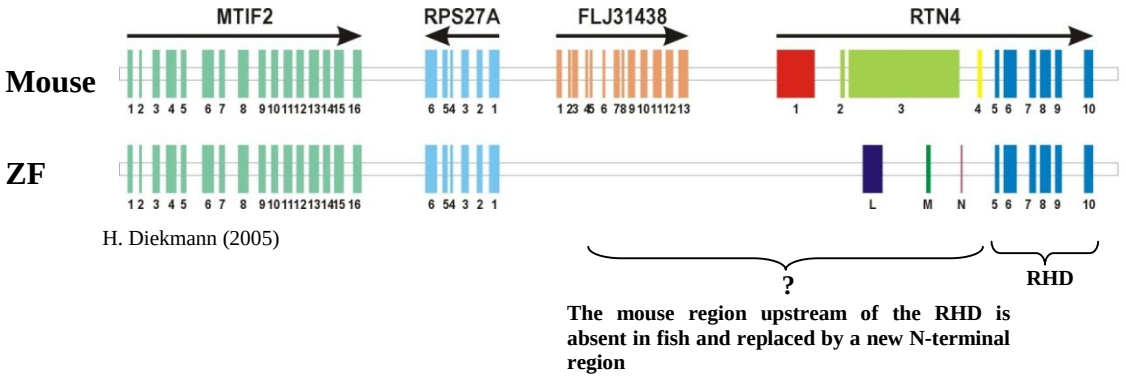

Fig 37. Model of the evolution of fish rtn-4 N-termini. Exchange of the genomic region directly upstream of the reticulon homology domain (RHD).

But why the highly conserved RHD with the Nogo-66 domain exists in fish in a version which is not inhibitory to growing axons remains elusive. Mammalian and fish Nogo-66 differ in roughly 33% of the amino acids (Figure 7). It is conceivable that the exchanges of the aa cause a change in the 3-D structure of Nogo-66. It needs to be determined whether in Rat-Nogo66 amino acids (aa) changes would cause disruption of the α-helical domain (He et al., 2003), implying a different affinity to the relevant receptor(s) and activation of different signal transduction pathways. Genetics can be a good tool to find out which amino acid(s) are crucial for functional inhibitory Nogo-66, by mutating the fish version into rat version and testing different mutants in axon growth assays. Another possibility is that the structural alterations as a consequence of amino acid exchanges may impair Nogo-66 binding to NgR receptors and thus disrupt receptor-ligand dependent growth inhibition, which then raises the question which ligand, if not ZF-Nogo66, would bind to ZF-NgR(s). The question, to which receptor Rat-Nogo66 may bind, and whether ZF-NgR(s) signal via Rho and Rho-kinase (Niederoest et al., 2002; Fournier et al., 2003) to provoke actin depolymerisation and hence growth cone collapse, requires further investigations. Thus, these inhibitory systems may be lost in fish to allow successful regeneration.

2) Gain of inhibition in land vertebrate: Most of the known RTN-4 proteins in different species have a relatively short N-terminal sequence, which is similar to that of Nogo-B and -C. The very long N-terminal sequence of Nogo-A appears very late in evolution, at the frog level, probably emerging during the transition from fish to land vertebrates (Oertle et al., 2003a) and suggest that Nogo-A is the result of a fusion between an ancient rtn homology domain at the C-terminus and a Nogo-A specific exon at the N-terminus, whereby the protein may have adopted a new function that of neurite growth inhibitor in oligodendrocytes. This

will be in line with the well known, high regeneration potential of the CNS after lesion in fish, which lack Nogo-A.

It is known in mammals that the highly conserved Nogo-66 domains of different RTN family members are functionally different. It has been shown by *in vitro* assays that the inhibitory activity is specific for Nogo-66 from RTN-4 and not found in RTN-1, 2 and 3 (GrandPré et al., 2000). Therefore, since lower vertebrates like fish have the RTN4-Nogo66 in a non-inhibitory version, they probably have no other inhibitory family members. Thus, inhibitory Nogo-66 might have been acquired with the Nogo-A specific region in land vertebrates to restrict regeneration plasticity.

In land vertebrates, Nogo-A is not only present in mammals, but also in birds (chick, *Gallus gallus*). Nogo-A is found in myelinating oligodendrocytes where it exerts its inhibitory activity for axon regeneration with the onset of myelination (O'Neill et al., 2004). Amphibians (frog, *Xenopus leavis*) also possess Nogo-A (Klinger et al., 2004). Frogs have an intermediate position in axon regeneration between different classes, because, in contrast to the optic nerve, frog spinal cord axons fail to regenerate after lesion. In addition, *in vitro* assays have shown that unlike the frog tectum opticum, the the spinal cord is nonpermissive for axon regeneration, which speaks for absence of inhibitors such as Nogo-A in the visual system. Moreover, IN-1 has been shown to stain myelinated tracts of frog spinal cord but not optic nerve (Lang et al., 1995). Using antibodies against Nogo-A, the inhibitor has been detected in myelinated fiber tracts of the spinal cord, optic nerve, tectum opticum and in isolated oligodendrocytes (Klinger et al., 2004), suggesting that Nogo-A in frog myelin might contribute to the failure of spinal cord regeneration. But how can the optic nerve regenerate successfully despite the presence of the Nogo-A? One speculation is that IN-1 antibodies recognize a Nogo-A posttranslational modification or conformational epitope relevant for surface exposure and function, and found only in the spinal cord and not in the optic nerve. In addition, myelin and oligodendrocytes are growth supportive in the frog visual system (Lang et al., 1995). In reptiles, the lizard (*Lizard Gallotia Galloti*) appears to have non-permissive substrate properties in CNS myelin and oligodendrocytes that block axon growth from mammalian neurons which indicates the existence of mammalian-like neurite inhibitor (Lang et al., 1998). However, the sensitivity of lizard RGC axons to these non-permissive substrates and to the mammalian neurite growth inhibitors seems reduced compared with mammalian axons (Lang et al., 1998). Apparently lizard RGC neurons seem to have properties which allow them to grow through non-permissive territories and therefore regenerate successfully. The fact that lizard axons are less sensitive to non-permissive substrates may be due to the

absence of receptors for inhibitors such as the Nogo-A or Nogo-66 receptors or changed signal transduction (Lang et al., 1998). Furthermore, since the brain is highly complex in higher vertebrates like “mammals, birds and amphibians” than in lower vertebrates “fish”, the Nogo-A and the inhibitory version of Nogo-66 may be acquired during evolution to have a stabilizing role on neural connections once they have been formed and myelinated during development.

8. Possible functions of ZF rtn-4 during development

Despite active research on the RTN4-Nogo function in regeneration of the adult CNS, the biological functions of this molecule in the developing animals are not well understood. We have explored the zf-rtn4 gene expression during embryonic and larval development in purpose to try to understand whether it has a function in space and time during ZF development. Which function the conserved RHD region containing the Nogo-66 domain subserves in embryos and which role the N-terminal variable sequences l, m and n may play, which are exclusively present in fish and absent in all land vertebrates are open questions. As a first step we used the ISH technique to analyse the Rtn-4 mRNAs distribution and found that all three transcripts Rtn4-l, -m and -n are expressed in embryos in the same spatio-temporal pattern. They were expressed early during development at 6 hpf by cells from the embryonic shield, and are probably important for gastrulation. More interestingly, the expression proceeds in later embryos, specifically in the eye lens and in some brain structure but is stronger in the somites. This means that rtn-4 gene may have diverse functions in different cell types. Moreover, we found an increase of rtn-4 expression in the somites up to 40 hpf, but no expression at 48 hpf or older embryos. Therefore, rtn-4 may function during somite formation, which become later the dermis (dermatome), skeletal muscle (myotome), and vertebrae (sclerotome). Since the anti-sense riboprobes used in our experiment are specific for both common RHD and the variable l, m and n regions, we are not sure whether the same pattern will be found for the three transcripts. In addition, we found Rtn4-l expressed in the larval brain with a diffuse pattern in all structures, increasing from earlier to later larvae, indicating that Rtn-4 might play a role in CNS development. In future, it will be interesting to clarify which role rtn-4 plays in these tissues at increasing ages. First, studying its expression by immunostaining will help us to know where exactly it is expressed, in which stages, tissues and cell types and if the RNA pattern reflects the protein distribution. Moreover, to get inside into its role during development, functional studies have to be performed in order to alter gene expression. Recently, Broesamle et al (2009) observed defect

in ZF PNS neurons, with shorter and defasciculated axon phenotypes when they knocked down the rtn4-n isoform using the morpholino (MO) technique. They claim that ZF-RTN4/Nogo plays a developmental role in axon growth and pathfinding, and consider it as a repulsive guidance molecule in interaction with NgR receptor. If this Nogo property is involved in growth-promotion (shorter axon phenotype in morphants) this might correspond to our *in vitro* assay where Nogo-66 is growth-permissive. We also do not exclude the possibility that RTN-4/Nogo-66 can have a function as guidance molecule during CNS development. Moreover, Broesamle et al describe Nogo as a ligand for the NgR and thus repelling axons, but no protein expression and localization analysis or binding assays were performed.

Altogether, we conclude that in contrast to the mammalian Nogo-66, fish Nogo-66 has no inhibitory function and is growth-permissive for ZF axon growth. Fish Nogo-66 is present in the environment where axons regenerate and seems not to negatively affect their growth. Fish RGC axons respond to the inhibitory effect of Rat-Nogo66 probably via the NgR, which is located on the surface of growing axons.

V. Literature

Aguayo, A.J., David, S. and Bray, G.M. (1981) Influences of the glial environment on the elongation of axons after injury: transplantation studies in adult rodents. **J Exp Biol**. **95**:231-40.

Ankerhold, R. and Stuermer, C.A.O. (1999) Fate of oligodendrocytes during retinal axon degeneration and regeneration in the goldfish visual pathway. **J Neurobiol 41**:572-584.

Atwal, J.K., Pinkston-Gosse, J., Syken, J., Stawicki, S., Wu, Y., Shatz, C. and Tessier-Lavigne, M. (2008) PirB is a functional receptor for myelin inhibitors of axonal regeneration. **Science. 322**(5903):967-70.

Bandtlow, C.E., Schmidt, M.F., Hassinger, T.D., Schwab, M.E. and Kater, S.B. (1993) Role of intracellular calcium in NI-35-evoked collapse of neuronal growth cones. **Science. 259**(5091):80-3.

Bandtlow, C.E. and Löschinger, J. (1997) Developmental changes in neuronal responsiveness to the CNS myelin-associated neurite growth inhibitor NI-35/250. **Eur J Neurosci. 12**:2743-52.

Barton, W.A., Liu, B.P., Tzvetkova, D., Jeffrey, P.D., Fournier, A.E., Sah, D., Cate, R., Strittmatter, S.M. and Nikolov, D.B. (2003) Structure and axon outgrowth inhibitor binding of the Nogo-66 receptor and related proteins. **EMBO J. 22**(13):3291-302.

Bastmeyer, M., Beckmann, M., Nona, S.M., Cronly-Dillon, J.R. and Stuermer, C.A.O. Identification of astrocyte- and oligodendrocyte-like cells of goldfish optic nerves in culture. **Neurosci Lett. 101**(2):127-32.

Bastmeyer, M., Beckmann, M., Schwab, M.E. and Stuermer, C.A.O. (1991) Growth of regenerating goldfish axons is inhibited by rat oligodendrocytes and CNS myelin but not by goldfish optic nerve tract oligodendrocytelike cells and fish CNS myelin. **J Neurosci 11**:626-40.

Bastmeyer, M., Bähr, M. and Stuermer, C.A.O. (1993) Fish optic nerve oligodendrocytes support axonal regeneration of fish and mammalian retinal ganglion cells. **Glia. 8**:1-11.

Becker, T., Wullimann, M.F., Becker, C.G., Bernhardt, R.R. and Schachner, M. (1997) Axonal regrowth after spinal cord transection in adult zebrafish. **J Comp Neurol. 377(4)**:577-95.

Benfey, M. and Aguayo, A.J. (1982) Extensive elongation of axons from rat brain into peripheral nerve grafts. **Nature 296**: 150-2.

Bernhardt, R.R., Tongiorgi, E., Anzini, P. and Schachner, M. (1996) Increased expression of specific recognition molecules by retinal ganglion cells and by optic pathway glia accompanies the successful regeneration of retinal axons in adult zebrafish. **J Comp Neurol. 376**(2):253-64.

Bolin, L.M. and **Shooter, E.M**. (1994) Characterization of a schwann cell neurite-promoting activity that directs motoneuron axon outgrowth. **J Neurosci Res. 37**:23-35.

Bhatheja, K. and Field, J. (2006) Schwann cells origins and role in axonal maintenance and regeneration. **Int J Biochem Cell Biol. 38**(12):1995-9.

Bomze, H.M., Bulsara, K.R., Iskandar, B.J., Caroni, P. and Pate Sken, J. H. (2001) Spinal axon regeneration evoked by replacing two growth cone proteins in adult neurons **Nat Neurosci. 4**, 38 – 43.

Boyd, J.G., Gordon, T. (2003) Neurotrophic factors and their receptors in axonal regeneration and functional recovery after peripheral nerve injury. **Mol Neurobiol. 27**(3):277-324.

Bradbury, E.J., Moon, L.D., Popat, R.J., King, V.R., Bennett, G.S., Patel, P.N., Fawcett, J.W. and McMahon, S.B. (2002) Chondroitinase ABC promotes functional recovery after spinal cord injury. **Nature. 416**(6881):636-40.

Broesamle, C., Huber, A.B., Fiedler, M., Skerra, A. and Schwab, M.E. (2000) Regeneration of lesioned corticospinal tract fibers in the adult rat induced by a recombinant, humanized IN-1 antibody fragment. **J Neurosci. 20**(21):8061-8.

Broesamle, C. and Halpern, M.E. (2009) Nogo–Nogo receptor signaling in PNS axon outgrowth and pathfinding. **Mol Cell Neurosci. 40**(4):401-9.

Bregman, B.S., Kunkel-Bagden, E., Schnell, L., Dai, H.N., Gao, D. and Schwab, M.E. (1995) Recovery from spinal cord injury mediated by antibodies to neurite growth inhibitors. **Nature. 378**(6556):498-501.

Buffo, A., Zagrebelsky, M., Huber, A.B., Skerra, A., Schwab, M.E., Strata, P. and Rossi, F. (2000) Application of neutralizing antibodies against NI-35/250 myelin-associated neurite growth inhibitory proteins to the adult rat cerebellum induces sprouting of uninjured Purkinje cell axons. **J Neurosci 20**:2275-2286.

Buss, A., Pech, K., Merkler, D., Kakulas, B.A., Martin, D., Schoenen, J., Noth, J., Schwab, M.E. and Brook, G.A. (2005) Sequential loss of myelin proteins during Wallerian degeneration in the human spinal cord. **Brain. 128**:356-64.

Cai, D., Shen, Y., DeBellard, M., Tang, S. and Filbin, M.T. (1999) Prior exposure to neurotrophins blocks inhibition of axonal regeneration by MAG and myelin via a cAMP-dependent mechanism. **Neuron. 22**(1):89-101.

Cai, D., Qiu, J., Cao, Z., McAtee, M., Bregman, B.S. and Filbin, M.T. (2001) Neuronal cyclic AMP controls the developmental loss in ability of axons to regenerate. **J Neurosci. 21**(13):4731-9.

Cai, D., Deng, K., Mellado, W., Lee, J., Ratan, R.R. and Filbin, M.T. (2002) Arginase I and polyamines act downstream from cyclic AMP in overcoming inhibition of axonal growth MAG and myelin *in vitro*. **Neuron. 35**(4):711-9.

Cao, Y., Shumsky, J.S., Sabol, M.A., Kushner, R.A., Strittmatter, S., Hamers, F.P., Lee, D.H., Rabacchi, S.A. and Murray, M. (2008) Nogo-66 receptor antagonist peptide (NEP1-40) administration promotes functional recovery and axonal growth after lateral funiculus injury in the adult rat. **Neurorehabil Neural Repair 22**(3):262-78.

Carbonetto, S., Evans, D. and Cochard, P. (1987) Nerve fiber growth in culture on tissue substrata from central and peripheral nervous systems. **J Neurosci. 7**(2):610-20.

Caroni, P. and Schwab, M.E. (1988) Antibody against myelin-associated inhibitor of neurite growth neutralizes nonpermissive substrate properties of CNS white matter. **Neuron. 1**(1):85-96.

Caroni, P., Savio, T. and Schwab, M.E. (1988) Central nervous system regeneration: oligodendrocytes and myelin as non-permissive substrates for neurite growth. **Prog Brain Res. 78**:363-70.

Carulli, D., Laabs, T., Geller, H.M. and Fawcett, J.W. (2005) Chondroitin sulfate proteoglycans in neural development and regeneration. **Curr Opin Neurobiol. 15**(2):252.

Chen, M.S., Huber, A.B., van der Haar, M.E., Frank, M., Schnell, L., Spillmann, A.A., Christ, F. and Schwab, M.E. (2000) Nogo-A is a myelin-associated neurite outgrowth inhibitor and an antigen for monoclonal antibody IN-1. **Nature 403**:434-9.

Cohen, A.H. and Wallén, P. (1980) The neuronal correlate of locomotion in fish. "Fictive swimming" induced in an *in vitro* preparation of the lamprey spinal cord. **Exp Brain Res.41**(1):11-8.

DeBellard, M.E., **Tang, S**., **Mukhopadhyay, G**., **Shen, Y.J**. **and Filbin, M.T**. (1996) Myelin-associated glycoprotein inhibits axonal regeneration from a variety of neurons via interaction with a sialoglycoprotein. **Mol Cell Neurosci. 7**(2):89-101.

Deininger, S.O., Rajendran, L., Lottspeich, F., Przybylski, M., Illges, H., Stuermer, C.A.O. and Reuter, A. (2003) Identification of teleost Thy-1 and association with the microdomain/lipid raft reggie proteins in regenerating CNS axons. **Mol Cell Neurosci. 22**(4):544-54.

Diekmann, H., Klinger, M., Oertle, T., Heinz, D., Pogoda, H-M., Schwab, M.E. and Stuermer, C.A.O. (2005) Analysis of the reticulon gene family demonstrates the absence of the neurite growth inhibitor Nogo-A in fish. **Mol Biol Evol 22**:1635-48.

Dimou, L., Schnell, L., Montani, L., Duncan, C., Simonen, M., Schneider, R., Liebscher, T., Gullo, M. and Schwab, M.E. (2006) Nogo-A-deficient mice reveal strain-dependent differences in axonal regeneration. **J Neurosci. 26**(21):5591-603.

Dodd, D.A., Niederoest, B., Bloechlinger, S., Dupuis, L., Loeffer, J-P. and Schwab, M.E. (2005) Nogo-A, -B and -C are found on the cell surface and interact together in many different cell types. **JBC 280**:12494-12502.

Domeniconi, M., Cao, Z., Spencer, T., Sivasankaran, R., Wang, K., Nikulina, E., Kimura, N., Cai, H., Deng, K. and Gao, Y. (2002) Myelin-associated glycoprotein interacts with Nogo-66 receptor to inhibit neurite outgrowth. **Neuron 35**:283.

Domeniconi, M., Zampieri, N., Spencer, T., Hilaire, M., Mellado, W., Chao, M.V. and Filbin, M.T. (2005) MAG induces regulated intramembrane proteolysis of the p75 neurotrophin receptor to inhibit neurite outgrowth. **Neuron. 46**(6):849-55.

Easter, Jr. S.S. and Stuermer, C.A.O. (1984) An evaluation of the hypothesis of shifting terminals in goldfish optic tectum. **J Neurosci 4**, 1052-1063.

Everly, J.L., Brady, R.O. and Quarles, R.H. (1973) Evidence that the major protein in rat sciatic nerve myelin is a glycoprotein. **J Neurochem. 21**(2):329-34.

Fan, J., Mansfield, S.G., Redmond, T., Gordon-Weeks, P.R. and Raper, J.A. (1993) The organization of F-actin and microtubules in growth cones exposed to a brain-derived collapsing factor. **J Cell Biol. 121**(4):867-78.

Fawcett, J.W. (1992) Intrinsic neuronal determinants of regeneration. **Trends Neurosci. 15**(1):5-8.

Fournier, A.E., GrandPre, T. and Strittmatter, S.M. (2001) Identification of a receptor mediating Nogo-66 inhibition of axonal regeneration. **Nature 409**:341-346.

Fournier, A.E., Gould, G.C., Liu, B.P., Strittmatter, S.M. (2002) Truncated soluble Nogo receptor binds Nogo-66 and blocks inhibition of axon growth by myelin. **J Neurosci 22**(20):8876-83.

Fournier, A.E., Takizawa, B.T. and Strittmatter, S.M. (2003) Rho kinase inhibition enhances axonal regeneration in the injured CNS. **J Neurosci. 23**(4):1416-23.

Freund, P., Wannier, T., Schmidlin, E., Bloch, J., Mir, A., Schwab, M.E. and Rouiller, E.M. (2007) Anti-Nogo-A antibody treatment enhances sprouting of corticospinal axons rostral to a unilateral cervical spinal cord lesion in adult macaque monkey. **J Comp Neurol. 502**(4):644-59.

Fuentes, E.O., Leemhuis, J., Stark, G.B. and Lang, E.M. (2008) Rho kinase inhibitors Y27632 and H1152 augment neurite extension in the presence of cultured Schwann cells. **J Brachial Plex Peripher Nerve Inj. 25:** 3-19.

Gaze, R.M. (1970) The formation of nerve connections. **Academic Press, London.**

GrandPre, T., Nakamura, F., Vartanian, T. and Strittmatter, S.M. (2000) Identification of the Nogo inhibitor of axon regeneration as a Reticulon protein. **Nature 403**:439-44.

GrandPre, T., Li, S. and Strittmatter, S.M. (2002) Nogo-66 receptor antagonist peptide promotes axonal regeneration. **Nature. 417**:547–551.

Haenisch, C., Diekmann, H., Klinger, M., Gennarini, G., Kuwada, J.Y. and Stuermer, C.A.O. (2005) The neuronal growth and regeneration associated Cntn1 (F3/F11/Contactin) gene is duplicated in fish: expression during development and retinal axon regeneration. **Mol Cell Neurosci. 28**(2):361-74.

He, X.L., Bazan, F.J., McDermott, G., Park, J.B., Wang, K., Tessier-Lavigne, M., He, Z. and Garcia, K.C. (2003) Structure of the Nogo receptor ectodomain: a recognition module implicated in myelin inhibition. **Neuron 38**:177-185.

Hirsch, S., Cahill, M.A. and Stuermer, C.A.O. (1995) Fibroblasts at the transection site of the injured goldfish optic nerve and their potential role during retinal axonal regeneration. **J Comp Neurol 360**:599-611.

Horn, K.P., Busch, S.A., Hawthorne, A.L., van Rooijen, N. and Silver, J. (2008) Another barrier to regeneration in the CNS: activated macrophages induce extensive retraction of dystrophic axons through direct physical interactions. **J Neurosci 28**:9330-9341.

Hsieh, S.H-K., Ferraro, G.B. and Fournier, A.E. (2006) Myelin-associated inhibitors regulate cofilin phosphorylation and neuronal inhibition through LIM kinase and slingshot phosphatase **J. Neurosci 26** (3): 1006.

Huber, A.B., Weinmann, O., Brösamle, C., Oertle, T. and Schwab, M.E. (2002) Patterns of Nogo mRNA and protein expression in the developing and adult rat and after CNS lesions. **J Neurosci. 22**(9):3553-67.

Hunt, D., Coffin, R. S. and Anderson, P. N. (2002). the Nogo receptor, its ligands and axonal regeneration in the spinal cord; a rieview. **J Neurocytol 31**:93-120.

Karimi-Abdolrezaee, S., Eftekharpour, E., Wang, J., Morshead, C.M. and Fehlings, M.G. (2006) Delayed transplantation of adult neural precursor cells promotes remyelination and functional neurological recovery after spinal cord injury. **J Neurosci. 26**(13):3377-89.

Kim, J.E., Li, S., GrandPre, T., Qiu, D. and Strittmatter, S.M. (2003a) Axon regeneration in young adult mice lacking Nogo-A/B. **Neuron. 38**(2):187-99.

Kim, J.E., Bonilla, I.E., Qiu, D. and Strittmatter, S.M. (2003b) Nogo-C is sufficient to delay nerve regeneration. **Mol Cell Neurosci. 23**(3):451-9.

Klinger, M., Taylor, J.S., Oertle, T., Schwab, M.E., Stuermer, C.A.O. and Diekmann, H. (2004) Identification of Nogo-66 Receptor (NgR) and homologous genes in fish. **Mol Biol Evol 21**:38-47.

Kottis, V., Thibault, P., Mikol, D., Xiao, Z.C., Zhang, R., Dergham, P. and Braun, P.E. (2002) Oligodendrocyte-myelin glycoprotein (OMgp) is an inhibitor of neurite outgrowth. **J Neurochem. 82**(6):1566-9.

Lauren, J., Hu, F., Chin, J., Liao, J., Airaksinen, M.S. and Strittmatter, S.M. (2007) Characterization of myelin ligand complexes with neuronal Nogo-66 receptor family members. **J Biol Chem. 282(8):**5715-25. Epub 2006 Dec 21.

Landreth, G.E. and Agranoff, B.W. (1979) Explant culture of adult goldfish retina: a model for the study of CNS regeneration. **Brain Res. 161**(1):39-55.

Lang, D.M., Rubin, B.P., Schwab, M.E. and Stuermer, C.A.O. (1995) CNS myelin and oligodendrocytes of the Xenopus spinal cord--but not optic nerve--are nonpermissive for axon growth. **J Neurosci. 15**(1 Pt 1):99-109.

Lang, D.M., Monzón-Mayor, M., Bandtlow, C.E. and Stuermer, C.A.O. (1998) Retinal axon regeneration in the lizard Gallotia galloti in the presence of CNS myelin and oligodendrocytes. **Glia. 23**(1):61-74.

Lang, D.M., Warren, J.T.Jr., Klisa, C. and Stuermer, C.A.O. (2001) Topographic restriction of TAG-1 expression in the developing retinotectal pathway and target dependent reexpression during axon regeneration. **Mol Cell Neurosci. 17**(2):398-414.

Leppert, C.A., Diekmann, H., Paul, C., Laessing, U., Marx, M., Bastmeyer, M. and Stuermer, C.A.O. (1999) Neurolin Ig domain 2 participates in retinal axon guidance and Ig domains 1 and 3 in fasciculation. J Cell Biol. 144(2):339-49.

Li, M., Shi, J., Wei, Z., Teng, F.Y., Tang, B.L., Song, J. (2004) Structural characterization of the human Nogo-A functional domains. Solution structure of Nogo-40, a Nogo-66 receptor antagonist injured spinal cord regeneration.**Eur J Biochem 271**(17):3512-22.

Li, S., Liu, B. P., Budel, S., Li, M., Ji, B., Walus, L., Li, W., Jirik, A., Rabacchi, S., Choi, E., Worley, D., Sah, W., Pepinsky, B., Lee, D., Relton, J. and Strittmatter, S.M. (2004) Blockade of Nogo-66, myelin-associated glycoprotein, and oligodendrocyte myelin glycoprotein by soluble Nogo-66 receptor promotes axonal sprouting and recovery after spinal injury. **J Neurosci 24**:10511-20.

Li, S., Kim, J.E., Budel, S., Hampton, T.G. and Strittmatter, S.M. (2005) Transgenic inhibition of Nogo-66 receptor function allows axonal sprouting and improved locomotion after spinal injury. **Mol Cell Neurosci 29**(1):26-39.

Liebscher, T., Schnell, L., Schnell, D., Scholl, J., Schneider, R., Gullo, M., Fouad, K., Mir, A., Rausch, M., Kindler, D., Hamers, F.P. and Schwab, M.E. (2005) Nogo-A antibody improves regeneration and locomotion of spinal cord-injured rats. **Ann Neurol. 58**(5):706-19.

Liu, B.P., Fournier, A., GrandPré, T. and Strittmatter, S.M. (2002) Myelin-associated glycoprotein as a functional ligand for the Nogo-66 receptor. **Science. 297**(5584):1190-3.

Lu, P. and Tuszynski, M.H. (2008) Growth factors and combinatorial therapies for CNS regeneration. **Exp Neurol. 209**(2):313-20. Review.

Málaga-Trillo, E., Solis, G.P., Schrock, Y., Geiss, C., Luncz, L., Thomanetz, V. and Stuermer, C.A.O. (2009) Regulation of embryonic cell adhesion by the prion protein. **PLoS Biol 7** (3):e55.

Mason, M. R. J., Lieberman, A. R., Latchman, D. S. and Anderson, P. (2003) FKBP12 mRNA expression is upregulated by intrinsic CNS neurons regenerating axons into peripheral nerve grafts in the brain. **Exper Neurology. 181**: 181-189.

McClellan, A.D. (1990) Locomotor recovery in spinal-transected lamprey: role of functional regeneration of descending axons from brainstem locomotor command neurons. **Neuroscience.37**(3):781-98.

McGee, A.W. and Strittmatter, S.M. (2003) The Nogo-66 receptor: focusing myelin inhibition of axon regeneration. **Trends Neurosci. 26**(4):193-8. Review.

McKeon, R.J., Schreiber, R.C., Rudge, J.S. and Silver, J. (1991) Reduction of neurite outgrowth in a model of glial scarring following CNS injury is correlated with the expression of inhibitory molecules on reactive astrocytes. **J Neurosci. 11**(11):3398-411.

Meyenburg, J. Van., Brösamle, C., Metz, G.A.S. and Schwab, M.E. (1998) Regeneration and sprouting of chronically injured corticospinal tract fibers in adult rats promoted by NT-3 and the mAb IN-1, which neutralizes myelin-associated neurite growth inhibitors. **Exp Neurol 154**:583-594.

Mi, S., Lee, X., Shao, Z., Thill, G., Ji, B., Relton, J., Levesque, M., Allaire, N., Perrin, S., Sands, B., Crowell, T., Cate, R.L., McCoy, J.M. and Pepinsky, R.B. (2004) LINGO-1 is a component of the Nogo-66 receptor/p75 signaling complex. **Nat Neurosci. 7**(3):221-8.

Mimura, F., Yamagishi, S., Arimura, N., Fujitani, M., Kubo, T., Kaibuchi, K. and Yamashita, T. (2006) Myelin-associated glycoprotein inhibits microtubule assembly by a Rho-kinase-dependent mechanism. **J Biol Chem. 281**(23):15970-9.

Mukhopadhyay, G., Doherty, P., Walsh, F.S., Crocker, P.R. and Filbin, M.T. (1994) A novel role for myelin-associated glycoprotein as an inhibitor of axonal regeneration. **Neuron. 13**(3):757-67.

Munderloh, C., Solis, G.P., Bodrikov, V., Jaeger, F.A., Wiechers, M., Málaga-Trillo, E. and Stuermer, C.A.O. (2009) Reggies/flotillins regulate retinal axon regeneration in the zebrafish optic nerve and differentiation of hippocampal and N2a neurons. **J Neurosci. 29(20)**:6607-15.

Ng, J., Nardine, T., Harms, M., Tzu, J., Goldstein, A., Sun, Y., Dietzl, G., Dickson, B.J. and Luo, L. (2002) Rac GTPases control axon growth, guidance and branching. **Nature. 416**(6879):442-7.

Niederoest, B., Oertle, T., Fritsche, J., McKinney, R.A. and Bandtlow, E. (2002) Nogo-A and myelin-associated glycoprotein mediate neurite growth inhibition by antagonistic regulation of RhoA and Rac1. **J Neurosci 22**:10368-10376.

Oertle, T., Klinger, M., Stuermer, C.A.O. and Schwab, M.E. (2003a) Phylogenetic evolution and nomenclature of the RTN/Nogo gene family. **FASEB J 17**, 1238-1247.

Oertle, T., et al. (13 co-authors) (2003b) Nogo-A inhibits neurite outgrowth and cell spreading with three discrete regions. **J Neurosci 23**:5393–5406.

O'Neill, P., Whalley, K. and Ferretti, P. (2004) Nogo and Nogo-66 receptor in human and chick: implications for development and regeneration. **Dev Dyn. 231**(1):109-21.

Paschke, K.A., Lottspeich, F. and Stuermer, C.A.O. (1992) Neurolin, a cell surface glycoprotein on growing retinal axons in the goldfish visual system, is reexpressed during retinal axonal regeneration. **J Cell Biol. 117**(4):863-75.

Park, J.B., Yiu, G., Kaneko, S., Wang, J., Chang, J., He, X.L., Garcia, K.C. and He, Z. (2005) A TNF receptor family member, TROY, is a coreceptor with Nogo receptor in mediating the inhibitory activity of myelin inhibitors. **Neuron. 45**(3):345-51.

Pellitteri, R., Zicca, A., Mancardi, G.L., Savio, T. and Cadoni, A. (2001) Schwann cell-derived factors support serotoninergic neuron survival and promote neurite outgrowth. **Eur J Histochem. 45**:367-76.

Pot, C., Simonen, M., Weinmann, O., Schnell, L., Christ, F., Stoeckle, S., Berger, P., Rülicke, T., Suter, U. and Schwab, M.E. (2002) Nogo-A expressed in Schwann cells impairs axonal regeneration after peripheral nerve injury. **JCB. 159:** 29–35.

Prinjha, R., Moore, S.E., Vinson, M., Blake, S., Morrow, R., Christie, G., Michalovich, D., Simmons, D.L. and Walsh, F.S. (2000) Inhibitor of neurite outgrowth in humans. **Nature 403**: 383-384.

Ramon y Cajal, S. (1890) Cajal's degeneration and regeneration of the nervous system. Oxford university. **press, Oxford**.

Ramon y Cajal, S. (1928) Cajal's degeneration and regeneration of the nervous system. Oxford university. **press, Oxford**.

Schmidt, J.T., Turcotte, J.C., Buzzard, M. and Tieman, D.G. (1988) Staining of regenerated optic arbors in goldfish tectum: progressive changes in immature arbors and a comparison of mature regenerated arbors with normal arbors. **J Comp Neurol 269**:565-591.

Schnell, L., Schwab, M.E. (1990) Axonal regeneration in the rat spinal cord produced by an antibody against myelin-associated neurite growth inhibitors. **Nature. 343** (6255):269-72.

Schrock, Y., Solis, G.P. and Stuermer, C.A.O. (2009) Regulation of cell spreading, focal adhesion formation and filopodia extension by the cellular prion protein. **FEBS Letts 583**:389-93.

Schulte, T., Paschke, K.A., Laessing, U., Lottspeich, F. and Stuermer, C.A.O. (1997) Reggie-1 and reggie-2, two cell surface proteins expressed by retinal ganglion cells during axon regeneration. **Development. 124**(2):577-87.

Schwab, M.E. (2004) Nogo and axon regeneration. **Curr Opin Neurobiol. 14**(1):118-24. Review.

Schwalb, J.N., Gu, M-f., Stuermer, C.A.O, Bastmeyer, M., Hu, G-f., Baulis, N., Irvin, N. and Benowitz, L.I. (1996) Optic nerve glia secrete a low molecular weight factor that stimulates retinal ganglion cells to regenerate axons in goldfish. **Neuroscience 72**, 901-911.

Seymour, A.B., Andrews, E.M., Tsai, S.Y., Markus, T.M., Bollnow, M.R., Brenneman, M.M., O'Brien, T.E., Castro, A.J., Schwab, M.E. and Kartje, G.L. (2005) Delayed treatment with monoclonal antibody IN-1 1 week after stroke results in recovery of function and corticorubral plasticity in adult rats. **J Cereb Blood Flow Metab. 25**(10):1366-75.

Silver, J. and Miller, J.H. (2004) Regeneration beyond the glial scar. **Nat Rev Neurosci 5**:146-156.

Simonen, M., Pedersen, V., Weinmann, O., Schnell, L., Buss, A., Ledermann, B., Christ, F., Sansig, G., van der Putten, H. and Schwab, M.E. (2003) Systemic deletion of the myelin-associated outgrowth inhibitor Nogo-A improves regenerative and plastic responses after spinal cord injury. **Neuron. 38**(2):201-11.

Spillmann, A.A, Bandtlow, C.E., Lottspeich, F., Keller, F. and Schwab, M.E. (1998) Identification and characterization of a bovine neurite growth inhibitor (bNI-220). **J Biol Chem. 273**(30):19283-93.

Steinmetz, M.P., Horn, K.P., Tom, V.J., Miller, J.H., Busch, S.A., Nair, D., Silver, D.J. and Silver, J. (2005) Chronic enhancement of the intrinsic growth capacity of sensory neurons combined with the degradation of inhibitory proteoglycans allows functional regeneration of sensory axons through the dorsal root entry zone in the mammalian spinal cord.**J Neurosci. 25**(35):8066-76.

Strobel, G. and Stuermer, C.A.O. (1994) Growth cones of regenerating retinal axons contact a variety of cellular profiles in the transected goldfish optic nerve. **J Comp Neurol. 346**:435-448.

Stuermer, C.A.O. and Easter, Jr. S.S. (1984) Rules of order in the retinotectal fascicles of goldfish. **J Neurosci 4**, 1045-1051

Stuermer, C.A.O. (1988a) The trajectories of regenerating retinal axons in the goldfish tectum. I. A comparison of normal and regenerated axons at late regeneration stages. **J Comp Neurol. 267**:55-68.

Stuermer, C.A.O. (1988b) The trajectories of regenerating retinal axons in the goldfish tectum. II. Exploratory branches and growth cones on axons at early regeneration stages. **J Comp Neurol. 267**:69-91.

Stuermer, C.A.O., Bastmeyer, M., Bahr, M., Strobel, G. and Paschke, K. (1992) Trying to understand axonal regeneration in the CNS of fish. **J Neurobiol. 23**:537-50.

Tozaki, H., **Kawasaki, T**., **Takagi, Y**. **and Hirata, T**. (2002) Expression of Nogo protein by growing axons in the developing nervous system. **Brain Res Mol Brain Res. 104**:111-9.

Venkatesh, K., Chivatakarn, O., Lee, H., Joshi, P.S., Kantor, D.B., Newman, B.A., Mage, R., Rader, C. and Giger, R.J. (2005) The Nogo-66 receptor homolog NgR2 is a sialic acid-dependent receptor selective for myelin-associated glycoprotein. **J Neurosci. 25**(4):808-22.

Vielmetter, J. and Stuermer, C.A.O (1989) Goldfish retinal axons respond to position-specific properties of tectal cell membranes *in vitro*. **Neuron 2**:1331-1339.

Weinmann, O., Schnell, L., Ghosh, A., Montani, L., Wiessner, C., Wannier, T., Rouiller, E., Mir, A. and Schwab, M.E. (2006) Intrathecally infused antibodies against Nogo-A penetrate the CNS and downregulate the endogenous neurite growth inhibitor Nogo-A. **Mol Cell Neurosci. 32**(1-2):161-73.

Wang, K.C., Koprivica, V., Kim, J.A., Sivasankaran, R., Guo, Y., Neve, R.L. and He, Z. (2002) Oligodendrocyte-myelin glycoprotein is a Nogo receptor ligand that inhibits neurite outgrowth. **Nature 417**:941-944.

Wang, X., Chun, S.J., Treloar, H., Vartanian, T., Greer, C.A. and Strittmatter, S.M. (2002) Localization of Nogo-A and Nogo-66 receptor proteins at sites of axon-myelin and synaptic contact. **J Neurosci. 22**(13):5505-15.

Wanner, M., Lang, D.M., Bandtlow, C.E., Schwab, M.E., Bastmeyer, M. and Stuermer, C.A.O. (1995) Re-evaluation of the growth-permissive substrate properties of gildfish optic nerve myelin and myelin proteins. **J Neurosci 15**:7500-8.

Yamashita, T., Higuchi, H. and Tohyama, M. (2002) The p75 receptor transduces the signal from myelin-associated glycoprotein to Rho. **J Cell Biol. 157**(4):565-70.

Yiu, G. and He, Z. (2006) Glial inhibition of CNS axon regeneration. **Nat Rev Neurosci. 7**(8):617-27. Review.

Zheng, B., Ho, C., Li, S., Keirstead, H., Steward, O. and Tessier-Lavigne, M. (2003) Lack of enhanced spinal regeneration in Nogo-deficient mice. **Neuron 38** (2):213-24.